Title
Molecular mechanisms by which Mycobacterium leprae survives in human macrophages

Author
Mehta, Manali D.

Publication Date
2016

Peer reviewed|Thesis/dissertation

UNIVERSITY OF CALIFORNIA

Los Angeles

Molecular mechanisms by which *Mycobacterium leprae* survives in human macrophages

A dissertation submitted in partial satisfaction of the requirements for the degree Doctor of Philosophy in Microbiology, Immunology, and Molecular Genetics

by

Manali Dhirendra Mehta

2016

ABSTRACT OF THE DISSERTATION

Molecular mechanisms by which *Mycobacterium leprae* survives in human macrophages

by

Manali Dhirendra Mehta

Doctor of Philosophy in Microbiology, Immunology, and Molecular Genetics

University of California, Los Angeles, 2016

Professor Robert L. Modlin, Chair

Leprosy, a chronic infectious disease caused by *Mycobacterium leprae*, is a powerful model to study the human immune response because the clinical manifestations of disease present as a spectrum correlating with the level of immune response to the pathogen. Research investigating mechanisms of host defense and *M. leprae*-induced suppression of antimicrobial pathways continues to provide insight into which immune pathways are essential for containment of mycobacterial infections. Here, we utilized three bioinformatics approaches to identify mechanisms of modulation of host immune responses by mycobacteria and gain a clearer understanding of disease pathogenesis and potential targets of mitigation, including: i) integration of microRNA and mRNA gene expression profiling of disseminated lepromatous leprosy (L-lep) versus self-containing tuberculoid leprosy (T-lep) lesions to identify microRNAs capable of downregulating antimicrobial peptide production, ii) overlap of highly expressed

receptors on IL-15-derived M1 and IL-10-derived M2 macrophages (MΦ) with known drivers of MΦ polarization to discern ligands capable of reeducating MΦ phenotype and function, and iii) comparison of transcriptome profiles of *M. leprae*-infected monocyte-derived MΦ and leprosy skin lesions to identify candidate genes contributing to suppression of host immune responses and bacterial survival.

We provide evidence illustrating the ability of *M. leprae* to induce specific microRNAs and host genes to alter host immune responses. *M. leprae*, but not *M. tuberculosis*, can induce upregulation of microRNA-21, which then targets and downregulates antimicrobial peptide production and mycobacterial killing. Differential cytokine expression coupled with the presence of mycobacterial ligands can alter MΦ polarization correlating to a change in phagocytic function and expression of antimicrobial genes. Lastly, *M. leprae* can induce expression of the autophagy regulator NUPR1, which is more highly expressed in L-lep lesions. As more data are gathered on (i) the functional consequences of host genes regulated during mycobacterial infections on the immune response and ii) how these genes are regulated by the pathogens, it may provide an opportunity for directed therapeutic intervention.

The dissertation of Manali Dhirendra Mehta is approved.

Genhong Cheng

Sherie Morrison

Dinesh Rao

Robert L. Modlin, Committee Chair

University of California, Los Angeles

2016

DEDICATION

This dissertation is dedicated to all those, past and present, that have taken on the fight to rid the world of social stigmas associated with leprosy and other debilitating diseases.

"I sought my soul, but my soul I could not see.
I sought my God, but my God eluded me.
I sought my brother, and I found all three."
by William Blake
- Favorite quote of Baba Amte, founder of Anandwan

TABLE OF CONTENTS

LIST OF FIGURES

ACKNOWLEDGMENTS

Chapter 1 and other sections of this dissertation contains edited portions of the full citation Mehta MD, Liu PT. microRNAs in mycobacterial disease: friend or foe? *Frontiers in Genetics*. 2014 Jul 15;5:231. Copyright 2014 by Creative Commons Attribution License (CC BY). doi: 10.3389/fgene.2014.00231. Chapter 2 is a reprint of the full citation Liu PT, Wheelwright M, Teles R, Komisopoulou E, Liu PT, Wheelwright M, Teles R, Komisopoulou E, Edfeldt K, Ferguson B, Mehta MD, Vazirnia A, Rea TH, Sarno EN, Graeber TG, Modlin RL. MicroRNA-21 targets the vitamin D-dependent antimicrobial pathway in leprosy. *Nature Medicine*. 2012 Jan 29;18(2):267-73. Copyright 2012. Chapter 3 was written in collaboration with Montoya D (co-author); other contributors include Ferguson B, Teles R, Cruz D, Krutzik SR, Pellegrini M, and Modlin RL. Contributors for Chapter 4 include Lu J, Teles R, Aliyari S, Parvatiyar K, Realegeno S, Kelly-Scumpia KM, Sarno EN, Rea TH, Ochoa MT, Pellegrini M, Modlin RL.

Funding was provided by Microbial Pathogenesis Training Grant (T32-AI07323).

VITA

2005-2009	B.A. Molecular and Cellular Biology, emphasis Immunology University of California, Berkeley Berkeley, California
2007-2009	Research Assistant University of California, Berkeley Berkeley, California
2009-present	Graduate Student Researcher UCLA Department of Microbiology, Immunology, and Molecular Genetics Los Angeles, California
2011-2012	Teaching Assistant Bacterial Pathogenesis UCLA Department of Microbiology, Immunology, and Molecular Genetics Los Angeles, California
2011-2012	Teaching Assistant Bacterial Pathogenesis UCLA Department of Microbiology, Immunology, and Molecular Genetics Los Angeles, California
2013-2014	Microbial Pathogenesis Training Grant
2013	Microbiology, Immunology, and Molecular Genetics Travel Award
2015	Keystone Symposium Travel Award

PUBLICATIONS AND PRESENTATIONS

1. Liu PT, Wheelwright M, Teles R, Komisopoulou E, Liu PT, Wheelwright M, Teles R, Komisopoulou E, Edfeldt K, Ferguson B, Mehta MD, Vazirnia A, Rea TH, Sarno EN, Graeber TG, Modlin RL. MicroRNA-21 targets the vitamin D-dependent antimicrobial pathway in leprosy. *Nature Medicine*. 2012 Jan 29;18(2):267-73.

2. Mehta MD, Liu PT, Modlin RL. Role of microRNAs in regulation of immune response to infection with *Mycobacterium leprae*. AAI Annual Meeting 2012.
3. Mehta MD, Liu PT, Modlin RL. microRNAs induced during *Mycobacterium leprae* infection and their effects on immune response. AAI Annual Meeting 2013.
4. Mehta MD, Liu PT. microRNAs in mycobacterial disease: friend or foe? *Frontiers in Genetics*. 2014 Jul 15;5:231.
5. Mehta MD, Montoya DJ, Teles R, Kelly-Scumpia K, Realegeno SE, Modlin RL. In vitro *Mycobacterium leprae* infection results in host response skewed towards a Type I IFN profile. UCLA Immunobiology of Leprosy Symposium 2015.

CHAPTER 1:

Introduction

Leprosy, a chronic infectious disease caused by *Mycobacterium leprae*, is the leading cause of permanent physical disability among communicable diseases[1]. Infection occurs primarily in the skin and peripheral nerves[2] and can result in physical deformities and peripheral neuropathy characterized by a sensory deficit. At the time of diagnosis, up to 60% of patients have already sustained irreversible peripheral nerve damage[3.4.5] and are at risk for sequelae long after the disease has been cured, increasing the need for early detection and treatment.

With the application of Multidrug Therapy (MDT) consisting of dapsone, rifampicin, and clofazimin in 1981, there is now a 98% cure rate of leprosy[3,6]. Still, there is evidence of relapse and the mode and effect of MDT on transmission of leprosy[7-10] is unclear. With the lack of data regarding transmission and the social stigma surrounding leprosy-induced disfigurements resulting in hesitation in seeking diagnosis and treatment, the number of cases has plateaued since 2005. Currently, there are close to 200,000 new cases per year[11]. Fortunately, although the negative connotations associated with leprosy has led to infected patients being ostracized from their homes, there has been a huge outgrowth of leprosy centers around the world aimed in treating and rehabilitating those with leprosy.

Learning from Leprosy:

With the lack of progress in elimination of the global incidence of leprosy, research on the host defense against *M. leprae* and disease pathogenesis continues to provide insight into which immune pathways are essential for containment of mycobacterial infections. Leprosy is a powerful model to study the human immune response because it presents as a spectrum where the clinical manifestations correlate with the level of immune response to the pathogen contributing to host defense or pathogenesis (Figure 1)[12]. At the ends of the spectrum are the tuberculoid (T-lep) and lepromatous (L-lep) forms, in which the infection presents as self-limited

or disseminated granulomatous lesions in the skin, respectively. Comparisons of T-lep versus L-lep skin lesions have yielded significant insight regarding the adaptive and innate immune responses essential in protection against *M. leprae* infection. Skin lesions from T-lep patients exhibit an immune response characterized by a Type II interferon (IFN) profile[13], Th1 cytokines such as IL-15, and macrophages (MΦ) programmed to express the vitamin D-mediated antimicrobial pathway[14] and to induce autophagy upon immune stimulation[15]. In contrast, L-lep lesions are typified by a Type I IFN profile[13], Th2 cytokines such as IL-10, and an accumulation of MΦ programmed to express enhanced phagocytic activity but lacking expression of antimicrobial factors[14].

Type II vs Type I Interferon:

The differential expression of Type II vs. Type I IFNs at the site of disease in leprosy is thought to be contribute to development of the T-lep and L-lep clinical forms, respectively[13], where the level of severity of mycobacterial disease closely correlates with the level of responsiveness to Type II interferon, IFN-γ[16,17]. IFN-γ, a known inducer of macrophage activation and antimicrobial pathways, activates a heterodimeric IFN-γ receptor (IFNGR) composed of two chains, IFNGR1 and IFNGR2. Accordingly, IFNGR-deficient mice are more susceptible to mycobacterial infection. Genetic studies investigating patients with mutations limiting expression or functionality of either receptor chain reveal poorer prognosis with mycobacterial disease[19-31], highlighting the nonredundant role of IFN-γ in protection against mycobacterial infection. In T-lep, cells of both the adaptive (Th1) and innate (Natural Killer) immune system secrete IFN-γ[32], which can then activate neighboring MΦ to mount an appropriate response to intracellular pathogens. *In vitro*, IFN-γ can promote mycobacterial killing in human monocytes or MΦ via multiple mechanisms, including induction of: i) the vitamin D antimicrobial pathway[33] and ii) autophagy[15].

In contrast, the gene expression profile of L-lep skin lesions exhibits an IFN-β, or Type I IFN, profile[13], which signals through a distinct receptor complex IFNAR composed of IFNAR1 and IFNAR2. While IFNGR-deficient mice are more susceptible to mycobacterial infection, IFNAR-deficient mice are more resistant to infection, suggesting that Type I IFN can antagonize IFN-γ responses[34,35]. Indeed, IFN-β can downregulate expression of IFNGR and downstream immune pathways including the vitamin D antimicrobial pathway[14] and antigen presentation[36-39]. IFN-β induces the M2-polarizing cytokine IL-10, which can suppress the conversion of vitamin D to its active form by suppressing Cyp27B1 expression. This inhibition ultimately leads to an inability to induce production of antimicrobial peptides CAMP and DEFB4 and enhanced bacterial viability[13].

M1 versus M2 MΦ:

In addition to type II and type I interferons, T-lep and L-lep lesions also contain MΦ of distinct phenotype and function and differential expression of IL-15 and IL-10[40,41], cytokines known to regulate macrophage function. T-lep lesions contain macrophages that are well-differentiated and contain little to no bacteria. Reflective of IL-15-derived M1 MΦ, these MΦ are $CD209^{+}CD163^{lo}$ and express components of the vitamin D antimicrobial pathway capable of mycobacterial killing[14]. In contrast, MΦ prominent in L-lep lesions are $CD209^{+}CD163^{hi}$, resembling IL-10-derived M2 MΦ. They express higher levels of scavenger receptors and show enhanced phagocytic function but lack expression of the antimicrobial pathway to promote bacterial clearance. Consistently, these MΦ have a large mycobacterial load and are ill-defined[42].

Host Defense:

Vitamin D antimicrobial pathway:

Induction of the vitamin D-dependent antimicrobial pathway can be achieved following activation of the adaptive or innate immune responses. In adaptive immunity, Th1 cells produce IFN-γ, which can activates MΦ by signaling through the IFNGR. In innate immunity, detection of *M. leprae* is mediated, in part, by the pattern recognition receptor heterodimer, Toll-like receptor 2 and 1 (TLR2/1)[43]. Stimulation with either IFN-γ or TLR2/1L on monocytes results in induction of the vitamin D receptor (VDR) and CYP27B1 in an IL-15-dependent manner[44,45]. The CYP27B1 gene product (CYP27b1), a cytochrome P450 hydroxylase, is responsible for the conversion of the circulating prohormone form of vitamin D (25-hydroxyvitamin D3, 25D) into its active hormone form (1,25α-dihydroxyvitamin D, 1,25D). If the extracellular concentration of 25D is sufficient, CYP27b1 will convert 25D into 1,25D, resulting in activation of the VDR and expression of antimicrobial peptides cathelicidin (CAMP) and human beta defensin-2 (DEFB4)[46]. Convergence of IL-1β signaling and vitamin D transcriptional activation is required for the TLR-induced expression of DEFB4[46]. Triggering of TLR2/1 was found to modulate IL-1β activity and increase the cell's responsiveness to IL-1β by simultaneously i) inducing IL-1β secretion, ii) increasing expression of cell surface IL-1 receptor 1 (IL-1R1), and iii) decreasing the baseline secretion of IL-1 receptor antagonist (IL-1RA).

Autophagy:

During optimal growth conditions, mTOR, or mammalian target of rapamycin, suppresses autophagy. In times of stress or nutrient deficiency, however, the cell undergoes the process of autophagy to break down cytoplasmic contents for the regeneration of amino acids and energy sources to permit cell survival[68]. Autophagy is generally subcategorized into three categories:

macroautophagy, microautophagy, and chaperone-mediated autophagy. Macroautophagy, or more generally termed autophagy, is the most common and initiates with the formation of a double membrane-containing phagophore. Portions of the cytosol containing aged or damage organelles and proteins are incorporated into the phagophore as the membrane elongates. During this time, LC3 is recruited to the phagophore where it stays until the phagophore fuses with the autolysosome and is degraded along with the rest of its contents[69,70]. Although autophagy most commonly occurs through macroautophagy, it can also occur via invagination of the lysosomal membrane (microautophagy)[71] or selective targeting of proteins to the lysosome (chaperone-mediated autophagy)[72.73].

Infection with intracellular bacteria can resemble nutrient-deficient states within the MΦ due to bacterial hijacking of host iron and metabolic intermediates required for bacterial persistence. As such, phagocytic cells can employ autophagy as a host defense mechanism to eliminate intracellular infections[74-77]. Indeed, autophagy is critical for mounting an effective immune response to mycobacterial infection[78-80]. After phagocytosis, mycobacteria suppress phagolysosomal fusion and acidification[81,82], but induction of autophagy can overcome this suppression and deliver mycobacteria to antimicrobial peptide-containing autolysosomes[83]. Stimulation with IFN-γ[33,84,85], recognition of mycobacterial lipid MDP[86], or nutrient sensing such as vitamin D can induce autophagy during mycobacterial infection.

Mechanisms of immune evasion:

<u>microRNA-21:</u>

MicroRNAs are small noncoding RNAs about 22 nucleotides in length that post-transcriptionally regulate the amount of mRNA in the cell. Encoded in the genome within intergenic or exonic regions or derived from introns of other genes[47,48], microRNAs are initially

transcribed by RNA polymerase II or III in the form of a long primary miRNA transcripts[49-51] and processed by the enzyme Drosha into smaller pre-miRNA containing a hairpin structure[52-55] prior to nuclear export[56-58]. Once in the cytoplasm, pre-miRNAs undergo a final processing step by Dicer RNase to produce mature miRNAs[59.60] that can then be loaded onto the RNA-induced silencing complex (RISC). With their 7mer or 8mer seed sequence, microRNAs can bind to 3' untranslated regions (UTR) of complementary mRNAs and sterically inhibit translation or target the mRNA for degradation[61].

The first microRNA, lin-4, was discovered in the early 1990s[62]. Since then, the number of microRNAs has grown to include over 1800 microRNAs estimated to regulate about 30% of the human transcriptome. Several microRNAs have been implicated in human pathologies including cancer, autoimmune diseases, and microbial infections[63]. An increasing amount of evidence also supports a role for microRNAs in regulation of host responses to mycobacterial infection[64]. Initially described as an oncogenic microRNA, microRNA-21 (miR-21) has been extensively studied in the context of host immunity. miR-21 is upregulated after activation of the myeloid precursor monocyte, during differentiation into macrophages, neutrophils, and immature dendritic cells, and after stimulation by immune regulators such as lipopolysaccharide[65] and TGF-β[66]. While the functions of miR-21 are complex and still being studied, several reports have provided evidence suggesting an anti-inflammatory role for miR-21. miR-21 can inhibit the expression of IL-12p35, a subunit of a major Th1 driving cytokine[67], and indirectly enhance the production of IL-10, a major Th2 driving cytokine[65].

NUPR1:

NUPR1, also known as p8 and Com1, was initially discovered in 1997 when it was found to be more highly expressed during acute pancreatitis[87]. It is conserved in mammals,

Drosophila[88], Xaenopus[96], and C. elegans but shares little homology to other proteins of known function[97]. Despite this lack of sequence similarity, NUPR1 shares several biochemical properties with high-mobility group proteins in the HMG-I/Y subfamily[97] including a high isoelectric point and high percentage of proline and glycine amino acids.

Predictions into the structure of NUPR1 protein have indicated the presence of a basic Helix-Loop-Helix motif characteristic of transcription factors. Accordingly, NUPR1 has is reported to bind DNA upon phosphorylation by protein kinase A. In addition to a seven-fold increase in DNA binding[97], phosphorylated NUPR1 exhibits increased secondary structure and stability.

Since the discovery of NUPR1, several studies have elucidated basic properties of NUPR1. The open reading frame is comprised of three exons alternatively spliced into two NUPR1 transcripts encoding an 82 and 100 amino acid peptide, It is important to note, however, that the majority of the literature that exists to date is representative of only the smaller isoform. Interestingly, though NUPR1 is small in size, it contains a nuclear localization sequence and requires active transport to enter the nucleus, suggesting NUPR1 has binding partners prior to entry into the nucleus. Induction of NUPR1 occurs after cellular stresses such as hypoxia or starvation[88], as well as after stimulation with demyelinating agents[89], cell cycle arrest[90], TGF-β[91], TNF-α[92,93], glucose[94], and 1,25D3[95].

The lack of paralog in yeast enabled a yeast two-hybrid screen to identify binding partners of NUPR1 including MSL-1[98]. NUPR1 can alter transcriptional profiles by inhibiting the histone acetylase activity of MSL-1. Several other binding partners are known, revealing a role of NUPR1 in multiple pathways including autophagy[99-102], apoptosis[103,104], demyelination[89], and transcriptional regulation[98,105-107]. Studies investigating the role of NUPR1 in autophagy, however, have yielded conflicting results. In two studies, NUPR1 inhibited autophagy through downregulation of autophagy inducer BNIP3[99] or correlation with AURKA expression[100]. In

contrast, NUPR1 can also promote the induction of autophagy by upregulation of mTOR inhibitor TRB3[101] or long non-coding RNA expression from TGFB2 that serves as a microRNA sponge for microRNAs that inhibit autophagy[102]. NUPR1 plays a role in regulation of cell cycle; however, it still remains to be determined whether NUPR1 plays a role in microbial infections.

FIGURE 1: The spectrum of leprosy

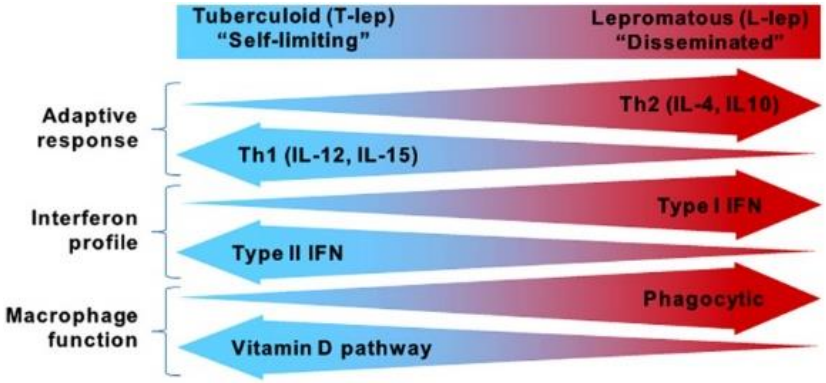

Figure 1: The spectrum of leprosy

Characteristics of the innate and adaptive immune responses in either end of the leprosy spectrum.

CHAPTER 2:

MicroRNA-21 targets the vitamin D-dependent antimicrobial pathway in leprosy

nature medicine

MicroRNA-21 targets the vitamin D–dependent antimicrobial pathway in leprosy

Philip T Liu[1,2], Matthew Wheelwright[2], Rosane Teles[2], Evangelia Komisopoulou[3,4], Kristina Edfeldt[2], Benjamin Ferguson[2], Manali D Mehta[5], Aria Vazirnia[5], Thomas H Rea[6], Euzenir N Sarno[7], Thomas G Graeber[3,4,8–10] & Robert L Modlin[2,5]

Leprosy provides a model to investigate mechanisms of immune regulation in humans, given that the disease forms a spectrum of clinical presentations that correlate with host immune responses. Here we identified 13 miRNAs that were differentially expressed in the lesions of subjects with progressive lepromatous (L-lep) versus the self-limited tuberculoid (T-lep) disease. Bioinformatic analysis revealed a significant enrichment of L-lep–specific miRNAs that preferentially target key immune genes downregulated in L-lep versus T-lep lesions. The most differentially expressed miRNA in L-lep lesions, hsa-mir-21, was upregulated in *Mycobacterium leprae*–infected monocytes. By directly downregulating Toll-like receptor 2/1 heterodimer (TLR2/1)-induced *CYP27B1* and *IL1B* expression as well as indirectly upregulating interleukin-10 (IL-10), hsa-mir-21 inhibited expression of the genes encoding two vitamin D–dependent antimicrobial peptides, *CAMP* and *DEFB4A*. Conversely, knockdown of hsa-mir-21 in *M. leprae*–infected monocytes enhanced expression of *CAMP* and *DEFB4A* and restored TLR2/1-mediated antimicrobial activity against *M. leprae*. Therefore, the ability of *M. leprae* to upregulate hsa-mir-21 targets multiple genes associated with the immunologically localized disease form, providing an effective mechanism to escape from the vitamin D–dependent antimicrobial pathway.

Interactions between the host immune response and the invading pathogen at the site of disease are crucial to the outcome of the infection. Leprosy, caused by the intracellular bacterium *M. leprae*, provides an extraordinary model for studying host-pathogen interactions in humans because the disease presents as a spectrum in which the clinical manifestations correlate with the level of immune response to the pathogen[1]. This allows for the investigation of the factors that contribute to the balance between host defense, persistence and pathogenesis at the site of disease in humans. At one end of the spectrum, in T-lep, the infection is self-limited, and skin lesions are typified by an adaptive immune response characterized by T helper type 1 (T_H1) cytokines[2,3] and an innate immune response characterized by macrophages programmed to express the vitamin D–mediated antimicrobial pathway[4]. At the other end of the spectrum, in L-lep, the infection is disseminated with lesions typified by an adaptive immune response characterized by T_H2 cytokines[2,3] and an innate immune response characterized by macrophages programmed to express a phagocytic activity[4]. To gain insight into the mechanisms that regulate host defense versus persistence in human infectious disease, we investigated miRNA expression in leprosy skin lesions.

RESULTS

Gene and miRNA profile in leprosy

The mRNA and miRNA expression profiles in skin lesions were determined in biopsy specimens from six individuals with T-lep and five individuals with L-lep collected at the time of diagnosis and classified according to the clinical and histopathological criteria of Ridley[1] (**Supplementary Fig. 1**). Unsupervised hierarchal clustering analysis of the mRNA profiles revealed two major groups in which the L-lep and T-lep samples were segregated (**Supplementary Fig. 2**). In contrast, hierarchal clustering analysis of the miRNA profiles performed on the same samples indicated two major miRNA patterns, with each group containing a mixture of both L-lep and T-lep samples (**Supplementary Fig. 2**). These results indicate that the principal component of the measured miRNA expression patterns in leprosy did not differentiate the lesion types.

To identify lesion-specific differences, we used a supervised approach. Differentially expressed miRNAs between the two clinical groups were identified by ranking miRNAs probes according to statistical significance (*t* test) and limited to sequences present in the miRBase database (version 14). There was a fivefold higher number

[1]Orthopaedic Hospital Research Center, University of California–Los Angeles, Los Angeles, California, USA. [2]Division of Dermatology, Department of Medicine, David Geffen School of Medicine, University of California–Los Angeles, Los Angeles, California, USA. [3]Crump Institute for Molecular Imaging, University of California–Los Angeles, Los Angeles, California, USA. [4]Department of Molecular and Medical Pharmacology, University of California–Los Angeles, Los Angeles, California, USA. [5]Department of Microbiology, Immunology and Molecular Genetics, University of California–Los Angeles, Los Angeles, California, USA. [6]Department of Dermatology, University of Southern California School of Medicine, Los Angeles, California, USA. [7]Leprosy Laboratory Institute Oswaldo Cruz, Rio de Janeiro, Brazil. [8]Institute for Molecular Medicine, University of California–Los Angeles, Los Angeles, California, USA. [9]Jonsson Comprehensive Cancer Center, University of California–Los Angeles, Los Angeles, California, USA. [10]California NanoSystems Institute, University of California–Los Angeles, Los Angeles, California, USA. Correspondence should be addressed to P.T.L. (ptliu@mednet.ucla.edu).

Received 29 December 2010; accepted 26 October 2011; published online 29 January 2012; doi:10.1038/nm.2584

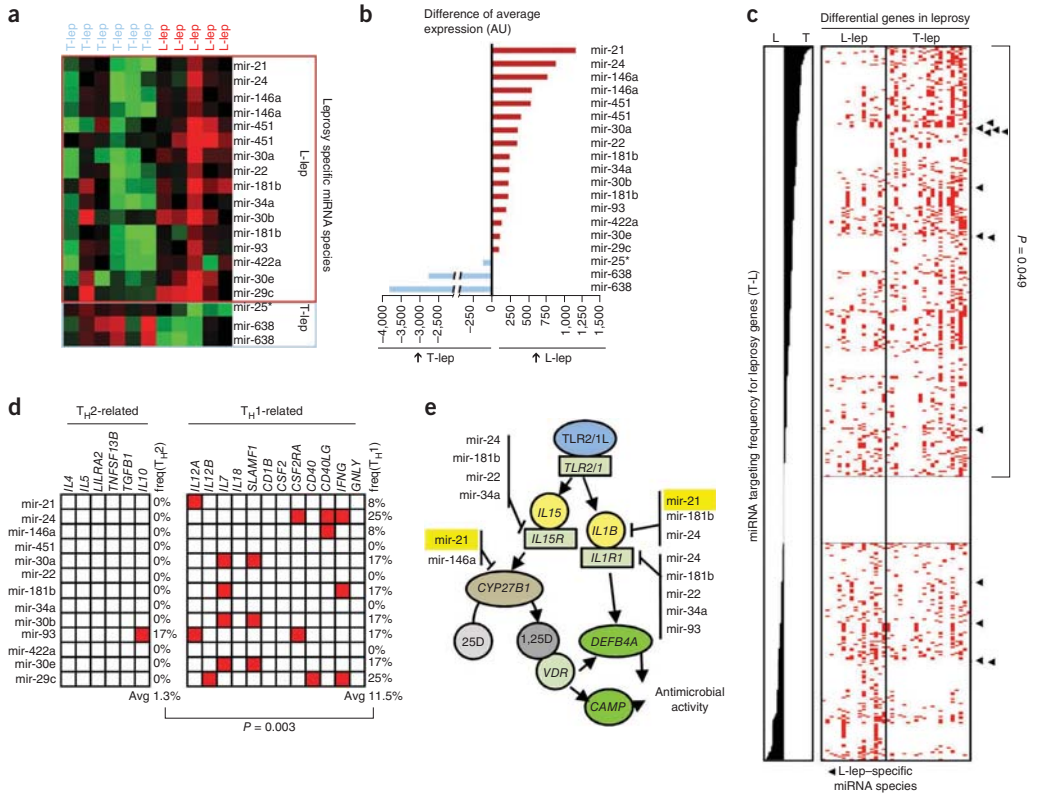

Figure 1 MiRNA expression and targeting profile in leprosy. (**a**,**b**) MiRNA probes that are differentially expressed between T-lep and L-lep lesions, depicted as normalized data (**a**) and raw expression values (**b**). AU, arbitrary units. (**c**) All miRNA species represented on the microarray platform ranged by targeting preference score. Arrowheads indicate L-lep–specific miRNA species. (**d**) Targeting preference of the L-lep– or T-lep–specific miRNA species for T_H2- or T_H1-related genes. Red boxes represent a predicted target site within the 3′ UTR of the indicated gene. (**e**) L-lep–specific miRNA species and predicted targeting of genes in the TLR2/1L-induced vitamin D–dependent antimicrobial pathway.

of differentially expressed miRNAs in the L-lep samples (16 probes representing 13 annotated miRNA species) versus the T-lep samples (three probes representing two unique miRNA species) (**Fig. 1a**). To compare the magnitude of differential expression between these miRNA species, we compared the un-normalized intensity values of the probes. The difference in intensity of the hsa-mir-21 probe was the greatest among the miRNA species differentially upregulated in L-lep versus T-lep lesions (**Fig. 1b**).

Targeting of immune genes by leprosy-specific miRNAs

Because the differentially expressed miRNA species were predominantly enriched in L-lep lesions, we hypothesized that regulation of miRNA expression at the site of the progressive disease inhibits expression of genes involved in host defense against the pathogen. We tested this hypothesis by integrating a prediction algorithm for miRNA binding sites in the 3′ untranslated regions (3′ UTRs) of mRNA species within curated sets of host immune response signature genes known to be differentially expressed in leprosy lesions, including T_H1- versus T_H2-related genes as well as the genes of the vitamin D pathway (**Supplementary Note**). All miRNA species represented on the microarray platform were ranked by their 'targeting preference score', calculated as the difference in frequency for targeting of the T-lep compared to L-lep signature genes (**Supplementary Fig. 3** and **Supplementary Note**). We next evaluated the enrichment of leprosy-disease-type–specific miRNA species by the Kolmogorov-Smirnov–based permutation test. On the basis of this analysis, we found the L-lep–specific miRNA species to be significantly associated with the miRNAs most strongly predicted to preferentially target T-lep signature genes ($P = 0.049$; **Fig. 1c**). Thus, L-lep–specific miRNAs may be a mechanism for the *M. leprae*–induced downregulation of T-lep host immune response signature genes in L-lep lesions.

In relation to the local immune response, the L-lep–specific set of miRNA species were predicted to have binding sites in the 3′ UTRs of T_H1-related signature genes, known to be differentially expressed in T-lep versus L-lep lesions, with an average targeting frequency of 11.5%. In contrast, the L-lep–specific set of miRNAs species showed a significantly ($P = 0.0003$) lower targeting frequency for T_H2-related genes, known to be differentially expressed in L-lep versus T-lep

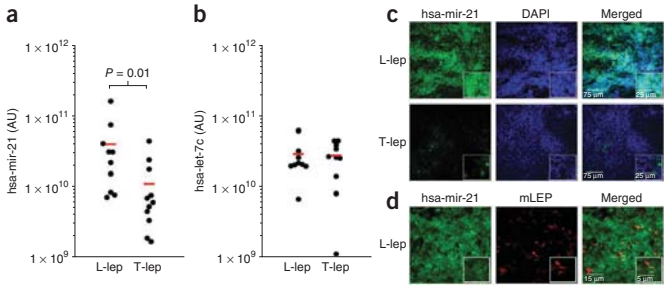

Figure 2 Expression of hsa-mir-21 in leprosy. (**a**,**b**) Expression levels of hsa-mir-21 (**a**) and hsa-let-7c (**b**) comparing L-lep versus T-lep lesions by qPCR. The levels of hsa-mir-21 and hsa-let-7c are normalized to 36B4 levels in the same tissue and depicted as values from individual lesions (filled circles) as well as the average (horizontal bars) of 10 L-lep lesions and 11 T-lep lesions. (**c**) Skin biopsy sections from subjects with L-lep or T-lep probed with a hsa-mir-21–specific oligomer using FISH. Cellular nuclei were visualized using DAPI. Data are representative experiment of four individual L-lep samples and three individual T-lep samples. (**d**) Skin biopsy section derived from subjects with L-lep and probed for hsa-mir-21 and *M. leprae* using FISH in conjunction with a monoclonal antibody specific for *M. leprae*, detected by confocal microscopy. The images are representative of three individual subjects.

lesions, with an average targeting frequency of 1.3% (**Fig. 1d**). Notably, multiple L-lep–specific miRNA species targeted two key genes in the vitamin D–dependent antimicrobial pathway, encoding cytochrome P450, family 27, subfamily B, polypeptide 1 (*CYP27B1*) and IL-1β (*IL1B*), but not the genes encoding the antimicrobial peptides induced by this pathway, cathelicidin (LL-37, encoded by *CAMP*) and defensin β4A (*DEFB4A*)[5,6] (**Fig. 1e**). Taken together, these results indicate that the L-lep–specific miRNAs target and potentially downregulate host defense genes in leprosy.

Regulation of hsa-mir-21 in leprosy

We verified the tissue expression of the most differentially expressed miRNA, hsa-mir-21, in L-lep lesions by real-time PCR (qPCR) and fluorescent *in situ* hybridization (FISH) in additional leprosy tissue sections. By qPCR, hsa-mir-21 levels were significantly higher (3.5-fold, $P = 0.01$) in 10 L-lep versus 11 T-lep lesions (**Fig. 2a**). An unrelated miRNA, hsa-let-7c, that was not differentially expressed in disease lesions by microarray analysis, was expressed at similar levels between the L-lep and T-lep lesions (**Fig. 2b**). Although the skin biopsies are composed predominately of granulomas in the dermis, we could not rule out that the differential expression of hsa-mir-21 came from nonimmune cells. Therefore, using FISH we determined that the frequency of hsa-mir-21–positive cells in the granulomatous regions was 25-fold higher in the L-lep lesions versus the T-lep lesions (98% versus 4% of nucleated cells, $P = 0.001$) (**Fig. 2c**). In the L-lep lesions, the hsa-mir-21–positive cells were located within the granulomas, in the same microanatomic locations as *M. leprae* (**Fig. 2d**). It was not possible to determine the frequency of cells expressing hsa-mir-21 and containing *M. leprae*, as these are found in distinct subcellular compartments: microRNAs are located in the cytoplasm and the pathogen resides within phagosomes. We used a scrambled probe as a negative control to demonstrate the absence of nonspecific binding in either lesion type (**Supplementary Fig. 4a**), and a positive control probe for the U6 noncoding small nuclear RNA showed equivalent RNA integrity (**Supplementary Fig. 4b**). Taken together, these three approaches, microarray, qPCR and FISH, provide evidence for the differential expression of hsa-mir-21 in L-lep versus T-lep lesions.

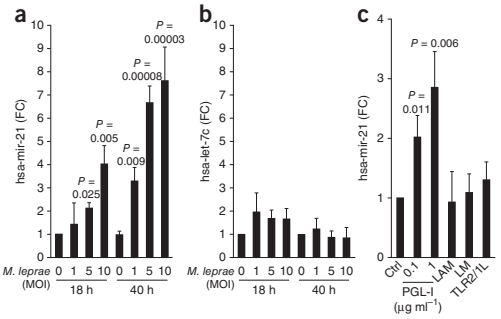

Figure 3 Regulation of hsa-mir-21 levels in primary human monocytes by *M. leprae*. (**a**,**b**) Levels of hsa-mir-21 (**a**) and hsa-let-7c (**b**) in primary human monocytes infected with *M. leprae* at an MOI of 0, 1, 5 or 10 for 18 h and 40 h. Data are mean fold change (FC) compared to no-infection control ± s.e.m., $n = 3$–5. (**c**) Levels of hsa-mir-21 in primary human monocytes after treatment with PGL-I, LAM (10 μg ml^{-1}), LM (10 μg ml^{-1}) or TLR2/1L for 18 h. Data are mean fold change compared to the vehicle control–treated cells ± s.e.m., $n = 3$–10.

Given that we identified both *M. leprae* and hsa-mir-21 in the granulomas, we hypothesized that *M. leprae* induced hsa-mir-21 expression in monocytes and macrophages, the predominant cell type in a granuloma and the primary cell type infected by *M. leprae*. We infected human peripheral blood monocytes with live *M. leprae* at different multiplicities of infection (MOIs) for 18 and 40 h and measured hsa-mir-21 levels by qPCR. We efficiently infected monocytes with *M. leprae* (**Supplementary Fig. 5**), which triggered an upregulation of hsa-mir-21 in a dose-dependent and time-responsive manner, with a 4.1-fold change ($P = 0.005$) at 18 h and 7.6-fold change ($P = 0.00003$) at 40 h, both at an MOI of 10 (**Fig. 3a**). In contrast, *M. leprae* infection of monocytes did not result in detectable upregulation of hsa-let-7c (**Fig. 3b**).

To explore the mechanism by which *M. leprae* infection induces hsa-mir-21, we compared the ability of several key cell wall biomolecules to trigger hsa-mir-21 expression. Treatment of monocytes with phenolic glycolipid-I (PGL-I) induced a 2.9-fold increase in hsa-mir-21 expression, whereas the *M. leprae* lipoarabinomman (LAM) and lipomannan (LM), as well as a synthetic triacylated lipopeptide (a TLR2/1 ligand, TLR2/1L), did not significantly induce hsa-mir-21 (**Fig. 3c**). Together, these data indicate that hsa-mir-21 is present at the site of disease in leprosy, is associated with the progressive and disseminated form (L-lep) of the disease, is specifically induced in monocytes by *M. leprae* infection and is triggered by an *M. leprae*–specific glycolipid, PGL-I. It is therefore likely that *M. leprae* infection of macrophages induces the upregulation of hsa-mir-21 at the site of infection.

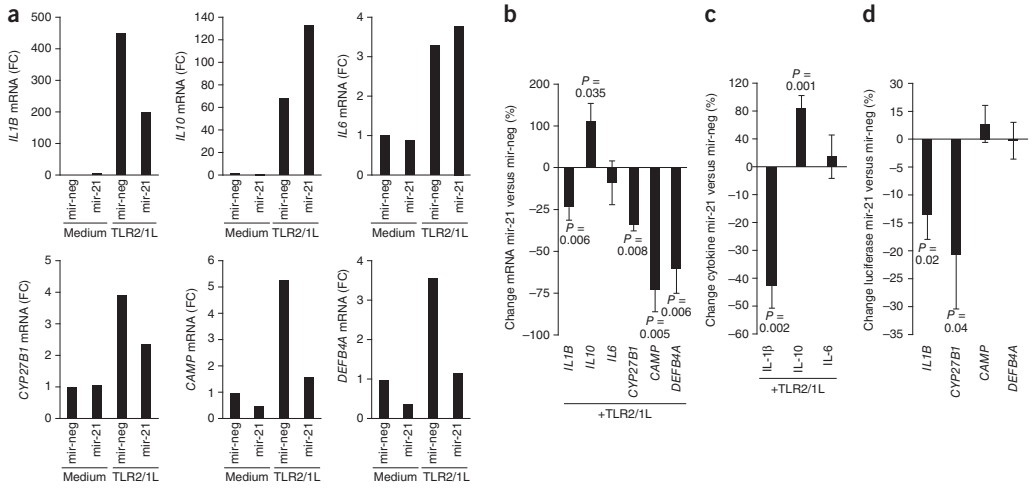

Figure 4 The ability of hsa-mir-21 to regulate the innate immune response in human monocytes. Primary human monocytes were transfected with the mature hsa-mir-21 (mir-21) oligomer or a nontargeting control (mir-neg) then treated with TLR2/1L for 18 h and 24 h. (**a**) Gene expression of *IL1B* at 18 h, *IL10* at 24 h, *IL6* at 16 h, *CYP27B1* at 16 h, *CAMP* at 24 h and *DEFB4A* at 24 h, as evaluated by qPCR. Data shown are representative experiments from more than five individual donors. (**b**) Change in gene expression comparing mir-21– to mir-neg–transfected cells after TLR2/1L simulation. Data are average percentage change mir-21 versus mir-neg ± s.e.m., $n = 3$–11. (**c**) Change in cytokine protein levels in culture supernatants comparing mir-21– to mir-neg–transfected cells after TLR2/1L stimulation. Data are average percentage change mir-21 versus mir-neg ± s.e.m., $n = 4$–6. Representative experiment is shown in **Supplementary Figure 6**. (**d**) Change in luciferase activity of cells co-transfected with a 3′ UTR luciferase reporter construct (*IL1B, CYP27B1, CAMP* or *DEFB4A*) and either mir-21 or mir-neg. Data are mean percentage change of each individual 3′ UTR construct comparing mir-21 versus mir-neg ± s.e.m., $n = 4$–6. Representative experiment is shown in **Supplementary Figure 8**.

Regulation of the vitamin D pathway by hsa-mir-21

It was noteworthy that of all the L-lep–specific miRNAs, only hsa-mir-21 had the potential to target both *IL1B* and *CYP27B1* (**Fig. 1e**), which are both required for TLR-induced, vitamin D–dependent expression of *CAMP* and *DEFB4A*[5,6]. We investigated the ability of hsa-mir-21 to regulate the expression of these antimicrobial genes by transfecting primary human monocytes with either the mature hsa-mir-21 oligomer or a nontargeting control oligomer, followed by activation with TLR2/1L. To determine the transfection efficiency of the miRNA oligomers into primary monocytes, we used a fluorescently tagged nontargeting control oligomer, which showed that 71% ($P = 0.002$) of the monocytes were miRNA positive (**Supplementary Fig. 6**). As a control for targeting specificity, we determined that overexpression of hsa-mir-21 downregulated interferon-γ–induced *IL12A* mRNA, a previously described direct target[7] (**Supplementary Fig. 7**). The presence of hsa-mir-21 during TLR2/1L activation of monocytes resulted in the downregulation of *IL1B* mRNA by 24% ($P = 0.006$, representative experiment in **Fig. 4a** and averaged in **Fig. 4b**). Despite the absence of predicted hsa-mir-21 target sites in the 3′ UTR of *IL10*, transfection of hsa-mir-21 enhanced TLR2/1-induced *IL10* mRNA levels by 110% ($P = 0.035$, **Fig. 4a**,**c**), consistent with studies in mouse cells[8]. In contrast, *IL6* mRNA, another cytokine without hsa-mir-21 target sequences, was not affected (**Fig. 4a**,**c**). TLR2/1-induced IL-1β secretion was reduced by 45% ($P = 0.003$), IL-10 release was enhanced by 85% ($P = 0.001$) and IL-6 levels did not change (representative experiment in **Supplementary Fig. 8** and averaged in **Fig. 4c**). Therefore, the effects of hsa-mir-21 on TLR2/1-induced cytokine mRNAs and secreted proteins were consistent.

Transfection of hsa-mir-21 also resulted in a 34% decrease in TLR-induced expression of CYP27B1 mRNA ($P = 0.008$, **Fig. 4a**,**b**). Given that hsa-mir-21 downregulated TLR2/1-induced IL-1β and CYP27B1 mRNA expression, we examined the effect of hsa-mir-21 on TLR2/1-induced antimicrobial peptide gene expression. Notably, TLR2/1 induction of *CAMP* and *DEFB4A* mRNAs was significantly inhibited by transfection of hsa-mir-21, by 73% ($P = 0.005$) and 60% ($P = 0.006$), respectively (**Fig. 4a**,**b**). Given that hsa-mir-21 upregulated IL-10, we investigated the effect of recombinant IL-10 on TLR2/1-induced gene expression. The addition of rIL-10 inhibited TLR2/1-induced mRNA expression of *CAMP* by 26% and *DEFB4A* by 35%, whereas the inhibition of *IL12B* was 76% (**Supplementary Fig. 9a**,**b**). Therefore, hsa-mir-21–mediated enhancement of IL-10 induction may partially contribute to the inhibition of antimicrobial gene expression.

We assessed whether hsa-mir-21 directly binds the TLR2/1-induced, vitamin D–dependent antimicrobial pathway genes with a 3′ UTR reporter assay. hsa-mir-21 directly bound the 3′ UTRs of both *CYP27B1* and *IL1B* but did not bind the 3′ UTRs of either *CAMP* or *DEFB4A* (**Fig. 4d**, **Supplementary Fig. 10** and **Supplementary Note**). These data indicate that hsa-mir-21 inhibits TLR2/1-mediated *CAMP* and *DEFB4A* expression directly by regulating key epigenetic targets including *CYP27B1* and *IL1B* and indirectly through induction of the immunomodulatory cytokine IL-10.

Role of hsa-mir-21 in the response to infection

Given the ability of hsa-mir-21 to downregulate key genes in the TLR2/1-induced antimicrobial pathway, and the observation that *M. leprae* induces hsa-mir-21 in monocytes, we investigated whether hsa-mir-21 contributes to inhibition of the innate immune response during *M. leprae* infection. We transfected monocytes with an hsa-mir-21–specific antisense oligomer (anti–mir-21), infected the transfected

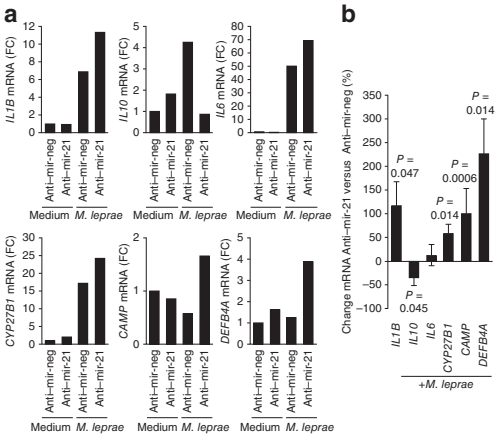

Figure 5 Role of hsa-mir-21 expression during *M. leprae* infection. Primary human monocytes were transfected with the antagomir against hsa-mir-21 (anti–mir-21) oligomer or a nonspecific control (anti–mir-neg) then infected with live *M. leprae* at an MOI of 10 for 18 h. Gene expression of *IL1B*, *IL10*, *IL6*, *CYP27B1*, *CAMP* and *DEFB4A* was evaluated by qPCR. (**a**) Representative experiments from more than four individual donors. (**b**) Change in gene expression comparing anti–mir-21– to anti–mir-neg–transfected cells following *M. leprae* infection for 18 h. Data are average percentage change anti–mir-21 versus anti–mir-neg ± s.e.m., $n = 4$–8.

monocytes with live *M. leprae*[9] for 18 h and then measured mRNA expression. The presence of anti–mir-21 (versus a control oligomer (anti–mir-neg), followed by *M. leprae* infection, resulted in a significant reduction of hsa-mir-21 levels by 70% ($P = 0.00002$, **Supplementary Fig. 11a**,**c**). Consistent with the hsa-mir-21 overexpression experiment, anti–mir-21 enhanced *IL12A* mRNA expression in the *M. leprae*–infected monocytes ($P = 0.006$, **Supplementary Fig. 11b**,**c**).

Relevant to the vitamin D–dependent innate immune pathway, anti–mir-21 increased *IL1B* mRNA expression in the *M. leprae*–infected monocytes by 118% ($P = 0.047$, **Fig. 5a**,**b**). In contrast, *IL10* mRNA was downregulated by 34% ($P = 0.045$), and there was no significant change in *IL6* mRNA levels (**Fig. 5a**,**b**). Notably, knockdown of hsa-mir-21 resulted in a significant increase in mRNA levels of *CYP27B1* (59%, $P = 0.014$), *CAMP* (100%, $P = 0.0006$) and *DEFB4A* (227%, $P = 0.014$) (**Fig. 5a**,**b**). These results provide evidence that monocytes and macrophages can detect *M. leprae* infection and trigger the vitamin D–dependent antimicrobial pathway; however, this response is inhibited by the pathogen's upregulation of hsa-mir-21.

Effects of hsa-mir-21 on innate antimicrobial activity

We investigated the role of hsa-mir-21 in regulating the TLR2/1-induced macrophage antimicrobial activity by overexpressing hsa-mir-21 during *Mycobacterium tuberculosis* infection. For these experiments, we used the avirulent *M. tuberculosis* H37Ra strain, as it does not contain a PGL-I homolog and failed to induce expression of hsa-mir-21 in monocytes upon infection (**Supplementary Fig. 12a**), despite induction of *IL6* mRNA in the same cells (**Supplementary Fig. 12b**). We transfected monocytes with hsa-mir-21 or a control oligomer, infected them with *M. tuberculosis* H37Ra overnight, subsequently treated them with TLR2/1L for 3 d and assessed bacterial viability by qPCR according to the ratio of 16S RNA to the IS6110 genomic repeat element DNA[10]. TLR2/1L induced an antimicrobial activity against *M. tuberculosis* in monocytes transfected with a control oligomer (**Fig. 6a**), at a level consistent with previous studies using the standard colony-forming unit assay (**Supplementary Note**)[6]. However, overexpression of hsa-mir-21 blocked the antimicrobial response and resulted in an increase in *M. tuberculosis* viability in TLR2/1L-activated cells (**Fig. 6a**). Also, in unstimulated cells, hsa-mir-21 increased bacterial viability. Overall, *M. tuberculosis* viability in TLR2/1L-treated as compared to control monocytes was significantly higher in the presence of hsa-mir-21 ($P = 0.01$, **Fig. 6b**).

To address the role of *M. leprae*–induced hsa-mir-21 in regulation of TLR2/1-induced antimicrobial activity, monocytes were transfected with anti–mir-21 or anti–mir-neg, then infected with live *M. leprae*. The transfected and infected cells were treated with the TLR2/1L for 3 d and antimicrobial activity assessed by qPCR by measuring the ratio of 16S RNA to RLEP DNA[10]. In anti–mir-neg transfected cells, TLR2/1-activation increased bacterial viability, consistent with previous findings indicating enhanced *M. tuberculosis* growth in TLR2/1-stimulated cells in the absence of *CAMP* and *DEFB4A*[6]. Strikingly, in anti–mir-21 transfected monocytes, TLR2/1-activation resulted in decreased bacterial viability (**Fig. 6c**). The anti–mir-21 oligomer had no effect on *M. leprae* viability in unstimulated monocytes (**Fig. 6c**).

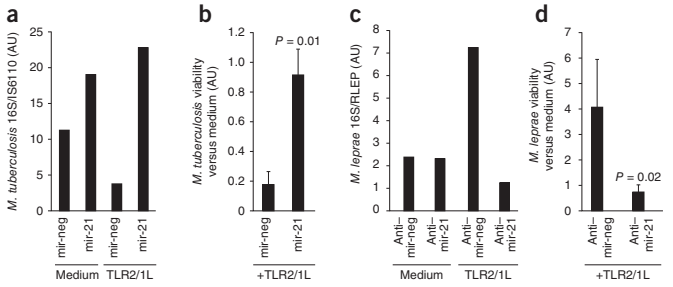

Figure 6 Role of hsa-mir-21 in TLR2/1-mediated antimicrobial activity. Primary human monocytes were transfected with the mature hsa-mir-21 (mir-21) oligomer or a nontargeting control (mir-neg) and then infected with live *M. tuberculosis* H37Ra at an MOI of 0.5 for 18 h. The monocytes were then treated with TLR2/1L (10 μg ml^{-1}) for 3 d. Levels of 16S rRNA and IS6110 DNA were assessed by qPCR. (**a**) The ratio of 16S rRNA to IS6110 DNA levels as a representative experiment from three donors. (**b**) Fold change in *M. tuberculosis* viability comparing TLR2/1L- versus medium-treated monocytes. Data are the mean fold change ± s.e.m., $n = 3$. Primary human monocytes were transfected with the antagomir against hsa-mir-21 (anti–mir-21) oligomer or a nonspecific control (anti–mir-neg) and then infected with live *M. leprae* at an MOI of 10 for 18 h. The monocytes were then treated with the TLR2/1L (10 μg ml^{-1}) for 3 d. Levels of 16S rRNA and RLEP DNA were assessed by qPCR. (**c**) Data are the ratio of 16S rRNA to RLEP DNA levels as a representative experiment from five donors. (**d**) Fold change in *M. leprae* viability comparing TLR2/1L– versus medium-treated monocytes. Data are the mean fold change ± s.e.m., $n = 5$.

In five donors tested, *M. leprae* viability in TLR2/1-stimulated cells was significantly lower in the presence of anti–mir-21 ($P = 0.02$, **Fig. 6d**). Together, the data from these infection experiments demonstrate the biologic relevance of hsa-mir-21 in innate host defense: the expression of hsa-mir-21 is sufficient to block TLR2/1-induced antimicrobial responses and the silencing of hsa-mir-21 induction restores TLR2/1-mediated antimicrobial activity.

DISCUSSION

Host-pathogen interactions determine the outcome of the immune response to microbial infection. Our data provide evidence that the human pathogen *M. leprae* regulates the miRNA profile at the site of infection in humans with leprosy and interferes with the host antimicrobial response. We used a unique bioinformatic strategy, combining an enrichment analysis of leprosy-disease-type–specific miRNA species ranked by 3′ UTR mRNA targeting preference and evaluated by the Kolmogorov-Smirnov-based permutation test. Together, these analyses led to the identification of hsa-mir-21 as differentially expressed in the progressive L-lep form of leprosy, with the potential to target genes in the vitamin D antimicrobial pathway. Infection of human monocytes with live *M. leprae,* or treatment with the mycobacterial virulence factor PGL-I, induced expression of hsa-mir-21. Next, we showed that hsa-mir-21 functionally downregulates the TLR2/1-induced vitamin D antimicrobial pathway by directly targeting *CYP27B1* and *IL1B* and indirectly inducing IL-10, all leading to the inhibition of the antimicrobial peptides *CAMP* and *DEFB4A*. Silencing of hsa-mir-21 during *M. leprae* infection led to the enhanced expression of vitamin D pathway genes. Finally, introduction of hsa-mir-21 into monocytes was sufficient to block TLR2/1-induced antimicrobial activity against *M. tuberculosis*, and the silencing of hsa-mir-21 induction restored TLR2/1-mediated antimicrobial activity against *M. leprae.* Therefore, these data identify an evasion strategy in which a microbial pathogen regulates the host miRNA profile at the site of infection to inhibit the antimicrobial response.

Although *M. leprae* was the first human pathogen discovered[11], it still cannot be grown in the laboratory, providing a major obstacle to investigation of the immunology of leprosy. To our knowledge, it has not been possible to demonstrate immune-mediated antimicrobial activity against *M. leprae* in primary human cells[12]. A previous comparison of antimicrobial responses in mouse and human macrophages demonstrated that the combination of lipopolysaccharide and interferon-γ reduced the viability of intracellular *M. leprae* in mouse but not human macrophages[12]. Here we successfully demonstrate that immune activation of *M. leprae*–infected human monocytes decreases bacterial viability, finding that TLR2/1 activation induced a fourfold reduction in *M. leprae* viability only when hsa-mir-21 was silenced. In addition, overexpression of hsa-mir-21 blocked the TLR2/1-induced antimicrobial activity against *M. tuberculosis*, resulting in a fivefold increase in bacterial viability. Taken together, these data indicate the biological relevance of hsa-mir-21 in the host antimicrobial response.

We gained insight into the mechanism by which *M. leprae* induces a specific miRNA immune regulatory profile at the site of infection by finding that hsa-mir-21 was induced in monocytes after *M. leprae* infection or by treatment with *M. leprae*–derived PGL-I. Previously, PGL-I has been shown to inhibit monocyte responses[13,14], as well as associate with mycobacterial virulence[15]. Further studies are needed to elucidate the mechanism of induction and functional role of those miRNAs differentially expressed in L-lep lesions. Given that the degree of genetic diversity in *M. leprae* clinical isolates is not as broad as compared with other human pathogens[16], it is not likely that species subtypes differentially induce single miRNAs, as has been shown for *Francisella tularensis*[17]. To complement the study of miRNA profiles in disease lesions as shown here, additional insight can be obtained by profiling the miRNAs induced by a pathogen in an isolated cell type[18]. It should be possible to learn whether the ability of a pathogen to induce a single miRNA or set of miRNA species that targets and inhibits host immune responses provides a potential virulence mechanism that contributes to the pathogenesis of infectious disease[19].

Our data demonstrate that a single miRNA species, by both directly and indirectly regulating immune modulatory genes, can affect the downstream effectors of an innate immune–triggered antimicrobial pathway. Specifically, hsa-mir-21 inhibited TLR2/1-induced *CYP27B1* and *IL1B* gene expression and enhanced IL-10 expression, thereby preventing upregulation of the *CAMP* and *DEFB4* mRNAs, which encode antimicrobial peptides. These factors are all key to the outcome of the vitamin D antimicrobial pathway: (i) CYP27b1 converts vitamin D from an inactive to active state, leading to antimicrobial activity, (ii) IL-1β is required for DEFB4 induction and (iii) IL-10 is known to inhibit TLR-induced responses[20]. Consequently, hsa-mir-21 inhibits the innate immune response by its distinct gene regulatory activities: the indirect upregulation of an immunosuppressive cytokine and direct targeting of epigenetic components required for the TLR-induced, vitamin D–dependent antimicrobial pathway[5,6]. Consistent with this model, the genes directly targeted by hsa-mir-21, *CYP27B1* and *IL1B*, are downregulated in L-lep versus T-lep lesions[2,4]. Although the relationship between expression of miRNAs and gene targets in disease lesions is correlative, the demonstration that hsa-mir-21 is induced in human primary monocytes 18 h after *M. leprae* infection and its effect on the TLR-induced antimicrobial response suggest a role in disease pathogenesis. Our investigation of the effect of a single miRNA in leprosy provides a framework for analyzing the set of miRNAs that are differentially expressed at the site of disease to determine their cumulative role in regulating the host immune response, including autophagy and antimicrobial pathways.

The ability of anti–mir-21 to enhance the vitamin D–dependent antimicrobial pathway provides a potential therapeutic strategy to intervene in human infectious disease. In leprosy, the vitamin D antimicrobial pathway may contribute to disease outcome, on the basis of the preferential expression of antimicrobial pathway genes in the T-lep versus L-lep form[4], the correlation of the vitamin D receptor single-nucleotide polymorphism in humans with L-lep[21] and the reported successful use of vitamin D as a therapeutic adjuvant in the treatment of leprosy[22]. Potentially, the combination of vitamin D supplementation with targeted miRNA therapy could provide an optimal treatment approach to leprosy and other chronic infectious diseases in which the cellular immune response is dysregulated. This type of approach may be particularly worth exploring in the clinical setting of drug-resistant pathogens, including multi-drug-resistant, extremely drug-resistant and totally drug-resistant tuberculosis, in which antimicrobial therapy is losing its effectiveness. Finally, our findings may be relevant to other diseases, including infectious[23,24], autoimmune[25] and neoplastic[26,27] diseases in which vitamin D sufficiency has been shown to be required for optimal host immunity.

METHODS

Methods and any associated references are available in the online version of the paper at http://www.nature.com/naturemedicine/.

Accession codes. Accession numbers for genes, miRNAs, mRNA arrays and miRNA arrays are provided in **Supplementary Table 1**.

Note: Supplementary information is available on the Nature Medicine website.

ACKNOWLEDGMENTS

We would like to thank G. Cheng, R. O'Connell, J. Krahenbuhl, R. Lahiri and B. Bloom for their helpful discussions. The live *M. leprae* was provided by the US National Hansen's Disease Programs through the generous support of the American Leprosy Missions and Society of St. Lazarus of Jerusalem. This work was supported by US National Institutes of Health grants AI 022553, AI 047868, AR 040312 and AI 073539. P.T.L. is supported by US National Institutes of Health K22 Career Development Award AI 85025. K.E. is supported by a postdoctoral grant from the Wenner-Gren Foundations (Sweden). We would like to thank M. Schibler and the University of California–Los Angeles, California NanoSystems Institute, Advanced Light Microscopy Core Facility for their assistance with the confocal studies.

AUTHOR CONTRIBUTIONS

P.T.L. performed the experiments, supervised the project, analyzed the data and wrote the manuscript. M.W. performed the *in situ* hybridization experiments and a portion of the *M. leprae* infection, antimicrobial and monocyte transfection experiments. R.T. performed the microarray experiments. E.K. performed the bioinformatics analysis of the microarray data. K.E. performed the IL-10–related experiments. B.F. performed a portion of the *M. leprae* infection, antimicrobial and monocyte transfection experiments. M.D.M. performed a portion of the *M. leprae* infection and ligands experiments. A.V. performed a portion of the monocyte transfection experiments. T.H.R. and E.N.S. diagnosed patients with leprosy collected skin biopsy specimens. T.G.G. designed, supervised and performed bioinformatics analysis. R.L.M. supervised the project and wrote the manuscript.

COMPETING FINANCIAL INTERESTS

The authors declare no competing financial interests.

Published online at http://www.nature.com/naturemedicine/.
Reprints and permissions information is available online at http://www.nature.com/reprints/index.html.

1. Ridley, D.S. & Jopling, W.H. Classification of leprosy according to immunity. A five-group system. *Int. J. Lepr. Other Mycobact. Dis.* **34**, 255–273 (1966).
2. Yamamura, M. *et al.* Defining protective responses to pathogens: cytokine profiles in leprosy lesions. *Science* **254**, 277–279 (1991).
3. Salgame, P. *et al.* Differing lymphokine profiles of functional subsets of human CD4 and CD8 T cell clones. *Science* **254**, 279–282 (1991).
4. Montoya, D. *et al.* Divergence of macrophage phagocytic and antimicrobial programs in leprosy. *Cell Host Microbe* **6**, 343–353 (2009).
5. Liu, P.T. *et al.* Toll-like receptor triggering of a vitamin D–mediated human antimicrobial response. *Science* **311**, 1770–1773 (2006).
6. Liu, P.T. *et al.* Convergence of IL-1β and VDR activation pathways in human TLR2/1-induced antimicrobial responses. *PLoS ONE* **4**, e5810 (2009).
7. Lu, T.X., Munitz, A. & Rothenberg, M.E. MicroRNA-21 is up-regulated in allergic airway inflammation and regulates IL-12p35 expression. *J. Immunol.* **182**, 4994–5002 (2009).
8. Sheedy, F.J. *et al.* Negative regulation of TLR4 via targeting of the proinflammatory tumor suppressor PDCD4 by the microRNA miR-21. *Nat. Immunol.* **11**, 141–147 (2010).
9. Adams, L.B. *et al.* The study of *Mycobacterium leprae* infection in interferon-γ gene–disrupted mice as a model to explore the immunopathologic spectrum of leprosy. *J. Infect. Dis.* **185** (suppl. 1), S1–S8 (2002).
10. Martinez, A.N. *et al.* Molecular determination of *Mycobacterium leprae* viability by use of real-time PCR. *J. Clin. Microbiol.* **47**, 2124–2130 (2009).
11. Hansen, G.A. Undwersogelser angaende spedalskhedens arsager. *Norsk. Mag. Laegevid* **4**, 1–88 (1874).
12. Peña, M.T. *et al.* Expression and characterization of recombinant interferon γ (IFN-γ) from the nine-banded armadillo (*Dasypus novemcinctus*) and its effect on *Mycobacterium leprae*–infected macrophages. *Cytokine* **43**, 124–131 (2008).
13. Vachula, M., Holzer, T.J. & Andersen, B.R. Suppression of monocyte oxidative response by phenolic glycolipid I of *Mycobacterium leprae*. *J. Immunol.* **142**, 1696–1701 (1989).
14. Neill, M.A. & Klebanoff, S.J. The effect of phenolic glycolipid-1 from *Mycobacterium leprae* on the antimicrobial activity of human macrophages. *J. Exp. Med.* **167**, 30–42 (1988).
15. Tabouret, G. *et al. Mycobacterium leprae* phenolglycolipid-1 expressed by engineered *M. bovis* BCG modulates early interaction with human phagocytes. *PLoS Pathog.* **6**, e1001159 (2010).
16. Clark-Curtiss, J.E. & Walsh, G.P. Conservation of genomic sequences among isolates of *Mycobacterium leprae*. *J. Bacteriol.* **171**, 4844–4851 (1989).
17. Cremer, T.J. *et al.* MiR-155 induction by *F. novicida* but not the virulent *F. tularensis* results in SHIP down-regulation and enhanced pro-inflammatory cytokine response. *PLoS ONE* **4**, e8508 (2009).
18. Liu, Z. *et al.* Up-regulated microRNA-146a negatively modulate *Helicobacter pylori*–induced inflammatory response in human gastric epithelial cells. *Microbes Infect.* **12**, 854–863 (2010).
19. Sinsimer, D. *et al. Mycobacterium leprae* actively modulates the cytokine response in naive human monocytes. *Infect. Immun.* **78**, 293–300 (2010).
20. Krutzik, S.R. *et al.* Activation and regulation of Toll-like receptors 2 and 1 in human leprosy. *Nat. Med.* **9**, 525–532 (2003).
21. Roy, S. *et al.* Association of vitamin D receptor genotype with leprosy type. *J. Infect. Dis.* **179**, 187–191 (1999).
22. Herrera, G. Vitamin D in massive doses as an adjuvant to the sulfones in the treatment of tuberculoid leprosy. *Int. J. Lepr.* **17**, 35–42 (1949).
23. Rook, G.A.W. The role of vitamin D in tuberculosis. *Am. Rev. Respir. Dis.* **138**, 768–770 (1988).
24. Crowle, A.J., Ross, E.J. & May, M.H. Inhibition by 1,25(OH)2-vitamin D3 of the multiplication of virulent tubercle bacilli in cultured human macrophages. *Infect. Immun.* **55**, 2945–2950 (1987).
25. Munger, K.L., Levin, L.I., Hollis, B.W., Howard, N.S. & Ascherio, A. Serum 25-hydroxyvitamin D levels and risk of multiple sclerosis. *J. Am. Med. Assoc.* **296**, 2832–2838 (2006).
26. Lappe, J.M., Travers-Gustafson, D., Davies, K.M., Recker, R.R. & Heaney, R.P. Vitamin D and calcium supplementation reduces cancer risk: results of a randomized trial. *Am. J. Clin. Nutr.* **85**, 1586–1591 (2007).
27. Ahn, J. *et al.* Vitamin D–related genes, serum vitamin D concentrations and prostate cancer risk. *Carcinogenesis* **30**, 769–776 (2009).

ONLINE METHODS

Statistical analyses. Percentage change due to miRNA or antagomir was analyzed against no change with an unpaired Student's *t* test. Gene or miRNA induction studies were analyzed with an unpaired Student's *t* test against the medium control of each experiment. L-lep–specific miRNA targeting of T_H1- and T_H2- related genes was analyzed with an unpaired Student's *t* test. The miRNA targeting preference was determined with the Kolmogorov-Smirnov–based permutation analysis as noted in the **Supplementary Note**. Error bars represent the s.e.m. between individual donor values.

Leprosy biopsy specimens. The acquisition of all specimens was approved by the Medical Investigational Review Board 1 (MIRB1) of the University of California–Los Angeles; more details can be found in the **Supplementary Methods**. Scalpel or punch skin biopsy specimens were obtained after informed consent from individuals with tuberculoid leprosy and individuals with lepromatous leprosy at the time of diagnosis; therefore, all samples are representative of untreated disease.

Microarray analysis. For gene and miRNA expression profiling, the RNA from skin biopsy specimens was processed and analyzed by the University of California–Los Angeles Clinical Microarray Core Facility using the Affymetrix U133 Genechip and Asuragen using the Discovarray platform, respectively. Additional details pertaining hierarchical clustering, cluster dendrograms and heat maps are included in the **Supplementary Methods**.

***In situ* hybridization.** Leprosy skin biopsy specimens were snap frozen and sectioned to a thickness of 10 μm and then mounted onto a glass slide. The protocol has been previously described[28] and adapted for current use. Briefly, biotinylated hsa-mir-21–specific, U6–specific and nonspecific control probes were purchased (Exiqon) and hybridized to the tissue at 0.1 pg μl^{-1} for 1–4 h, followed by incubation with Streptavidin–horseradish peroxidase. Then, the sections were incubated with the TSA Plus Fluorescein System (PerkinElmer) according to the manufacturer's instructions. A coverslip was sealed to the slides with ProLong Gold with DAPI (Invitrogen), left to dry at 4 °C in the dark overnight and imaged using a Leica FLIM confocal microscope (Leica).

Live *Mycobacterium leprae*. Live and viable *M. leprae* bacteria were generously donated by J.L. Krahenbuhl. Additional information is included in the **Supplementary Methods**.

Quantitative PCR. For miRNA analysis, qPCR was performed using the TaqMan MicroRNA Cells-to-CT kit in conjunction with the TaqMan MicroRNA Assay for hsa-mir-21 (Applied Biosystems) or the NCODE miRNA cDNA Synthesis and qPCR Kit (Invitrogen) according to the manufacturers' recommended conditions. For mRNA studies, total RNA was isolated from monocytes by TRIzol (Invitrogen), and cDNA libraries were made using the iScript cDNA synthesis kit (BioRAD). qPCR reactions were carried out using the iQ SYBR Green qPCR Master Mix (BioRAD) according to the manufacturer's recommended conditions. The primer sequences for *36B4*, *CAMP*, *DEFB4A* and *CYP27B1* were previously published[5,6]; other primer sequences and calculations are included in the **Supplementary Methods**.

Transfection of monocytes. Monocytes were enriched from peripheral blood mononuclear cells using a Percoll (GE Healthcare) gradient as previously described[6] and then transfected with either the mature miRNA or the antagomir oligomers using the Amaxa Nucleofector system with the Human Monocyte Nucleofector transfection kit (Lonza) according to the manufacturer's recommended protocol. Additional details are included in the **Supplementary Methods**.

miRNA direct targeting analysis. MiRNA-targeting plasmids were prepared with endotoxin-free conditions using the Qiagen Endofree Maxi Kit (Qiagen) according to the manufacturer's recommended protocols. The constructs were co-transfected into HEK293 cells (ATCC) with either hsa-mir-21 mature oligomer or a nontargeting control oligomer with the Amaxa Nucleofector Transfection Cell Line V kit (Lonza) according to the manufacturer's optimized protocol. After transfection, the cells were rested for 2 h and then washed to replace the medium. The transfected cells were then incubated 37 °C for 16 h, and luciferase activity was measured using the Dual Glo-Luciferase Assay System (Promega) according to the manufacturer's recommended protocols. The miRNA effect is calculated as a ratio of the firefly to *Renilla* luciferase activities.

Antimicrobial assays. To assess *M. leprae* and *M. tuberculosis* H37Ra viability from infected macrophages, we adapted the previously described real-time PCR–based method for the assessment of bacterial viability, which compares 16S RNA levels to levels of a genomic DNA as a predictor of bacterial viability (**Supplementary Note**)[10]. Experimental details are included in the **Supplementary Methods**. The 16S and bacterial DNA values were calculated using the $\Delta\Delta C_T$ analysis, with the bacterial DNA value serving as the housekeeping gene. The *M. leprae* 16S and *M. leprae* repetitive genomic element primers used were as previously described[10]; other primer sequences are included in the **Supplementary Methods**.

Additional methods. Detailed methodology is described in the **Supplementary Methods**.

28. Silahtaroglu, A.N. *et al.* Detection of microRNAs in frozen tissue sections by fluorescence *in situ* hybridization using locked nucleic acid probes and tyramide signal amplification. *Nat. Protoc.* **2**, 2520–2528 (2007).

MicroRNA-21 targets the vitamin D-dependent antimicrobial pathway in leprosy

Philip T. Liu, Matthew Wheelwright, Rosane Teles, Evangelia Komisopoulou,
Kristina Edfeldt, Benjamin Ferguson, Manali D. Mehta, Aria Vazirnia, Thomas H. Rea,
Euzenir N. Sarno, Thomas G. Graeber, and Robert L. Modlin

Nature Medicine doi:10.1038/nm.2584

Supplemental Figure 1

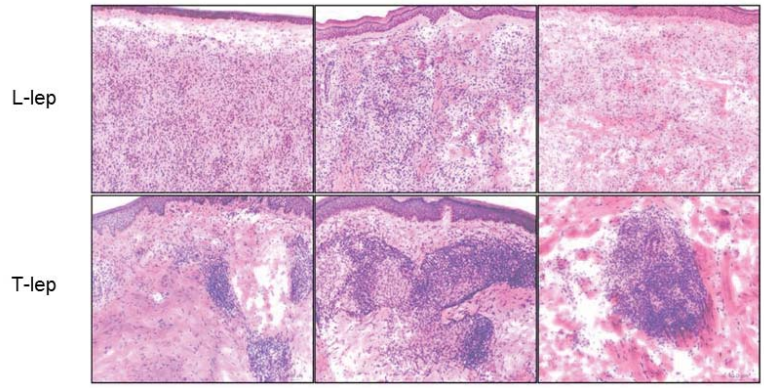

Supplemental Figure 1. Histology of leprosy skin biopsy specimens. Representative hematoxylin and eosin (H&E) stain for L-lep and T-lep skin biopsy specimens used for microarray and qPCR analysis.

Nature Medicine doi:10.1038/nm.2584

Supplemental Figure 2

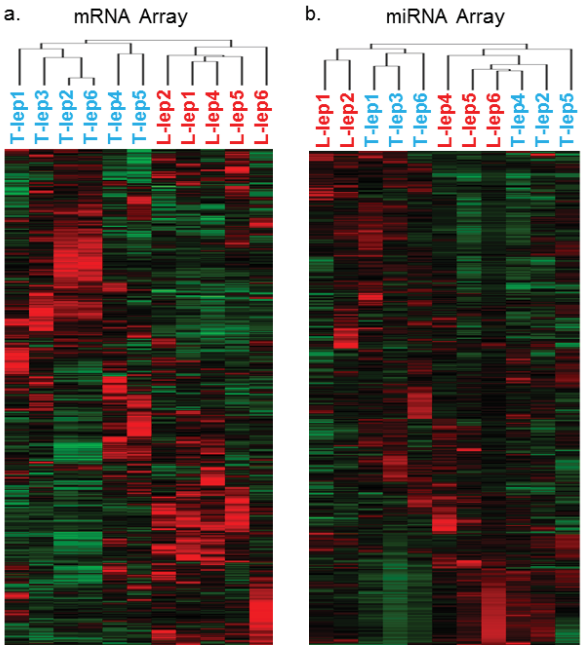

Supplemental Figure 2. mRNA and miRNA expression profile in leprosy skin biopsy specimens. Hierarchical clustering analysis of (**a**) mRNA and (**b**) miRNA microarrays performed on total RNA extracted from six T-lep and five L-lep skin biopsy specimens.

Nature Medicine doi:10.1038/nm.2584

Supplemental Figure 3

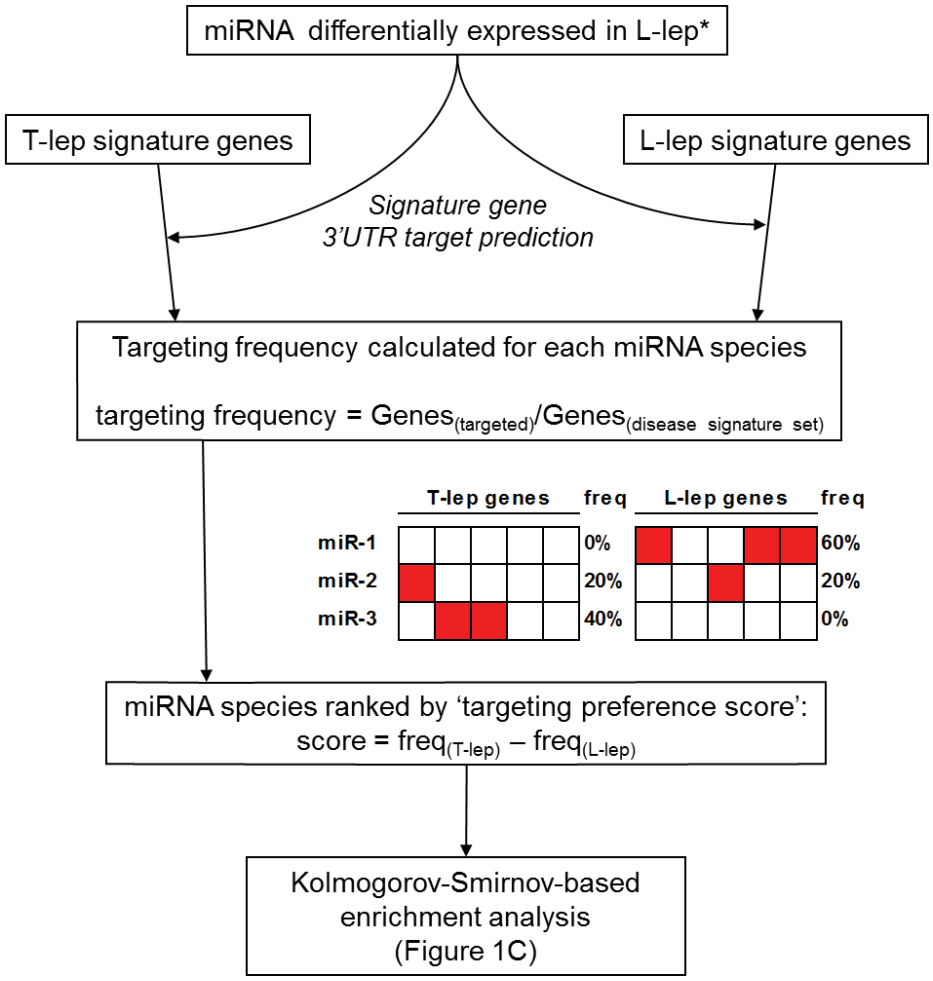

*T-lep specific miRNA were not included in analysis due to lack of statistical power from only two probes.

Supplemental Figure 3. Schematic of targeting enrichment analysis.

Nature Medicine doi:10.1038/nm.2584

Supplemental Figure 4

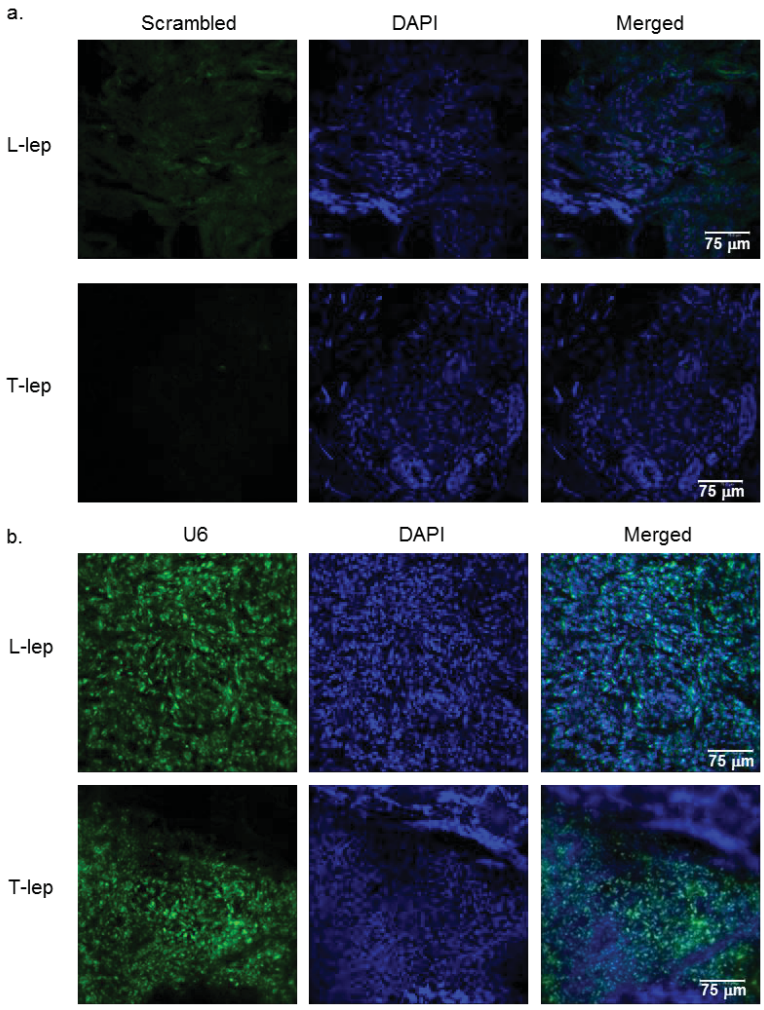

Supplemental Figure 4. *In situ* hybridization for detection of miRNA in leprosy skin biopsy specimens. Representative experiments of L-lep and T-lep skin biopsy specimens labeled with either the (**a**) scrambled negative control or (**b**) positive control oligo for the U6 non-coding small nuclear RNA (U6) using fluorescent *in situ* hybridization detected by confocal microscopy. Data is representative of three individual donors.

Nature Medicine doi:10.1038/nm.2584

Supplemental Figure 5

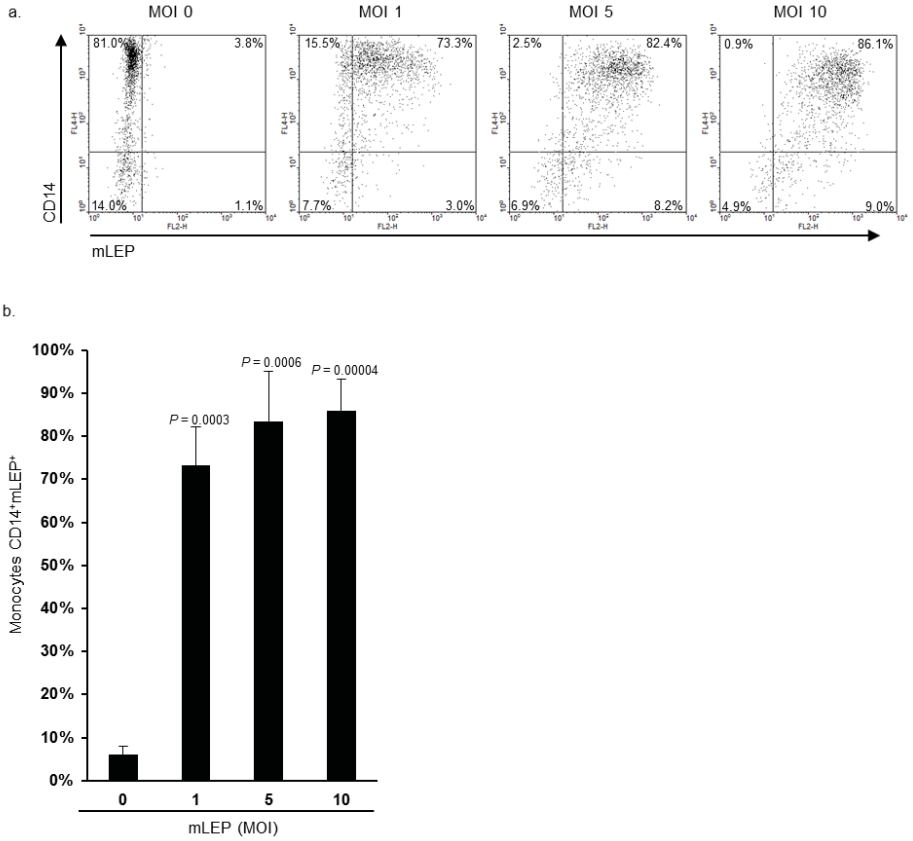

Supplemental Figure 5. *M. leprae* infection efficiency of primary human monocytes. Primary human monocytes were infected with PKH26-labeled live *M. leprae* at an MOI of one, five and ten for 18 h, and then co-labeled with a monoclonal antibody specific for CD14. Data shown is (**a**) representative of four individual donors, and (**b**) mean CD14 and *M. leprae* double positive cells ± SEM, *n* = 4.

Supplemental Figure 6

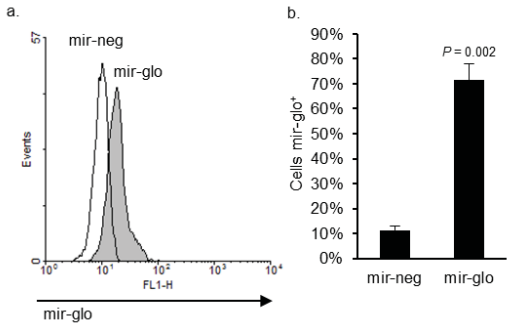

Supplemental Figure 6. Primary human monocyte transfection efficiency. Primary human monocytes were transfected with a Cy5-labeled non-targeting control miRNA oligo (mir-glo) or an unlabeled control oligo (mir-neg). Following transfection, the total mir-glo level in the transfected monocytes was evaluated using flow cytometry. Data shown is (**a**) representative of five donors, and (**b**) mean percent mir-glo positive cells ± SEM, $n = 5$.

Nature Medicine doi:10.1038/nm.2584

Supplemental Figure 7

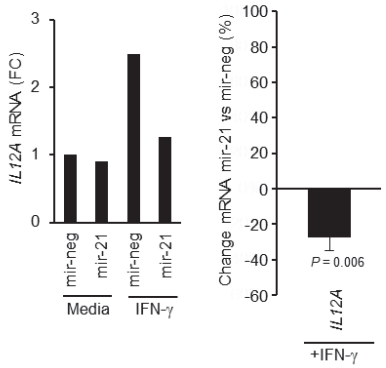

Supplemental Figure 7. Effects of hsa-mir-21 overexpression on the innate immune response. *IL12A* mRNA induction by IFN-γ following transfection of a non-targeting control oligo (mir-neg) or hsa-mir-21 mature oligo (mir-21) into primary human monocytes detected by qPCR. Data shown is representative experiment (left panel) and a summary of all experiments, shown as mean percent change (right panel) ± SEM, *n* = 5.

Nature Medicine doi:10.1038/nm.2584

Supplemental Figure 8

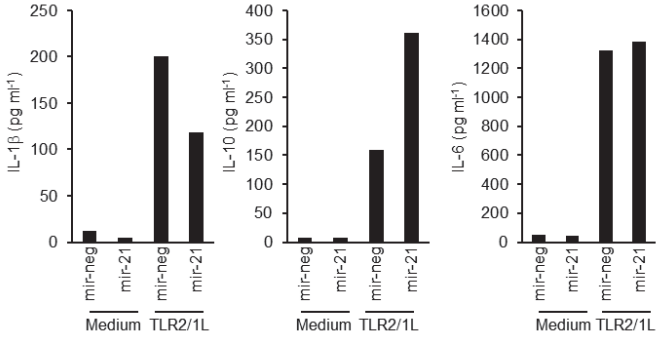

Supplemental Figure 8. Effects of hsa-mir-21 overexpression on the innate immune triggered cytokine response. IL-1β, IL-10 and IL-6 levels in the culture supernatants of mir-neg or mir-21 transfected cells followed by TLR2/1L stimulation as detected by CBA. Data shown is representative experiment of four to five independent donors.

Nature Medicine doi:10.1038/nm.2584

Supplemental Figure 9

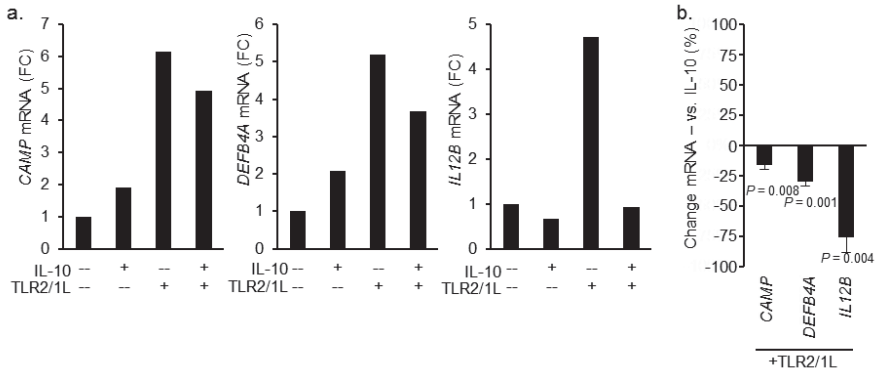

Supplemental Figure 9. Effect of exogenous IL-10 on TLR-induced antimicrobial expression. Expression levels by qPCR of *CAMP*, *DEFB4A* and *IL12B* in primary human monocytes treated with either recombinant IL-10, TLR2/1L or both. *IL12B* is a positive control for IL-10 mediated TLR2/1 inhibition. Data shown is (**a**) representative experiment and a (**b**) summary of all experiments, shown as mean percent change ± SEM in TLR2/1L stimulated cells (–– vs IL-10), $n = 3$.

Supplemental Figure 10

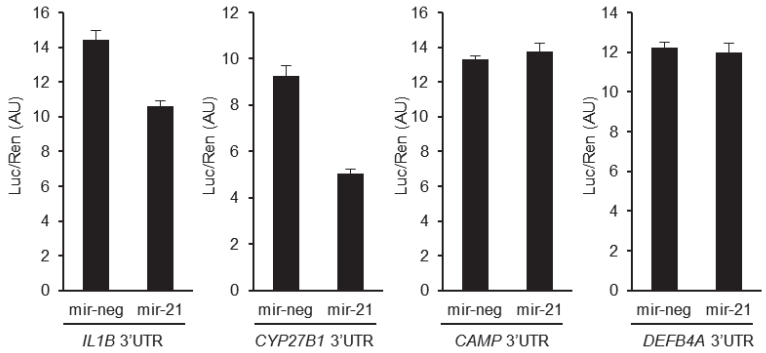

Supplemental Figure 10. Direct 3'UTR binding analysis. Luciferase activity normalized to the internal *Renilla* luciferase control activity of HEK-293 cells transfected with reporter constructs for the 3'UTR of *IL1B*, *CYP27B1*, *CAMP* or *DEFB4A*, with either mir-neg or mir-21 simultaneously. Data shown is representative of four to six independent experiments.

Nature Medicine doi:10.1038/nm.2584

Supplemental Figure 11

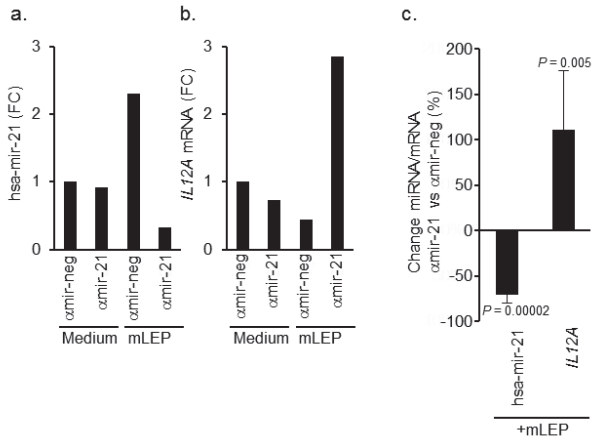

Supplemental Figure 11. Knockdown of hsa-mir-21 expression during *M. leprae* infection. Expression levels by qPCR of (**a**) hsa-mir-21 and (**b**) *IL12A* mRNA in primary human monocytes transfected with either a control anatgomir (αmir-neg) or an antagomir specific for hsa-mir-21 (αmir-21) followed by infection with *M. leprae* infection at MOI of ten. Data shown is (**a**-**b**) representative experiment and a (**c)** summary of all experiments, shown as mean percent change (αmir-neg vs αmir-21) ± SEM, *n* = 5-7.

Supplemental Figure 12

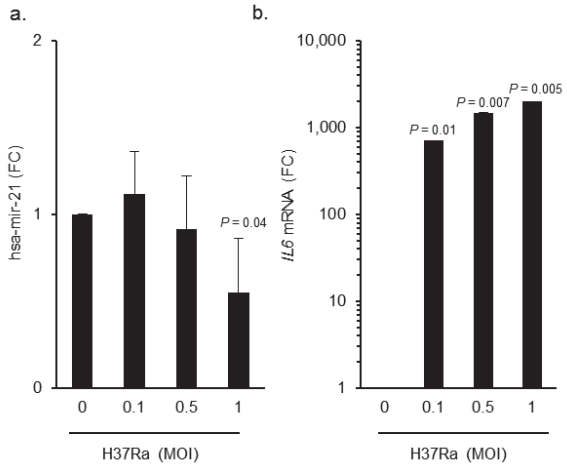

Supplemental Figure 12. Regulation of hsa-mir-21 by *M. tuberculosis*. Primary human monocytes were infected with *M. tuberculosis* H37Ra at MOI of 0.1, 0.5 and one for 18 h and the level of (**a**) hsa-mir-21 and (**b**) *IL6* mRNA was assessed by qPCR. Data shown is the mean fold change vs. MOI 0 ± SEM, *n* = 4-5.

Nature Medicine doi:10.1038/nm.2584

SUPPLEMENTAL TABLE
ACCESSION NUMBERS

Gene	**NCBI Accession**
CAMP	NM_004345
DEFB4A	NM_004942
CYP27B1	NM_000785
IL1B	NM_000576
IL6	NM_000600
IL10	NM_000572
IL12A	NM_000882
IL12B	NM_002187
36B4	NM_001002

miRNA	**miRBase Accession**
hsa-mir-21	MI0000077
hsa-let-7c	MI0000064

mRNA Array (GEO Title)	**GEO Accession**
T-lep1 (BT1)	GSM443590
T-lep2 (BT6)	GSM443591
T-lep3 (BT10)	GSM443678
T-lep4 (BT3)	GSM443592
T-lep5 (BT4)	GSM443622
T-lep6 (BT7)	GSM443625
L-lep1 (LL1)	GSM443583

L-lep2 (LL4)	GSM443586
L-lep4 (LL3)	GSM443585
L-lep5 (LL7)	GSM443588
L-lep6 (LL9)	GSM443589

miRNA Array	**GEO Acession**
T-lep1	GSM821609
T-lep2	GSM821610
T-lep3	GSM821611
T-lep4	GSM821612
T-lep5	GSM821613
T-lep6	GSM821614
L-lep1	GSM821604
L-lep2	GSM821605
L-lep4	GSM821606
L-lep5	GSM821607
L-lep6	GSM821608
Study	GSE33192

SUPPLEMENTAL NOTE

Leprosy specific gene sets

L-lep specific gene list: interleukin 4 (*IL4*) [1-3], interleukin 5 (*IL5*) [1, 3], leukocyte immunoglobulin-like receptor, subfamily A (with TM domain), member 2 (*LILRA2*) [4], tumor necrosis factor (ligand) superfamily, member 13b (*TNFSF13B*) [4], transforming growth factor, beta 1 (*TGFB1*) [5], interleukin 10 (*IL10*) [1, 3], CD163 molecule (*CD163*) [6], peroxisome proliferator-activated receptor gamma (*PPARG*) [7], apolipoprotein E (*APOE*) [7], CD36 molecule (thrombospondin receptor) (*CD36*) [6], macrophage scavenger receptor 1 (*MSR1*) [6, 7], macrophage receptor with collagenous structure (*MARCO*) [6, 7], chemokine (C-X-C motif) ligand 16 (*CXCL16*) [6], oxidized low density lipoprotein (lectin-like) receptor 1 (*OLR1*) [6], scavenger receptor class B, member 1 (*SCARB1*) [6], CD68 molecule (*CD68*) [6].

T-lep specific gene list: interleukin 12A (*IL12A*) [8], interleukin 12B (*IL12B*) [8], interleukin 7 (*IL7*) [9], interleukin 18 (*IL18*) [10], signaling lymphocytic activation molecule family member 1 (*SLAMF1*) [4, 11], CD1b molecule (*CD1B*) [12, 13], colony stimulating factor 2 (granulocyte-macrophage) (*CSF2*) [3], colony stimulating factor 2 receptor, alpha, low-affinity (granulocyte-macrophage) (*CSF2RA*) [13, 14], CD40 molecule, TNF receptor superfamily member 5 (*CD40*) [15], CD40 ligand (*CD40L*) [15], interferon, gamma (*IFNG*) [1, 2], interleukin 15 (*IL15*) [2], interleukin 2 receptor, beta (*IL2RB*) [16], interleukin 2 receptor, gamma (*IL2RG*) [16], interleukin 1, beta (*IL1B*) [3], interleukin 1 receptor, type I (*IL1R1*) [4], cytochrome P450, family 27, subfamily B, polypeptide 1 (*CYP27B1*) [6], vitamin D (1,25- dihydroxyvitamin D3) receptor (*VDR*) [6], cytochrome P450, family 24, subfamily A, polypeptide 1 (*CYP24A1*) [6], granulysin (*GNLY*) [17].

Targeting preference score

Nature Medicine doi:10.1038/nm.2584

The potential ability of the 468 annotated miRNA species represented on the microarray platform to target the 3'UTRs of the genes in the leprosy specific gene sets (defined above) were analyzed using the online database TargetScanHuman [18]. Given that the two leprosy specific gene sets have different numbers of genes, the targeting frequency of each individual miRNA species was calculated for the two sets of genes differentially expressed in T-lep and L-lep lesions. All miRNA species were ranked based on their 'targeting preference score', the degree of differential targeting of T-Lep versus L-lep signature genes (**Supplemental Fig. 2**). All miRNA species were rank ordered based on their targeting frequency score. This yielded three principal categories within the ranked list: i) preferentially targeting T-lep genes (preference score > 0), ii) no targeting preference (preference score = 0), and iii) preferentially targeting L-lep genes (preference score < 0).

The statistical significance of leprosy specific miRNA species enrichment was determined by 'Kolmogorov-Smirnov (KS)-based permutation analysis. Ranked lists annotated with the presence or absence of differential expression were scanned using all possible rank thresholds for the point of maximal enrichment as defined by the maximal KS distance. Permutation analysis was then performed by randomly reassigning the targeting preference scores used for ranking. The fraction of permutation cases resulting in a maximal KS distance greater than or equal to the observed maximum value was then defined as the permutation-based frequency of random occurrence, i.e. the permutation-based p-value. This procedure is analogous to the permutation approach used in Gene Set Enrichment Analysis (GSEA) [19]. Using this analysis the L-lep specific miRNA species were significantly enriched within the group of miRNA with a preference score greater than zero (**Fig. 1c**). In contrast the two T-lep specific miRNA species showed no statistical enrichment due to the lack of statistical power.

Direct 3'UTR binding

Nature Medicine doi:10.1038/nm.2584

In order to ascertain if hsa-mir-21 directly regulated the expression of the key antimicrobial genes, the ability of hsa-mir-21 to bind the three prime untranslated region (3'UTR) of these genes was assessed. Constructs containing the firefly luciferase gene with the 3'UTR of the gene of interest driven by the CMV promoter were co-transfected with a non-targeting oligo or hsa-mir-21 into HEK-293 cells. Following transfection, the resulting firefly luciferase activity was measured, and normalized to activity of the internal *Renilla* luciferase control on the plasmids. Presence of hsa-mir-21 resulted in the downregulation of luciferase activity in cells transfected with the *IL1B* and *CYP27B1* 3'UTR constructs. In contrast, hsa-mir-21 had no effect on the luciferase activity in cell transfected with the *CAMP* and *DEFB4A* 3'UTR constructs (Representative Experiment, **Supplemental Fig. 8**). In these assays, hsa-mir-21 downregulated luciferase activity by 14% (P = 0.02) in the *IL1B* 3'UTR and 21% (P = 0.04) in the *CYP27B1* constructs (**Fig. 4d**). These data indicate that hsa-mir-21 directly regulates two key components of the vitamin D antimicrobial pathway, *IL1B* and *CYP27B1*, leading to downstream inhibition of antimicrobial peptide gene expression.

PCR-based bacterial viability

This PCR-based assay is a powerful tool for the investigation of *M. leprae* biology as well as other mycobacterial pathogens both *in vivo* and *in vitro*. Although *M. leprae* can also be assessed using radiorespiromtery and BacLight, these approaches were not feasible here as the cell yield after transfection was limiting. However, as demonstrated by Martinez *et al.*, the PCR-based assay is comparable to both radiorespirometry and BacLight in its ability to determine *M. leprae* viability [20]. In addition to *M. leprae*, similar PCR based methods have been used to assess the viability in vitro of *M. tuberculosis* [21] as well as *M. avium* [22]. Levels of *M. tuberculosis* 16S RNA and IS6110 have been previously explored as a measurement of *M. tuberculosis* viability in sputum samples *in vivo* following chemotherapy treatment in patients [23]. In this study, the authors found that in patient's sputum, *M. tuberculosis* 16S RNA levels

rapidly declined upon initiation of antimicrobial therapy, whereas IS6110 DNA levels remained constant, which mirrors the expected results of an *in vitro* viability assay for *M. tuberculosis*.

In our previous studies of siRNA transfected monocytes stimulated with TLR2/1L, examining antimicrobial effects against H37Ra, we demonstrated a significant (P = 0.05) TLR2/1L-induced antimicrobial activity of 14.5% ± 1.3 by the CFU assay [24]. These results are comparable to the data shown in this manuscript using the real time PCR method, where we demonstrate a significant (P = 0.02) TLR2/1L-induced antimicrobial activity against H37Ra in mir-neg transfected monocytes of 18.0% ± 0.08. Given the similarities between the nontargeting siRNA control used in the previous study and the mir-neg non-targeting control used here (both 21 nucleotides long, double stranded RNA oligos), we feel that these results demonstrate that the real time PCR assay is comparable to the CFU assay.

Nature Medicine doi:10.1038/nm.2584

SUPPLEMENTAL METHODS

Reagents

Mature miRNA oligos and antagomir oligos were purchased (Applied Biosystems), resuspended in sterile DEPC-treated water at 20μM, stored in aliquots at 80°C, and used at 2.5μl per reaction. TLR2/1L is a synthetic 19kDa *M. tuberculosis* derived lipopeptide used at 10μg/ml (EMC Microcollections). Recombinant IFN-γ (BD Bioscience) and IL-10 (R&D Systems) were purchased and both used at 10ng/ml. Biotinylated LNA probes used for fluorescent in situ hybridization were purchased (Exiqon, Woburn, MA) and stored in small aliquots at -20°C. Strep-avidin horse radish peroxidase (*S*A-HRP, Thermo Fisher) was resuspended in DEPC-treated water at 1mg/ml, then stored in small aliquots at -20°C and diluted 1:2000 before use. miRNA Target Clones containing the 3'UTR of *IL1B*, *CYP27B1*, *CAMP* and *DEFB4* were purchased (Genecopoeia). HEK293 cells were purchased, and maintained according to the manufacturer's recommended conditions (ATCC). Human CD14 specific monoclonal antibody conjugated with APC was purchased and used as recommended by the manufacturer (BD Pharmingen).

Primer sequences

The following primers were designed: *IL6* Forward 5'-GAC CCA ACC ACA AAT GCC A-3', *IL6* Reverse 5'-CAT GTC CTG CAG CCA CTG G-3', *IL1B* Forward 5'-GCT TAT GTG CAC GAT GCA CC-3', *IL1B* Reverse 5'-GAG GCC CAA GGC CAC AG-3', *IL12A* Forward 5'-AGT GGA GGC CTG TTT ACC ATT GGA-3', *IL12A* Reverse 5'-AGG CCA GGC AAC TCC CAT TAG TTA-3', *IL10* Forward 5'-GAG AAC CAA GAC CCA GAC ATC AAG-3', *IL10* Reverse 5'-CAT TGT CAT GTA GGC TTC TAT GTA GTT G-3', hsa-mir-21 5'-CGG TAG CTT ATC AGA CTG ATG TTG A-3', and hsa-let-7c 5'-CGC TGA GGT AGT AGG TTG TAT GGT T-3'. For *M. tuberculosis*

H37Ra, the IS6110 genomic element was used and the primer sequences are as follows: 16S Forward 5'-GGT GCG AGC GTT GTC CGG AA-3', 16S Reverse 5'- CGC CCG CAC GCT CAC AGT TA-3', IS6110 Forward 5'-GGA AGC TCC TAT GAC AAT GCA CTA G-3', and IS6110 Reverse 5'-TCT TGT ATA GGC CGT TGA TCG TCT-3'.

Leprosy biopsy specimens

We have established a library of skin biopsy specimens collected from new untreated patients at the time of diagnosis from the Hansen's Disease Clinic at Los Angeles Country and University of Southern California Medical Center as well as the Leprosy Clinic at the Oswaldo Cruz Foundation in Brazil presenting between 2005-2010. The diagnosis and classification of patients was established by means of clinical and histopathological criteria of Ridley and Jopling [25]. T-lep patients were classified as borderline tuberculoid (BT) and L-lep patients classified as lepromatous (LL). For the microarray, qPCR and FISH studies presented here, skin biopsy specimens from T-lep and L-lep patients were randomly selected from the library, representing a total of 20 individual T-lep patients and 23 individual L-lep patients. Specimens were embedded in OCT medium, snap-frozen in liquid nitrogen and stored at -80°C until sectioning. Tissue sections were either mounted on slides for *in situ* hybridization or processed for RNA isolation.

Microarray analysis

Total RNA was isolated from six lepromatous and six tuberculoid leprosy lesions as previously described [13]. Data obtained from the miRNA analysis indicated that one lepromatous sample was to be excluded from further analysis due to low RNA quality. For the hierarchical clustering, the individual probe expression patterns were compared using a centered Pearson correlation coefficient. Cluster dendrograms were generated using the Cluster and TreeView software

programs from the Eisen Lab at http://rana.lbl.gov/ [26]. For heatmap-based visualization, expression values were mean subtracted with the sum of squares set equal to one [26].

Live *M. leprae*

M. leprae is grown in the footpad of nu/nu mice, harvested and treated with NaOH to remove mouse tissue, and the bacteria viability is assessed by determining the rate of palmitic acid oxidation, bacterial membrane integrity, and growth in the mouse footpad [27]. A portion of the *M. leprae* is then incubated with the fluorescent dye: PKH26. The NaOH treated *M. leprae* preps are shipped overnight at on ice, which was determined to have minimal impact on the bacteria viability.

Isolation and infection of monocytes

The collection and analysis of peripheral blood cells from healthy blood donors was approved by the committees on investigations involving human subjects of the University of California, Los Angeles, and all donors provided written informed consent. Mononuclear cells were isolated from peripheral blood of healthy donors using Ficoll-Paque as previously described [28]. Monocytes were purified by plastic adherence for two hours in RPMI 1640 (Invitrogen) supplemented with 1% fetal calf serum (Omega Scientific). Non-adherent cells were removed via vigorous washing and cultured in RPMI supplemented with antibiotics and 10% fetal calf serum, or 10% vitamin D-sufficient (100 nM) human serum for antimicrobial peptide gene expression studies or *M. leprae* infection studies. For *M. leprae* infection studies, monocytes were infected with single cell suspensions of *M. leprae* at a MOI of one, five, and ten then cultured at 33 °C for 18 or 40 h. Using PKH26-labled *M. leprae*, the infection efficiency of CD14 positive monocytes was determined using flow cytometry (**Supplemental Fig. 11a**), as previously described [24]. An average of 73%, 84% and 86% of monocytes in culture were *M. leprae* positive at a MOI of one, five, and ten, respectively (**Supplemental Fig. 11b**). At MOI

of ten, each infected cell contained an average of 2.1 ± 0.4 bacteria (average of three individual donors). Unless indicated, all experiments involving live *M. leprae* were conducted with a MOI of ten. For *M. tuberculosis* infection studies, monocytes were infected with single cell suspensions of *M. tuberculosis* H37Ra at a MOI of 0.1, 0.5 and one, and then cultured at 37 °C for 18 h, or with an MOI of 0.5 for transfected cells, as we previously described [24]. An MOI of 0.5 was optimized based on infectivity and viability of the transfected monocytes.

Quantitative PCR

For mRNA studies, the data was analyzed using the $\Delta\Delta C_T$ method as previously described [28] using *36B4* as the normalizer. The results are then calculated as a fold change to control treated cells. For miRNA studies, four different "normalizing" short RNA sequences were tested over several donors and experiments; however, none demonstrated sufficient stability for use as a qPCR normalizer, which corroborates published data [29]. Therefore, the samples were normalized to the same input cell number prior to applying the Cells-to-CT or NCODE kits, and analyzed using the ΔC_T method. The results are then calculated as a fold change to control cells.

Transfection of monocytes

Transfection efficiency was evaluated using the Cy5-labeled non-targeting miRNA oligo (mir-glo). Primary monocytes were transfected with mir-glo or an unlabeled control oligo (mir-neg), and mir-glo positive cells were assessed by flow cytometry (**Supplemental Fig. 12a**). In five independent experiments, the average number of mir-glo positive cells was 71% ± 6% (P = 0.002, **Supplemental Fig. 12b**). Following transfection, the cells were allowed to recover for two hours in the provided transfection medium, then washed and plated in RPMI and 10% FCS, or 10% pooled human vitamin D sufficient serum for the cathelicidin and DEFB4 studies. The

Nature Medicine doi:10.1038/nm.2584

cells transfected with the mature miRNA oligos were then stimulated with TLR2/1L (10 μg ml^{-1}) incubated for either 18 or 24 hours. The antagomir transfected cells were infected with live *M. leprae* (MOI 10) as above and incubated for 18 to 24 h. Total RNA was harvested following the incubation and quantitative PCR was performed.

Cytometric bead array

Supernatants from the transfected and stimulated monocytes were harvested at 18 and 24 h. IL-1β, IL-10 and IL-6 cytokine levels in the supernatants were assessed using Cytometric Bead Array Flex Set (BD Biosciences) according to the manufacturer's recommended protocols. The beads were visualized using a BD FACSCalibur (BD Biosciences) and analyzed with Flowjo Software (Tree Star).

Antimicrobial assays

Monocytes were first transfected as indicated, and infected overnight with an MOI of ten for *M. leprae*, and an MOI of 0.5 with *M. tuberculosis* H37Ra, then counted and viability assessed using trypan blue exclusion. Higher MOIs of H37Ra were toxic to the transfected monocytes. The infected cells were cultured in equal amounts of viable cells for all conditions tested, followed by stimulation with the TLR2/1L or medium for three days as indicated above. Following the incubation, the cells are harvested and divided. Half of the cells were lysed by boiling at 100 °C for 5 min then snap freezing at -80 °C, and total RNA was isolated from the remaining half using Trizol as detailed above, followed by RNA cleanup and on column DNAse digestion using RNeasy Miniprep Kit (Qiagen). cDNA was synthesized from the total RNA as described above. The bacterial 16S rRNA, and genomic element DNA levels were then assessed using real time PCR as detailed above from the cDNA and cellular lysate, respectively. In order to normalize for the total monocytes present in the culture, *36B4* was also

evaluated, which were capable of amplifying the human genomic DNA. Comparison of the bacterial DNA to the mammalian *36B4* levels was used to monitor infectivity between all the conditions in the assay as well as PCR quality.

Nature Medicine doi:10.1038/nm.2584

SUPPLEMENTAL REFERENCES

1. Yamamura,M. et al. Defining protective responses to pathogens: cytokine profiles in leprosy lesions. Science 254, 277-279 (1991).

2. Jullien,D. et al. IL-15, an immunomodulator of T cell responses in intracellular infection. J. Immunol. 158, 800-806 (1997).

3. Yamamura,M. et al. Cytokine patterns of immunologically mediated tissue damage. J. Immunol. 149, 1470-1475 (1992).

4. Bleharski,J.R. et al. Use of genetic profiling in leprosy to discriminate clinical forms of the disease. Science 301, 1527-1530 (2003).

5. Goulart,I.M., Figueiredo,F., Coimbra,T., & Foss,N.T. Detection of transforming growth factor-beta 1 in dermal lesions of different clinical forms of leprosy. Am. J. Pathol. 148, 911-917 (1996).

6. Montoya,D. et al. Divergence of macrophage phagocytic and antimicrobial programs in leprosy. Cell Host. Microbe 6, 343-353 (2009).

7. Cruz,D. et al. Host-derived oxidized phospholipids and HDL regulate innate immunity in human leprosy. J. Clin. Invest 118, 2917-2928 (2008).

8. Sieling,P.A. et al. IL-12 regulates T helper Type 1 cytokine responses in human infectious disease. J. Immunol. 153, 3639-3647 (1994).

9. Sieling,P.A. et al. IL-7 in the cell-mediated immune response to a human pathogen. J. Immunol. 154, 2775-2783 (1995).

10. Garcia,V.E. et al. IL-18 promotes type 1 cytokine production from NK cells and T cells in human intracellular infection. J Immunol 162, 6114-6121 (1999).

11. Garcia,V.E. et al. Signaling lymphocytic activation molecule expression and regulation in human intracellular infection correlate with Th1 cytokine patterns. J Immunol 167, 5719-5724 (2001).

12. Sieling,P.A. et al. CD1 expression by dendritic cells in human leprosy lesions: Correlation with effective host immunity. J Immunol 162, 1851-1858 (1999).

13. Krutzik,S.R. et al. TLR activation triggers the rapid differentiation of monocytes into macrophages and dendritic cells. Nat. Med. 11, 653-660 (2005).

14. Krutzik,S.R. et al. Activation and regulation of Toll-like receptors 2 and 1 in human leprosy. Nat. Med. 9, 525-532 (2003).

15. Yamauchi,P.S. et al. A role for CD40-CD40 ligand interactions in the generation of type 1 cytokine responses in human leprosy. J. Immunol. 165, 1506-1512 (2000).

16. Modlin,R.L. et al. In situ identification of cells in human leprosy granulomas with monoclonal antibodies to interleukin 2 and its receptor. J. Immunol. 132, 3085-3090 (1984).

Nature Medicine doi:10.1038/nm.2584

17. Ochoa,M.T. et al. T-cell release of granulysin contributes to host defense in leprosy. Nat. Med. 7, 174-179 (2001).

18. Lewis,B.P., Burge,C.B., & Bartel,D.P. Conserved seed pairing, often flanked by adenosines, indicates that thousands of human genes are microRNA targets. Cell 120, 15-20 (2005).

19. Subramanian,A. et al. Gene set enrichment analysis: a knowledge-based approach for interpreting genome-wide expression profiles. Proc. Natl. Acad. Sci. U. S. A 102, 15545-15550 (2005).

20. Martinez,A.N. et al. Molecular determination of Mycobacterium leprae viability by use of real-time PCR. J. Clin. Microbiol. 47, 2124-2130 (2009).

21. Munoz-Elias,E.J. et al. Replication dynamics of Mycobacterium tuberculosis in chronically infected mice. Infect. Immun. 73, 546-551 (2005).

22. Kralik,P., Nocker,A., & Pavlik,I. Mycobacterium avium subsp. paratuberculosis viability determination using F57 quantitative PCR in combination with propidium monoazide treatment. Int J Food Microbiol. 141 Suppl 1, S80-S86 (2010).

23. Desjardin,L.E. et al. Measurement of sputum Mycobacterium tuberculosis messenger RNA as a surrogate for response to chemotherapy. Am J Respir. Crit Care Med 160, 203-210 (1999).

24. Liu,P.T. et al. Convergence of IL-1beta and VDR activation pathways in human TLR2/1-induced antimicrobial responses. PLoS. ONE. 4, e5810 (2009).

25. Ridley,D.S. & Jopling,W.H. Classification of leprosy according to immunity. A five-group system. Int. J. Lepr. 34, 255-273 (1966).

26. Eisen,M.B., Spellman,P.T., Brown,P.O., & Botstein,D. Cluster analysis and display of genome-wide expression patterns. Proc. Natl. Acad. Sci. U. S. A 95, 14863-14868 (1998).

27. Lahiri,R., Randhawa,B., & Krahenbuhl,J.L. Effects of purification and fluorescent staining on viability of Mycobacterium leprae. Int. J Lepr. Other Mycobact. Dis. 73, 194-202 (2005).

28. Liu,P.T. et al. Toll-like receptor triggering of a vitamin D-mediated human antimicrobial response. Science 311, 1770-1773 (2006).

29. Peltier,H.J. & Latham,G.J. Normalization of microRNA expression levels in quantitative RT-PCR assays: identification of suitable reference RNA targets in normal and cancerous human solid tissues. RNA. 14, 844-852 (2008).

Nature Medicine doi:10.1038/nm.2584

CHAPTER 3:

Plasticity of macrophage IL-10 induced phagocytic and IL-15 induced antimicrobial programs

Title:

Plasticity of macrophage IL-10 induced phagocytic and IL-15 induced antimicrobial programs

Authors:

Dennis Montoya[1], Manali Mehta[2], Benjamin G. Ferguson[1], Rosane M.B. Teles[2], Daniel Cruz[3], Stephan R. Krutzik[2], Matteo Pellegrini[1], and Robert L. Modlin[2]

[1]Department of Molecular, Cell, and Developmental Biology,[2]Division of Dermatology, [3]Division of Cardiology, Department of Medicine David Geffen School of Medicine at University of California Los Angeles, CA 90095, USA

Abstract:

Macrophage (MΦ) polarization is triggered during the innate immune response to defend against microbial pathogens, but can also contribute to disease pathogenesis, providing an strong incentive to identify mechanisms to drive MΦ plasticity. In studying MΦ differentiation in leprosy, we found that IL-15 derived M1 MΦ have enhanced antimicrobial activity against intracellular mycobacteria, whereas IL-10 derived M2 MΦ have enhanced scavenger receptor expression, promoting phagocytosis, but lacking antimicrobial activity against intracellular bacteria. Examination of plasticity of M1 and M2 MΦ led to the finding that addition of IL-10 to M1 MΦ induced M2-like MΦ, but IL-15 had little effect on M2 MΦ. We determined the set of immune receptors that are present on M2 MΦ and known to drive M1 MΦ polarization, elucidating two candidates for inducing plasticity of M2 MΦ, Toll-like receptor 1 (TLR1) and

interferon-gamma receptor 1 (IFNGR1). Stimulation of M2 MΦ with TLR2/1 ligand or IFN-γ alone was not sufficient to completely change the M2 MΦ phenotype or function; however, co-addition led to skewing towards the M1 MΦ phenotype. These reeducated M1-like MΦ exhibited a decrease in phagocytic capabilities and recovery of the vitamin D dependent induction of antimicrobial peptide production as compared to M2 MΦ maintained in polarizing conditions. Although TLR2/1L stimulation alone was not sufficient to reeducate M2 MΦ, stimulation in concert with anti-IL-10 neutralizing antibody led to polarization to M1-like MΦ phenotype and function. Together, our data demonstrate an approach to induce MΦ plasticity that provides the potential for reeducating MΦ function in human infectious disease to promote host defense and modify pathogenesis.

Introduction:

Playing a crucial role in host defense against microbial pathogens[108], macrophage (MΦ) activation states and plasticity of macrophage polarization is being increasingly studied. MΦ are characterized by a diversity of activation states[109,110] but are broadly grouped into two categories based on their phenotypic and functional profiles: i) classically activated M1 MΦ produced by IFN-γ + LPS stimulation[111] and ii) alternatively activated M2 MΦ, which are further subcategorized into M2a, M2b, and M2c MΦ induced by stimulation of IL-4 or IL-13, immune complexes, and IL-10 or TGF-b, respectively[112,113]. Since the discovery of phagocytes in 1884, immunologists have generally linked two key functions of the innate immune response, phagocytosis and antimicrobial responses, as being co-regulated for optimal host defense. Previously, however, we discovered that the innate immune response, by selectively stimulating with cytokines IL-10 or IL-15, differentially activates MΦ phagocytic and antimicrobial responses, respectively[14]. The phenotype and phagocytic programs of IL-10- and IL-15-derived MΦ (M2 and M1 MΦ) closely resemble those identified in the skin lesions of two distinct types of leprosy, lepromatous (L-lep) and tuberculoid (T-lep) leprosy, respectively. M2 MΦ show enhanced phagocytic capabilities but are unable to initiate the vitamin D dependent antimicrobial response against mycobacteria. The lack of antimicrobial activity in conjunction with enhanced phagocytosis of a lipid energy source for mycobacteria is thought to lead to disease progression. In contrast, M1 MΦ induce expression of 25-hydroxylase enzyme, CYP27b1, in response to mycobacterial cell wall ligand (TLR2/1L), which converts inactive vitamin D (25D) into its active form 1,25D and leads to the production of antimicrobial peptides cathelicidin and beta-defensin 2 that are required for killing of mycobacteria[44,45]. In leprosy, some patients are able to convert from the lepromatous to tuberculoid form of the disease and vice versa, known as reversal reactions (RR), suggesting plasticity of MΦ polarization during disease progression. In fact, MΦ have shown some plasticity *in vivo* and *in vitro* after treatment

with various cytokines to reeducate M1 and M2 MΦ. Here we investigate mechanisms of reeducation of MΦ polarization of IL-10 and IL-15 MΦ in an effort to understand plasticity of MΦ polarization in mycobacterial infection that may prove useful for therapeutic intervention of MΦ-mediated disease.

Results:

IL-10 is sufficient to reprogram M1 MΦ, but IL-15 is not sufficient to reprogram M2 MΦ

To investigate whether established M1 MΦ and M2 MΦ phenotypes are reversible, adherent peripheral blood mononuclear cells were first differentiated with IL-15 or IL-10 for three days to generate $CD209^{+}CD163^{-}$ M1 MΦ or $CD209^{+}CD163^{+}$ M2 MΦ as previously described[14]. At day three, M2 MΦ show CD163 expression in 58% of $CD209^{+}$ cells in contrast to M1 MΦ, which have CD163 expression on only 6% of $CD209^{+}$ cells (Figure 1A). Differentiated MΦ were immunomagnetically sorted for $CD209^{+}$ to achieve greater than 95% purity and then stimulated with IL-10 or IL-15 for an additional three days to determine if their phenotype can be reprogrammed. After the additional three days of treatment, M1 MΦ in the presence of IL-15 retained their $CD209^{+}CD163^{-}$ phenotype (Figure 1B). Treatment of M1 MΦ with the M2 polarizing cytokine IL-10 significantly increased the percentage of $CD163^{+}$ cells from 0% to 63.7% at day six (Figure 1C), indicating IL-10 is sufficient to reprogram M1 MΦ. Conversely, M2 MΦ in the presence of IL-10 retained their $CD209^{+}CD163^{+}$ phenotype. IL-15 treatment, however, was not sufficient to reprogram M2 MΦ, as treatment of M2 MΦ with IL-15 resulted in an incomplete decrease in percentage of CD163 positive cells from 91% to 67% at day six.

Differential expression of MΦ receptors suggests ligands to alter M2 MΦ phenotype

It's been previously noted that the expression level of receptors may affect MΦ response to ligands[114]. Thus, we hypothesized that the MΦ receptor repertoire can change to induce

receptors which can be triggered to alter MΦ phenotype. Using previously published transcriptional signatures of adherent human peripheral blood mononuclear cells stimulated with IL-10 or IL-15, or time zero unstimulated cells[14], we compiled expression data for receptors known to be involved in driving MΦ polarization (Figure 2A). Concordant with Figure 1, M1 MΦ express IL-10 receptor genes IL10RA and IL10RB, thereby making them susceptible to the effects of IL-10 treatment. M2 MΦ, on the other hand, express decreased levels of IL-15 receptor complex genes IL15RA, IL2RB, and IL2RG, which may explain why IL-15 treatment was only partially able to reprogram M2 MΦ. Assessment of cell surface markers on M2 MΦ revealed heightened expression of other receptors known to drive M1 MΦ polarization, including many of the Toll-like receptor (TLR) family and interferon gamma receptor 1 (IFNGR1). Of these, TLR1 and IFNGR1 are known to be protective against mycobacterial infection and were significantly more highly expressed in L-lep versus T-lep lesions. Cell surface expression of inflammatory receptors TLR1 and IFNGR1, but not IFNGR2, was confirmed to be more highly expressed on M2 MΦ at day three as compared to M1 MΦ or freshly isolated monocytes by flow cytometry (Figure 2B).

TLR2/1L+ IFN-γ stimulation is sufficient to reprogram M2 MΦ

Due to the prominent expression of TLR1 and IFNGR1 on M2 MΦ, we speculated that activation of IFN-γ receptor or TLR1 may be sufficient to fully reprogram M2 to M1-like MΦ. To test whether stimulation of these receptors would lead to a complete change in the IL-10 phenotype, $CD209^{+}$ IL-10 MΦ were purified and stimulated with TLR2/1L, IFN-γ, or TLR2/1L and IFN-γ in combination, in addition to IL-10 or IL-15 for comparison, for three additional days. At day six, only the stimulation with TLR2/1L and IFN-γ in combination led to a complete decrease in CD163 surface expression to 17.5% as compared to IL-10 stimulated M2 MΦ at 84.4%

(Figure 2C). TLR2/1L, IFN-γ, and IL-15 stimulations only showed a moderate decrease in percentage of $CD163^+$ cells to 46.3%, 61.2%, and 66.9%, respectively. The effect on percentage of $CD163^+$ cells could not be enhanced by stimulating with increasing concentrations of IFN-γ (Supplementary Figure 1).

TLR2/1L-induced secretion of IL-10 counteracts suppression of CD163 expression

TLR activation is reported to be a key driver of M1 polarization, however stimulation with TLR2/1L failed to potently decrease CD163 expression. This incomplete repolarization may be due to an increase in IL-10 secretion as TLR2/1L treatment of human monocytes is reported to induce high levels of IL-10[115], which may counteract any decrease in CD163 expression. To identify factors which may antagonize the IL-10 induced program, an upstream analysis was performed by Ingenuity Pathways Analysis (Figure 3A). IFN-γ was identified as the most significant repressor of the IL-10-induced program with p-value 3.9×10^{-34}, suggesting that the ability of TLR2/1L+ IFN-γ to reverse M2 MΦ polarization is at least in part due to IFN-γ-mediated suppression of TLR2/1L-induced IL-10 secretion. To investigate whether IFN-γ can suppress the levels of IL-10 protein induction, M2 MΦ were stimulated with TLR2/1L or TLR2/1L in combination with IFN-γ for 24h, and IL-10 protein secretion was measured by ELISA. Similar to previously published data, stimulation with TLR2/1L alone induced secretion of 130±52pg/ml IL-10 protein (Figure 3B). Co-stimulation with IFN-γ repressed TLR2/1L-induced secretion of IL-10 by 52% to 63±18pg/ml. M2 MΦ were also stimulated with TLR2/1L for three days in the presence of αIL-10 neutralizing antibody or isotype control to determine if TLR2/1L-induced secretion of IL-10 prevented a complete decrease of CD163 expression. Stimulation in the presence of neutralizing antibody led to a complete down-regulation of CD163 expression to 15.3% positive cells versus 41.1% $CD163^+$ cells in the isotype control, thus confirming that

TLR2/1L-induced IL-10 secretion prevented a decrease in CD163 expression and complete MΦ reprogramming.

Reeducation of M2 MΦ to M1-like MΦ leads to a loss of phagocytic function

In addition to CD163 surface expression, M2 MΦ are characterized by enhanced phagocytic function and an increase in uptake of oxidized lipoprotein as compared to M1 MΦ[14]. To determine whether the change in MΦ phenotype also led to a change in MΦ function, M2 MΦ were cultured with stimuli as in Figure 2c and assayed for DiI-labeled oxLDL uptake via flow cytometry. Simultaneous stimulation of TLR2/1L and IFN-γ led to the highest decrease in oxLDL uptake, to 120 mean florescence intensity (MFI) from 455 MFI with IL-10 treatment (Figure 4A). TLR2/1L stimulation showed no significant decrease in oxLDL uptake, whereas IFN-γ (245 MFI) or IL-15 (265 MFI) showed an intermediate decrease. To determine whether this effect on oxLDL uptake was due to a fluctuation in receptor expression, we assessed the surface expression of CD36, a scavenger receptor highly induced by IL-10 and the major receptor for oxLDL. Surface CD36 expression was measured by flow cytometry after M2 MΦ were reeducated by TLR2/1L or IFN-γ, alone or in combination, or IL-10, and normalized to MFI oxLDL uptake. Figure 4B shows the surface expression of CD36 is most decreased in costimulation of TLR2/1L and IFN-γ while either stimulation alone did not have a statistically significant effect.

Reprogramming of M2 MΦ to M1-like MΦ correlates with an induction of antimicrobial activity

TLR2/1L or IFN-γ treatment of adherent monocytes can trigger activation of the vitamin D pathway, in which upregulation of 25 hydroxylase enzyme CYP27b1 leads to the conversion of intracellular inactive 25-hydroxyvitamin D (25D) to active 1,25-hydroxyvitamin D (125D)[44,33] {Liu 2008, Fabri 2011, Kristina paper}. 1,25D production and subsequent VDR activation leads to the production of antimicrobial peptides cathelicidin (*CAMP*) and human beta defensin 2 (*DEFB4*) which can directly kill mycobacteria such as leprosy and tuberculosis bacilli. While IL-10 MΦ are phagocytic and can take up many mycobacteria bacilli, they lack CYP27b1 expression and fail to metabolize 25D to 1,25D to induce antimicrobial peptide production, thus rendering them appealing hosts for mycobacteria to take up residence[14]. Given that TLR2/1L and IFN-γ treatment can reverse polarization of M2 MΦ, we investigated whether treatment could also enhance M1 MΦ function such as induction of the antimicrobial pathway. M2 MΦ were stimulated with TLR2/1L+IFN-γ, IL-10 or media alone for 24h to evaluate if these stimulations could induce expression of CYP27b1 enzyme. TLR2/1L+IFN-γ showed an induction of 11-fold over media alone, while IL-10 stimulation did not have a significant difference (Figure 5A). In addition, stimulation of reprogrammed M2 MΦ in the presence of exogenous 25D3 for 24h suggested that the CYP27b1 enzyme is active and can convert inactive 25D3 to its active form leading to antimicrobial peptide production (unpublished data). Results show that M2 MΦ stimulated with TLR2/1L + IFN-γ were able to induce expression of *CAMP* and *DEFB4*, while TLR2/1L alone did not significantly induce either antimicrobial peptide (Figure 5B). In summary, TLR2/1L + IFN-γ treatment is able to reeducate M2 MΦ into M1-like MΦ by decreasing CD163 expression, suppressing scavenger receptor expression and phagocytic function, and inducing Cyp27b1 expression to enable antimicrobial peptide production.

Discussion:

The induction of MΦ activation and polarization allows alteration of phenotype and function to mount an antimicrobial response but can also result in pathologic consequences. MΦ plasticity and reeducation allows for optimization of the immune response to appropriately respond to microbial infection. Here, we show that stimulation with IL-15 induced and maintained M1 MΦ polarization, but the addition of IL-10 induced reeducation to M2-like MΦ with enhanced phagocytic function. In contrast, IL-10 treatment induced and maintained M2 MΦ polarization; however, IL-15 was not sufficient to trigger plasticity. Analysis of M1 and M2 MΦ receptor expression led to the discovery that co-addition of IFN-γ and TLR2/1L, but not either one alone, to M2 MΦ induced conversion to M1-like MΦ, with upregulation of key components of the antimicrobial pathway. The regulation of MΦ plasticity allows flexibility in the innate immune response in defending the host against microbial pathogens.

M2 MΦ play a critical role in the initial response to tissue injury, clearing the site of tissue destruction of cellular debris and apoptotic cells, as well as eliminating invading pathogens, to allow for tissue repair and regeneration[116]. Uncontrolled production of inflammatory mediators by M1 MΦ coupled with a deficient population of anti-inflammatory M2 MΦ can subsequently lead to persistent injury. Thus, the ability to reeducate M1 MΦ to M2 MΦ can prove beneficial in cases of unresolved tissue injury and other pathologies driven by M1 MΦ. Here we show that IL-10 treatment could not only maintain M2 MΦ polarization, but it could also reeducate M1 MΦ to become more M2-like. One of the beneficial effects of IL-10 during inflammation was recently demonstrated by Jiang et al, showing that IL-10 treatment during particle challenge could lessen the harmful effects of inflammation on bone mineral density during joint replacement wear[117]. Other M2 MΦ-switching compounds such as pomegranate juice polyphenols, which have been reported to have anti-inflammatory properties in immune-

mediated diseases such as rheumatoid arthritis, LPS- or UVB-induced inflammation, or atherosclerotic vessel inflammation, also induce expression of IL-10, although the role of IL-10 has not been investigated[118]. Further exploration into reeducation of M1 MΦ and the effects of IL-10 treatment during inflammation are needed to ascertain the ability of IL-10 to promote MΦ switching and aid in inhibition of disease progression.

In the context of intracellular infections, M2 MΦ are not protective and promote disease pathogenesis, whereas M1 MΦ can induce antimicrobial responses and clear the pathogen. Several studies have highlighted the ability of intracellular pathogens to promote M2 MΦ polarization and even reeducate M1 MΦ to M2-like MΦ to enhance bacterial survival[119], demonstrating the importance of appropriate MΦ polarization to mount an effective immune response to infection. Additionally, reeducation to M1 MΦ has also displayed antitumor effects[120,121], further substantiating the need to identify mechanisms of M2 to M1 MΦ switching. Here we show that while IL-15 is insufficient to reverse polarization of differentiated M2 MΦ due to a downregulation of IL-15 receptor expression, treatment with IFN-γ + TLR2/1L was able to reeducate M2 MΦ, decrease phagocytic function, and induce expression of antimicrobial genes such as CYP27b1, CAMP, and DEFB4. Thus, M2 to M1 MΦ switching can be a powerful tool in initiating host defense against intracellular pathogens. Further exploration into mechanisms of M2 MΦ reeducation is needed for development of therapeutics for intracellular pathogens and tumor development.

With the characterization of MΦ cell types and their relative protective roles in tissue injury, infection, and tumor development, recent efforts have delved into the application of MΦ-based cell therapies as a means to alter MΦ polarization to mount appropriate responses[122]. Here we propose another mechanism to alter MΦ function, with the identification of ligands capable of MΦ reeducation.

Materials and Methods:

Reagents:

IL-10 (R&D Systems) and IL-15 (graciously provided by Dr. Thomas Waldmann) were used for macrophage differentiation. Antibodies for cell surface staining are as follows: CD163 (BD PharMingen), CD209 (BD PharMingen), CD36 (BD PharMingen), TLR1 (EBioscience), IFNGR1 (R&D), IFNGR2 (R&D), and isotypes (Thermofisher). Synthetic 19kDa lipoprotein derived from mycobacteria (EMC Microcollections) and recombinant human IFN-γ (BD Biosciences) were used for macrophage reeducation. Anti-IL-10 (Invitrogen) and IgG1 isotype control (BioLegend) were used for neutralization studies.

Macrophage Differentiation and Reeducation:

Peripheral blood was acquired from healthy donors with informed consent (UCLA Institutional Review Board #125.15.0-f). As previously described, adherent monocytes were isolated[44] and differentiated[14] into M1 or M2 macrophages using 50ng/ml IL-15 or 10ng/ml IL-10, respectively. After 3 days of differentiation, cells were deadhered and viable cells were counted by Trypan blue counterstain. Macrophages were allocated for labeling of cell surface markers CD209 and CD163 as previously described[14] and purification using CD209+ beads (Miltenyi Biotec) according to manufacturer's protocol. $CD209^+$ macrophages were then stimulated for an additional three days with the following ligands alone or in combination: 50ng/ml IL-15, 10ng/ml IL-10, TLR2/1L (10ug/ml), IFN-γ (1.25ng/ml), and assessed for reeducation by cell surface labeling of CD209 and CD163.

IL-10 Secretion and Neutralization Studies:

IL-10 MΦ were treated with TLR2/1L alone or in combination with IFN-γ for 24h and supernatants were assayed for IL-10 protein levels by ELISA. For IL-10 neutralization studies, IL-10 MΦ were incubated with αIL-10 blocking antibody or isotype control prior to TLR2/1L treatment for 24h. Cells were then labeled for CD163 cell surface expression as previously described[14].

Endocytosis Assays:

Reeducated IL-10 MΦ were incubated for 4h at 37ºC with DiI(1,1'-dioctadecyl-3,3,3',3'-tetramethylindocarbocyanine perchlorate)-labeled $CuSO_4$-oxidized low-density lipoprotein (Intracel) and assayed for uptake as previously described[14]. Some macrophages were also labeled with CD36 antibody and mean fluorescence intensity was acquired by flow cytometry according to established methods[14].

Real-Time Quantitative PCR:

IL-10 MΦ were stimulated with IL-10, TLR2/1L+IFN-γ, or TLR2/1L for 24h and mRNA expression of CYP27b1, CAMP, or DEFB4 were assayed as previously described[14].

FIGURE 1: IL-10 is sufficient to reprogram M1 MΦ, but IL-15 is not sufficient to reprogram M2 MΦ

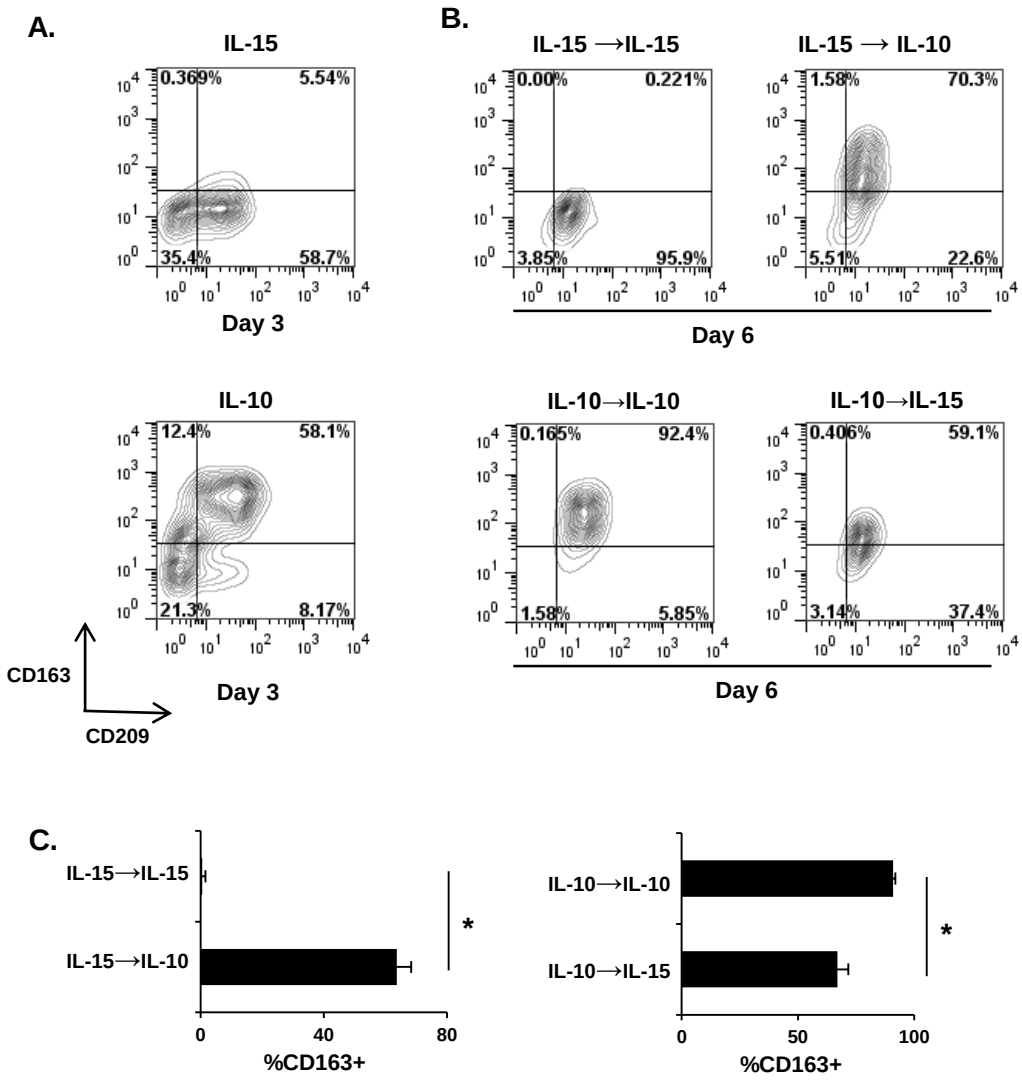

Figure 1: IL-10 is sufficient to reprogram M1 MΦ, but IL-15 is not sufficient to reprogram M2 MΦ

(A) Adherent PBMC were stimulated with IL-15 (above) or IL-10 (below) for three days and then labeled with antibodies to cell surface markers CD163 and CD209.

(B) IL-15-derived M1 MΦ (above) and IL-10-derived M2 MΦ (below) were washed and treated with either IL-15 or IL-10 for an additional three days (above) and labeled with antibodies to cell surface markers CD163 and CD209 at day 6.

(C) Quantification of percentage of $CD63^{+}$ cells from (B).

Flow diagrams are representative of n=3 and depicted as mean florescence intensity (MFI) subtracted from background (ΔMFI) for each antibody. *$p<0.05$

SUPPLEMENTARY FIGURE 1: Increasing concentrations of IFN-γ did not further decrease percentage of CD163⁺ cells

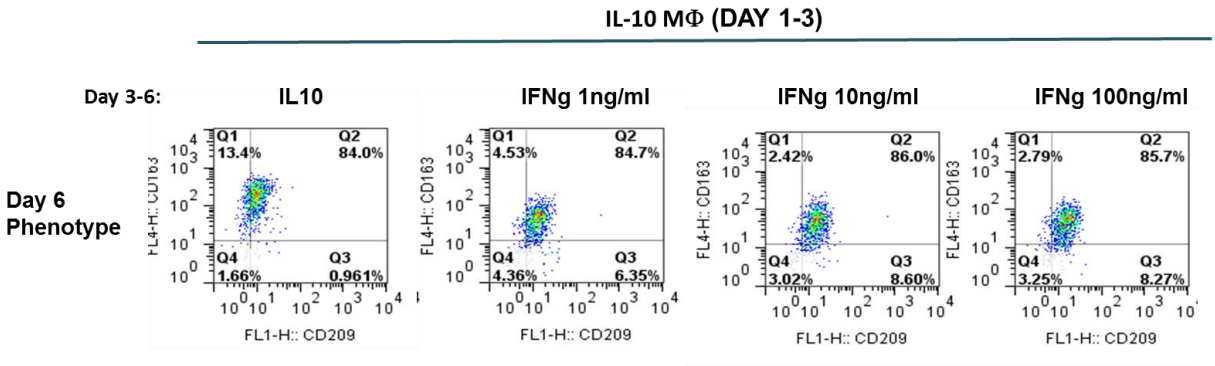

Figure S1: Increasing concentrations of IFN-γ did not further decrease percentage of CD163+ cells

IL-10-derived M2 MΦ were washed and treated with either IL-10 or IFN-γ at the concentrations indicated for an additional three days (above) and labeled with antibodies to cell surface markers CD163 and CD209 at day 6.

Flow diagrams are representative of n=3 and depicted as mean florescence intensity (MFI) subtracted from background (ΔMFI) for each antibody

FIGURE 2: Differential expression of MΦ receptors suggest ligands to change MΦ phenotype

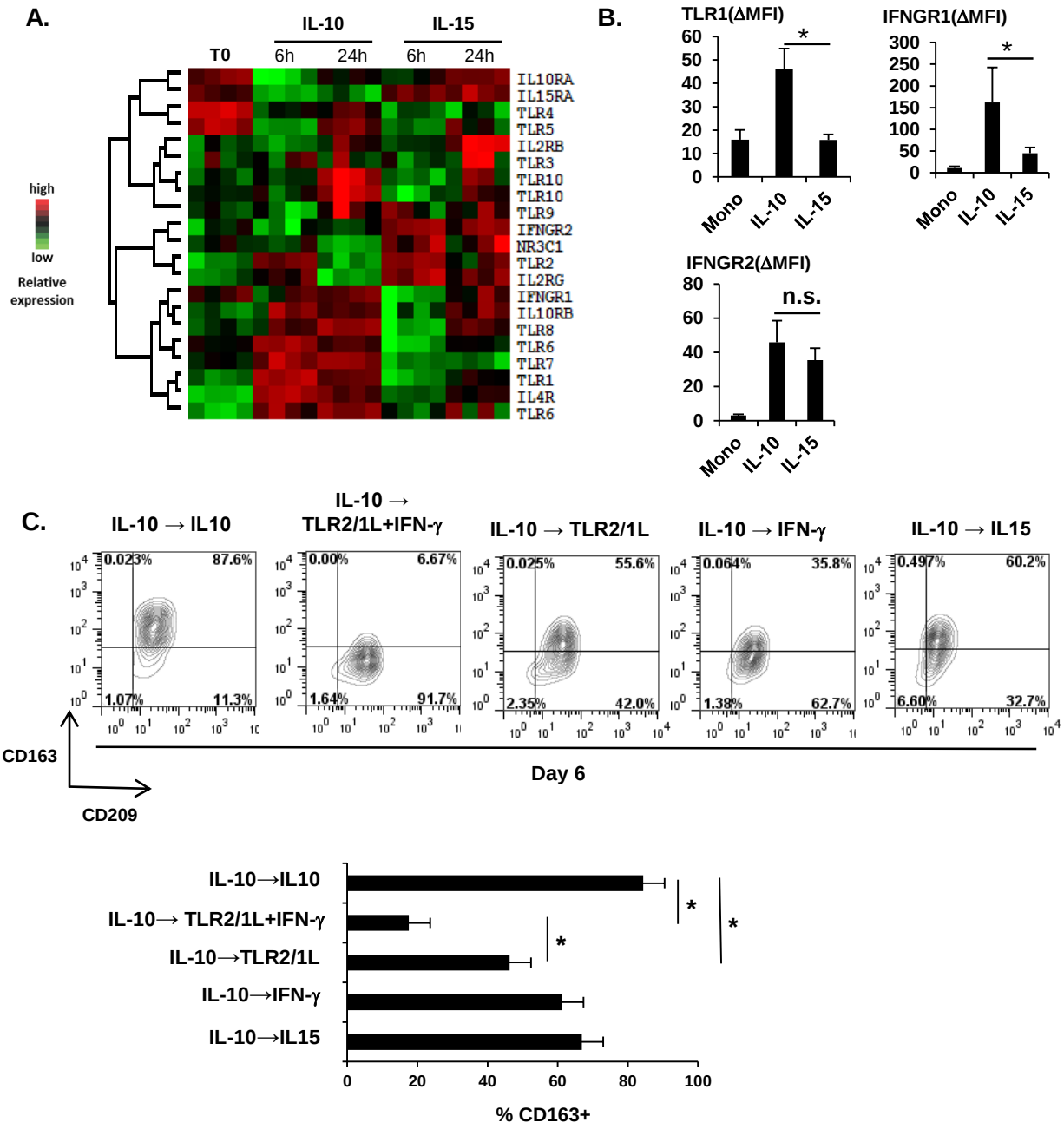

Figure 2. Differential MΦ receptors suggest ligands to change macrophage phenotype

(A) Heat map displaying receptor expression data from previously published transcriptional signatures of adherent human peripheral blood mononuclear cells stimulated with IL-10 or IL-15, or time zero unstimulated cells. Each row represents one gene and each column represents a sample taken at the time point indicated. Red indicates higher expression and green depicts lower expression.

(B) Adherent PBMC stimulated with IL-10 or IL15 for three days or freshly isolated monocytes were labeled with specific antibodies to TLR1, IFNGR1, or IFNGR2. Receptor expression is quantified as mean florescence intensity (MFI) subtracted from background (ΔMFI) for each antibody. n=3

(C) IL-10-derived M2 MΦ were treated with the ligand indicated for an additional three days and labeled with antibodies to cell surface markers CD163 and CD209 at day 6. Flow diagrams (above) are representative of n=3 and percentage of $CD163^{+}$ cells were quantified (below).

FIGURE 3: TLR2/1L-induced secretion of IL-10 prevents change in MΦ phenotype by TLR2/1L

A.

Upstream Regulator	Molecule Type	Predicted Activation State	Activation z-score	p-value of overlap
IFNG	cytokine	Inhibited	-2.970	3.89E-34
IRF7	transcription regulator	Inhibited	-5.279	1.07E-19
IFNA2	cytokine	Inhibited	-4.018	2.77E-18
poly rI:rC-RNA	chemical reagent	Inhibited	-3.804	2.50E-17

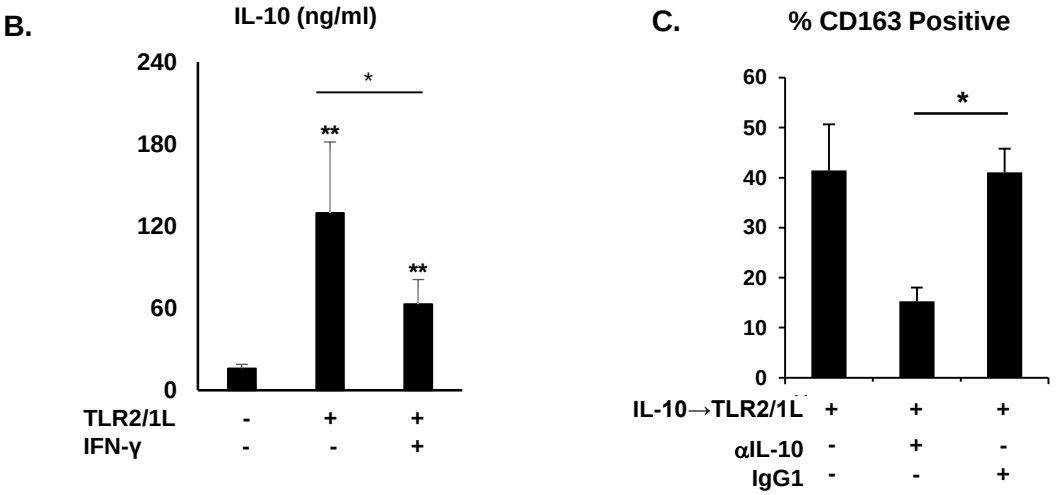

Figure 3: TLR2/1L-induced secretion of IL-10 prevents change in MΦ phenotype by TLR2/1L

(A) Top potential upstream regulators of the IL-10 induced gene program as determined by Ingenuity Pathways Analysis

(B) Quantification of IL-10 secretion after stimulation of IL-10-derived M2 MΦ with TLR2/1L, IFN-γ, or combination of TLR2/1L+IFN-γ for 24h.

(C) IL-10-derived M2 MΦ were incubated with αIL-10 blocking antibody or isotype control and then stimulated with TLR2/1L for 24h. Cells were then labeled with antibody to CD163 and percentage of CD163+ cells was assessed by flow cytometry.

Experiments are representative of n=3, *p<0.05, **p<0.01

FIGURE 4: Reprogramming of M2 to M1-like MΦ correlates with a loss of phagocytic function

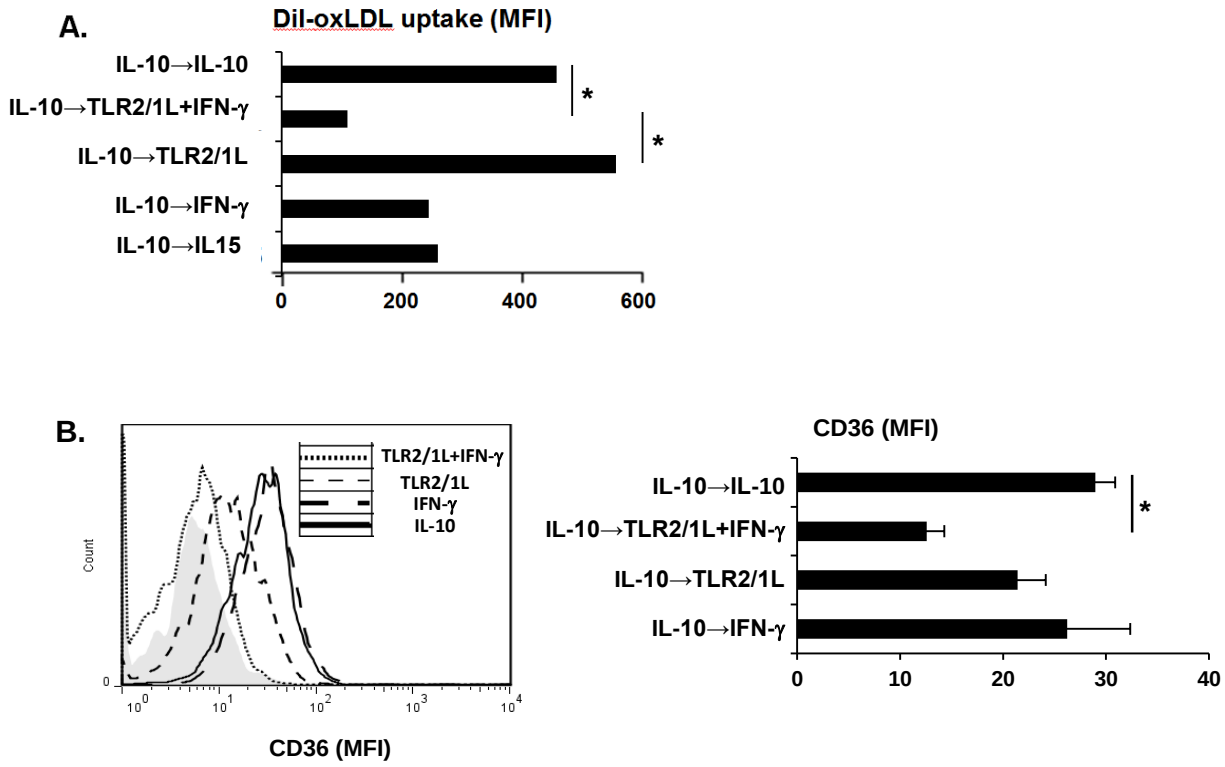

Figure 4: Reprogramming of M2 to M1-like MΦ correlates with a loss of phagocytic function

(A) IL-10-derived M2 MΦ were treated with the ligand indicated for an additional three days and then assayed for DiI-labeled oxLDL uptake via flow cytometry. Uptake was determined by MFI.

(B) IL-10-derived M2 MΦ were treated with the ligand indicated for an additional three days and then labeled with specific antibody to cell surface marker CD36. CD36 MFI is pictured as a histogram (left) and quantified (right).

Experiments are representative of n=3, *p<0.05

FIGURE 5: Reprogramming of M2 to M1-like MΦ correlates with an induction of antimicrobial activity

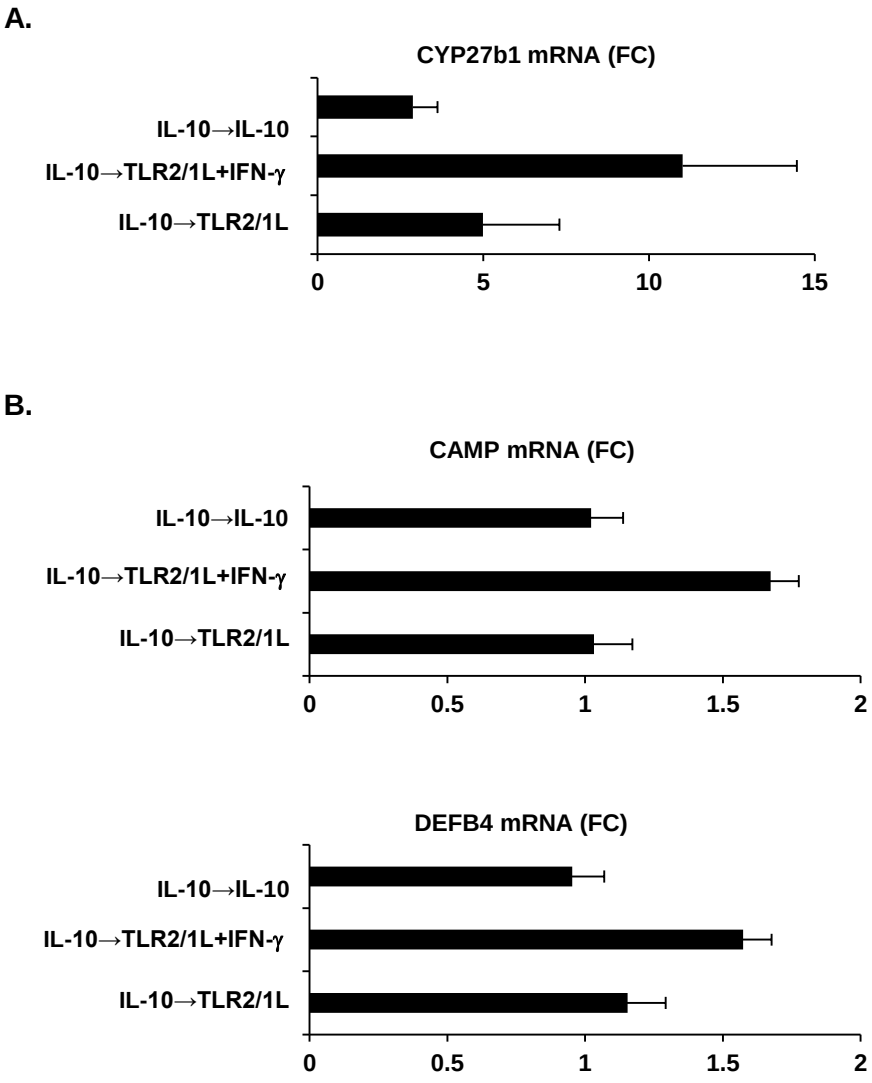

Figure 5: Reprogramming of M2 to M1-like MΦ correlates with an induction of antimicrobial activity

IL-10-derived M2 MΦ were stimulated with the ligand indicated for 24h and assayed for CYP27b1 (A), CATH (B), or DEFB4 (C) expression by qPCR. mRNA levels were normalized to h36b4 levels and fold change was determined as compared to media controls. Experiments are representative of n=3.

CHAPTER 4:

Elucidating *M. leprae*-induced gene programs that enhance bacterial survival

Introduction:

The induction of antimicrobial pathways in infected macrophages is a crucial part of the innate immune response to eliminate an invading pathogen. At the same time, however, the pathogen evades these host defense mechanisms by inhibiting innate immunity. Leprosy, caused by *Mycobacterium leprae*, provides an excellent model to study human pathways of host defense as well as mechanisms by which an intracellular pathogen escapes antimicrobial responses and establishes chronic infection. The disease presents as a clinical spectrum, with the two poles mirroring the immune response to infection[12]. At one end of the spectrum, tuberculoid leprosy (T-lep) represents a self-contained form of disease, with patient lesions characterized by production of the Type II interferon, IFN-γ, and activated macrophages with the capacity to kill intracellular mycobacteria[40,13,14]. At the other end of the spectrum, lepromatous leprosy (L-lep) represents the disseminated form of the disease, characterized by the production of Type I interferon and accumulation of macrophages displaying scavenger receptors[13,14]. These macrophages, although highly phagocytic, do not express genes encoding antimicrobial responses, thereby contributing to bacterial persistence.

The ability of activated macrophages to eliminate intracellular mycobacteria involves the induction of antimicrobial mediators. In mouse macrophages, the generation of nitric oxide is essential to kill *M. tuberculosis*. In human macrophages, activation leads to the induction of both vitamin D dependent and independent antimicrobial responses[44]. Activation of the vitamin D dependent pathway results in the production of the antimicrobial peptides cathelicidin and defensin beta 2. Many of these antimicrobial responses involve the induction of autophagy, which overcomes the ability of mycobacteria to block phagolysosomal fusion[81,82] and deliver the antimicrobial effector molecules to the compartment in which the pathogen resides.

There are several mechanisms by which intracellular mycobacteria evade innate immunity. One such pathway involves the ability of mycobacteria to induce Type I IFN[123,13] to block antimicrobial responses including the IL-10 dependent inhibition of induction of

antimicrobial peptides. To further explore how mycobacteria evade the innate immune response, we measured the gene expression profile induced by infection of macrophages with *M. leprae* with relevance to the human disease leprosy.

Results:

RNA Sequencing of *M. leprae*-infected MDM reveals an enrichment for a leprosy gene signature

To investigate the effect of *M. leprae* on the immune response in human macrophages, we performed RNA sequencing (RNASeq) on *in vitro* infected cells. $CD14^+$ monocytes were isolated from healthy human donors and cultured with M-CSF for five days to allow differentiation into macrophages (Supplementary Figure 1). Monocyte-derived macrophages (MDM) were then infected with *M. leprae* at a multiplicity of infection (MOI) of 10 with greater than 85% cells infected and RNA was harvested at 1, 2, 24, 48 hours and sequenced. Initially we studied a single donor, with the goal to validate our data with a second RNASeq experiment and subsequently by PCR and immunohistochemistry. A heat map illustrating hierarchical clustering of DESeq normalized counts depicts a cluster of genes expressed prior to and 1h and 2h after infection that are repressed at 24h and 48h (Figure 1A). In addition, a cluster of genes was more highly expressed after 24 and 48h. The *M. leprae*-induced gene signature was thus defined as those genes induced >1.5-fold at 24h or 48h post-infection.

To link the *M. leprae*-induced gene signature in human macrophages with gene expression in leprosy, we overlapped the *M. leprae*-induced genes with the gene expression profiles of leprosy skin lesions[14]. The top 500 genes most highly induced by *M. leprae* in MDM by fold change significantly correlated with genes more highly expressed in L-lep versus T-lep lesions, with an overlap of 62 genes, 3.6-fold greater than expected (Supplementary Figure 3). Gene Set Enrichment Analysis (GSEA) analysis of Hallmarks of the genes that overlap between

M. leprae infected MDM and L-lep lesions indicated a significant enrichment for 'Interferon Gamma Response (p-value $3.44x10^{-15}$),' 'Interferon Alpha Response' (p-value $9.65x10^{-13}$), and 'mTORC1 Signaling' (p-value $8.81x10^{-9}$) signatures (Figure 1C), all pathways that play an important role in mycobacterial infection.

RNASeq of *M. leprae*-infected MDM reveals an enrichment for Type I IFN signature

Given that Type I and Type II interferons signal through a common signaling molecule, we utilized an integrative bioinformatics approach to examine the relative contribution of Type I and Type II interferons in the *M. leprae*-induced gene signature. The *M. leprae*-induced gene signature was overlapped with curated IFN-β- and IFN-γ-specific gene expression profiles derived from RNASeq data from stimulated MDM (unpublished data), 71 genes were identified in common with the IFN-β-specific dataset, two-fold higher than expected with a signed log10 p-value of eight (Figure 1D). In contrast, there were only two genes in common with the IFN-γ-specific dataset, suggesting that the interferon signature was most likely solely due to an induction of Type I interferon. Taken together, the *M. leprae*-induced gene signature was enriched for Type I interferon genes characteristic of L-lep lesion gene profiles.

Transcriptome analysis highlights a significant cluster of genes enriched for autophagy

To gain a better understanding of the effect of *M. leprae* infection on host gene expression, we first performed a weighted correlation network analysis (WGCNA) to identify clusters of similarly coexpressed genes. WGCNA is a widely used bioinformatics tool for simplifying large datasets into modules of correlated genes with similar function. Significant modules can be analyzed separately or in contrast to each other to identify potential phenotypic or functional differences in gene expression that can ultimately be correlated with disease.

Based on the similar hierarchical clustering of 1h and 2h, as well as 24h and 48h, WGCNA was performed on single and combinations of time points post-infection. Analysis reduced the gene expression profile into 29 modules each comprised of 34 to 2795 genes, of which multiple modules were significant ($p<0.05$, correlation>0.9) (Figure 2A). The most highly significant module, 'MEgreenyellow', was composed of 1627 genes and enriched within the 24h+48h vector with p-value $6x10^{-04}$. Correlation scores of genes within the 'MEgreenyellow' module show a high module membership and significance between genes (Supplementary Figure 4).

Ingenuity IPA Core analysis of this module yielded gene ontology (GO) terms relevant to infection including 'Interferon Signaling' (-log(p-value) 7.83) and 'autophagy' (-log(p-value) 2.98), consistent with that seen in the overlap with L-lep lesions (Figure 2B). Depiction of 'MEgreenyellow' genes with a potential role in autophagy derived from siRNA screens[124] led to the discovery of a highly expressed autophagy regulator during *M. leprae* infection as well as in lepromatous leprosy: NUPR1 (Figure 2C). The top gene, NUPR1, was induced 46-fold in *M. leprae*-infected MDM and expressed 2.7-fold higher in L-lep versus T-lep.

Given the potentially interesting role of NUPR1 in autophagy, we decided to focus on NUPR1 and investigate its induction during infection. RNASeq revealed NUPR1 as one of the most highly induced genes during *M. leprae* infection of macrophages, increasing 46-fold after 48h (Figure 3A). This was validated in a subsequent RNASeq performed by collaborators (unpublished data, Supplementary Figure 2B) as well as by qPCR of *M. leprae*-infected MDM (Figure 3A). *M. leprae* induced NUPR1 17-fold at 24h and 67-fold at 48h post-infection. In summary, these data identify NUPR1 as a key gene induced in *M. leprae*-infected MDM, differentially expressed in L-lep versus T-lep lesions, and connected in a network to genes involved in autophagy.

M. leprae-mediated induction of NUPR1 is dependent on Type I IFN signaling

NUPR1 was one of the most highly upregulated genes within the 'MEgreenyellow' module, which was also enriched for Type I IFN signaling. Mining the RNASeq data used in Figure 1 of IFN-β- and IFN-γ-stimulated MDM, we found that NUPR1 was highly induced by IFN-β, increasing 553-fold, but only modestly induced by IFN-γ, 10.4-fold (Figure 3B). qPCR for NUPR1 after 24h interferon treatment confirmed this strong induction by IFN-β at 24h. A dose titration of IFN-β revealed a dependency of NUPR1 on IFN-β, where NUPR1 expression increased with increasing concentrations of IFN-β (Figure 3C).

To establish whether *M. leprae*-mediated induction of NUPR1 in MDM occurred through Type I IFN signaling, we incubated MDM with a blocking antibody to the Type I IFN receptor prior to infection. Antibodies to IFN-β cytokine have proven unsuccessful in fully eliminating Type I interferon signaling; however, several reports have shown dampening of signaling when using blocking antibody to one of the receptor chains, IFN-aR1. Incubation of MDM with αIFNAR antibody, but not Isotype antibody, prior to infection led to a drastic decrease in NUPR1 expression (Figure 3D), from 3.7-fold to 0.5-fold, thereby confirming NUPR1 is at least partially induced during infection through activation of Type I IFN signaling. Blocking of Type I IFN signaling was confirmed using IFN-β stimulation (Supplementary Figure 5).

NUPR1 protein is more highly expressed in L-lep lesions

The enrichment of NUPR1 mRNA in L-lep versus T-lep lesions as determined by microarray was 2.7-fold, with probe intensities of 8626.1 versus 3160.86, $p<0.01$[14] (Figure 4A). This was confirmed by qPCR, showing 5.6-fold higher NUPR1 expression in L-lep samples. To determine whether the message was turned into protein, we analyzed NUPR1 protein levels in lesional tissue by immunoperoxidase staining. Concordantly, more NUPR1 protein was seen in

L-lep versus T-lep lesions as well (Figure 4B). Using the online software Immunoratio[125], we quantified the overlap of NUPR1 immunoperoxidase staining with hematoxylin-stained nuclei as shown in Figure 4C, which shows a significant difference of NUPR1 protein levels of 75% cells in L-lep tissue versus 45% of cells in T-lep tissue ($p<0.05$).

Discussion:

Although the innate immune system attempts to mount an antimicrobial response to destroy intracellular pathogens such as mycobacteria, microbes have developed mechanisms to block antimicrobial activity and evade clearance. To address the question of how mycobacteria can alter the host immune response to promote its own survival, we measured the gene expression profile of MDM infected with a high MOI of *M. leprae*. Hierarchical clustering identified *M. leprae*-induced genes, which by bioinformatics analysis were found to be enriched for genes differentially expressed in L-lep vs. T-lep lesions and induced by Type I IFN. Further analysis revealed a gene network linked to autophagy containing NUPR1, which was highly expressed in L-lep lesions and induced by Type I IFN. Given that NUPR1 can block autophagy[99,100], which is required for a macrophage antimicrobial activity, these data provide one mechanism by which *M. leprae* evades the host immune response.

We identified NUPR1 as a potential gene involved in the pathogenesis of the disease leprosy using an integrated bioinformatics approach. NUPR1 was found to be induced: i) at 24 and 48h in *M. leprae* infected MDM, ii) in an autophagy-enriched gene module, 'MEgreenyellow', identified by WGCNA in the *M. leprae* infected MDM, iii) in L-lep vs. T-lep lesions; and, iv) in type I IFN treated MDM. Informatics analysis linked NUPR1 to an "mTORC1 signaling" pathway in the overlap of the *M. leprae*-induced gene signature and genes highly expressed in L-lep lesions induced genes as well as in a curated list of autophagy regulators in the 'MEgreenyellow' module. The ability to integrate gene expression data from *in vitro* infected

cells with gene expression profiles derived from the site of infection provides a powerful tool to identify relevant mechanisms of host defense and immune evasion.

NUPR1 was linked to autophagy based on a curated list of autophagy regulators derived from published siRNA screens, pathway analysis algorithms and text mining of the literature[124]; however, the literature investigating the role of NUPR1 in autophagy is conflicting. NUPR1 has been reported to play both positive and negative roles in autophagy by regulating expression of autophagy inducer BNIP3 (negative)[99], correlating with AURKA expression (negative)[100], upregulating the mTOR inhibitor TRB3 (positive)[101] or altering expression of long non-coding RNA from TGFB2 that serves as a microRNA sponge for autophagy-regulating microRNAs (positive)[102]. Preliminary analysis of gene expression of BNIP3, AURKA, and TRB3 suggest a negative role for NUPR1 during *M. leprae* infection, but further studies are needed to determine the function of NUPR1 in infection and whether it plays a role in i) autophagy, ii) subsequent bacterial viability, and iii) the ability of MΦ to present antigen to other cells.

Exploration into the mechanism of NUPR1 upregulation by *M. leprae* revealed NUPR1 induction to be dependent on type I IFN signaling. The differential expression of Type II vs. Type I IFNs at the site of disease in leprosy is thought to contribute to development of the T-lep and L-lep clinical forms, respectively[14], where the level of severity of mycobacterial disease closely correlates with the level of responsiveness to Type II interferon, IFN-γ. Previous studies have shown that IFN-β, a type I IFN, is induced following *in vitro* infection of monocytes and downregulates IFN-γ-induced antimicrobial activity in an IL-10-dependent manner[14]. Here we provide a possible mechanism by which IFN-β may be able to downregulate other IFN-γ-mediated antimicrobial activities such as autophagy via induction of NUPR1.

Immunohistochemistry analysis of NUPR1 expression in leprosy skin biopsies revealed NUPR1 mRNA is more highly expressed in L-lep versus T-lep lesions. This is mirrored in protein expression as well, where NUPR1 immunostaining in L-lep lesions revealed higher NUPR1 protein colocalization with hematoxylin nuclear staining. Intriguingly, although NUPR1

is a transcription factor and should be found in the nucleus, protein was found in both the nucleus and the cytosol in L-lep lesions. This is similar to previous studies investigating NUPR1 localization in pancreatic[126] and thyroid cancers[127]. Comparison of NUPR1 expression in thyroid carcinomas showed a correlation between higher NUPR1 cytosolic localization and more malignant papillary carcinomas of larger size or containing poorly differentiated lesions[127]. The reason for high cytoplasmic NUPR1 expression is still unclear and whether NUPR1 may have a function in the cytosol is yet to be determined. It may be interesting to see if NUPR1 can function in the binding and sequestering of other proteins from the nucleus. Further exploration needs to be done to address NUPR1 function correlating to NUPR1 localization within the cell.

While there appears to be multiple mechanisms by which macrophages can kill intracellular pathogens, mycobacteria have established methods by which to evade these host immune defenses. *In vitro*, *M. leprae* stimulates production of IFN-β, which not only induces the L-lep cytokine IL-10, but which also blocks components of the vitamin D-dependent antimicrobial pathway and suppresses production of antimicrobial peptides[14]. Here, we performed RNA sequencing on *M. leprae*-infected macrophages and found evidence suggesting *M. leprae* can also induce the expression of genes involved in regulation of autophagy, such as NUPR1, to modify the host immune response and evade bacterial killing. *M. leprae* induces NUPR1 in a type I IFN-dependent manner, suggesting a novel mechanism by which IFN-β may suppress other IFN-γ-mediated antimicrobial responses.

Materials and Methods

Antibodies and Cytokines

M-CSF (R&D Systems) was used for macrophage differentiation. IFN-β, recombinant human IFN-γ (BD Biosciences) were used for macrophage stimulations at the concentrations indicated. Antibodies used were as follows: Neutralization experiments: anti-IFNAR antibody (PBL Assay Science) and corresponding Isotype Antibody mIgG2a, k (BioLegend); Immunoperoxidase Staining: NUPR1 (Abbexa), corresponding Isotype antibody mIgG2b, and Biotinylated Goat anti-mouse IgG2b, Immunofluorescence: anti-LC3, IgG1, and Goat anti-mouse IgG1 Alexa488. For neutralization studies, MDM were incubated with anti-IFNAR1 blocking antibody or Isotype control prior to stimulation with M*. leprae* or IFN-β.

Macrophage Differentiation

Peripheral blood was acquired from healthy donors with informed consent (UCLA Institutional Review Board #125.15.0-f). $CD14^+$ monocytes were isolated from peripheral blood using a Ficoll-hypaque (GE Healthcare) density gradient and subsequent $CD14^+$ positive selection as previously described[128]. $CD14^+$ cells were then cultured for 5 days in RPMI 1640 supplemented with 10% FCS (Omega Scientific) and 50 ng/ml M-CSF to generate MDM.

RNASeq Library Preparation

1.5 million MDM were infected with *Mycobacterium leprae* at a multiplicity of infection (MOI) of 10 in RPMI 1640 + 10% FCS. Cells were lysed at varying time points (0h, 1h, 2h, 24h, 48h) post-infection using RLT Buffer supplemented with 1% B-mercaptoethanol. Samples were bead beated as previously described. Total RNA was then isolated using RNeasy columns according

to manufacturer's protocol and quantified by RiboQuantitation and Qubit (UCLA Core). RNA integrity number of all conditions were determined by Bioanalyzer to be >8. Depletion of ribosomal RNA and library preparation was performed using Ribozero Gold Epidemiology (EpiBio) and TruSeq Sample Preparation Kit (Illumina) as per manufacturer's protocols. Final libraries were reassessed for quality (Qubit and Bioanalyzer), multiplexed at two samples per lane, and sequenced on HiSeq 2000 sequencer (Illumina) with 50bp single-end reads.

Bioinformatics analysis

Sequenced reads were demultiplexed, aligned to the human reference genome hg19 (UCSC), and converted to DESeq normalized counts as previously described[128]. Hierarchical clustering was performed on normalized counts using Cluster 3.0 and graphically represented by TreeView. Weight Gene Network Correlation Analysis (WGCNA) was performed as previously described[128].

Real-time Quantitative PCR

Total RNA was obtained using TRIzol reagent (Invitrogen) and converted to cDNA using Iscript (BioRad) as previously described[44]. Quantitative PCR was performed using KAPA Sybr (KAPA Biosystems) and normalized to housekeeping gene h36b4. Arbitrary units were calculated using the $2^{-(\Delta\Delta Ct)}$ method. NUPR1 primer set was obtained from Quantitect. Primer for h36b4 is as previously described[44].

Leprosy biopsy specimens and immunoperoxidase labeling

Leprosy skin biopsy specimens were collected and processed as previously described[128]. Skin biopsies were cut into cryosections 4um in diameter and incubated with normal goat serum followed by staining with anti-NUPR1, anti-CD3, or isotype control. Sections were subsequently incubated with biotinylated goat anti-mouse IgG, ABC Elite system, and AEC Peroxidase Substrate Kit (Vector Laboratories) and counterstained with hematoxylin prior to mounting in crystal mounting medium (Biomeda). NUPR1 and CD3 staining was visualized and quantified using ImmunoRatio[125].

Live *M. leprae*

Live *M. leprae* was graciously provided to us by Dr. James L. Krahenbuhl of the National Hansen's Disease Programs, Health Resources Service Administration, Baton Rouge, LA. There, *M. leprae* was grown in nude mice footpad and treated with NaOH as previously described.

FIGURE 1: *M. leprae*-infected MDM induce a prominent type I IFN signature

A.

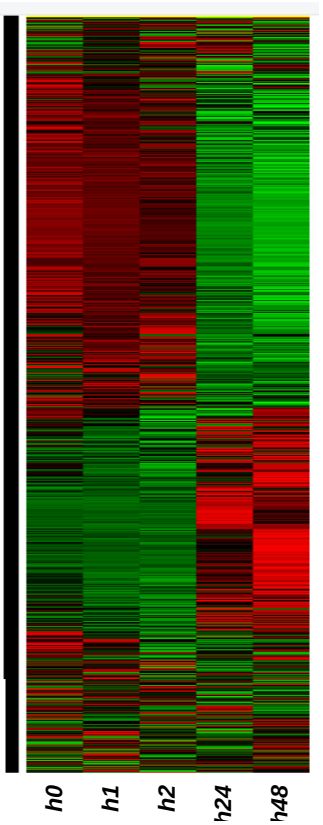

B.

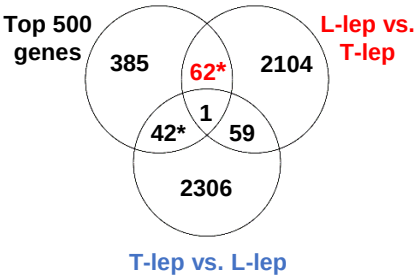

Gene Set Name	# Genes in Gene Set (K)	# Genes in Overlap (k)	k/K	p-value
Interferon_Gamma_Response	**200**	**12**	**0.06**	**5.90E-17**
Interferon_Alpha_Response	**97**	**10**	**0.1031**	**1.07E-16**
TNFa_Signaling_via_NFkB	200	6	0.03	3.16E-07
Hypoxia	200	4	0.02	1.59E-04
Xenobiotic_Metabolism	200	4	0.02	1.59E-04
UV_Response_Up	158	3	0.019	1.30E-03
Apoptosis	161	3	0.0186	1.37E-03
Reactive_Oxygen_Species_Pathway	49	2	0.0408	2.02E-03
MTORC1_Signaling	200	3	0.015	2.54E-03
IL6_JAK_STAT3_Signaling	87	2	0.023	6.22E-03
Androgen_Response	101	2	0.0198	8.30E-03

C.

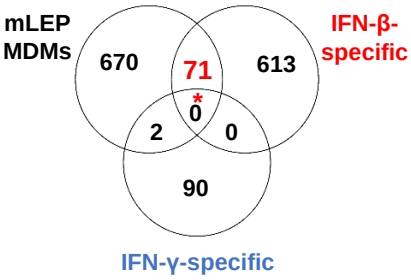

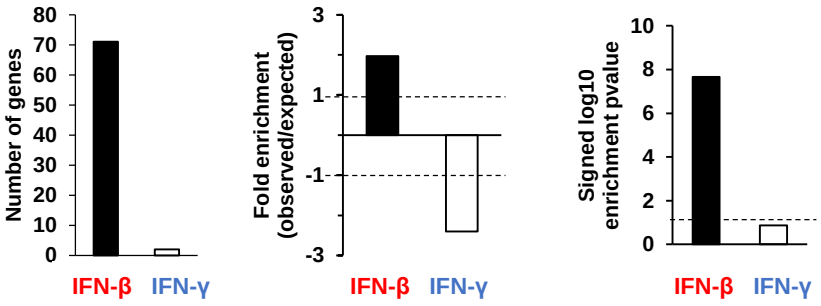

Figure 1: mLEP-infected MDMs reveals enrichment of lepromatous leprosy genes and a prominent Type I IFN signature

(A) Unsupervised single linkage hierarchical clustering of normalized DESeq counts obtained from RNA Sequencing of *M. leprae*-infected MDM at an MOI of 10. Each row corresponds to a gene and each column represents time post-infection as indicated. Red denotes higher expression whereas green indicates lower expression.

(B) Venn diagram depicting top 500 *M. leprae*-induced genes at 24 and 48h overlapped with genes more highly expressed in lepromatous (L-lep) and tuberculoid (T-lep) leprosy lesions (above). Significant genes determined as those with FC>1.5 in comparison to other lesion form with p<.05. Gene Set Enrichment Analysis displaying Hallmark pathways significantly enriched in 62* genes (below). * Denotes significant enrichment over expected as determined by hypergeometric means.

(C) Overlap of *M. leprae*-induced gene signature with IFN-β- and IFN-γ-specific genes (FC>1.5, p<.05, >3 FC versus other stimulation). Hypergeometric enrichment analysis shown as FC enrichment (observed/expected) with dotted line indicating greater than (positive) or less than (negative) expected. Significant of enrichment depicted as signed log10 enrichment p-value with dotted line indicating significance (signed log10 pvalue = 1.3).

SUPPLEMENTAL FIGURE 1: RNA Sequencing of *M. leprae*-infected MDM

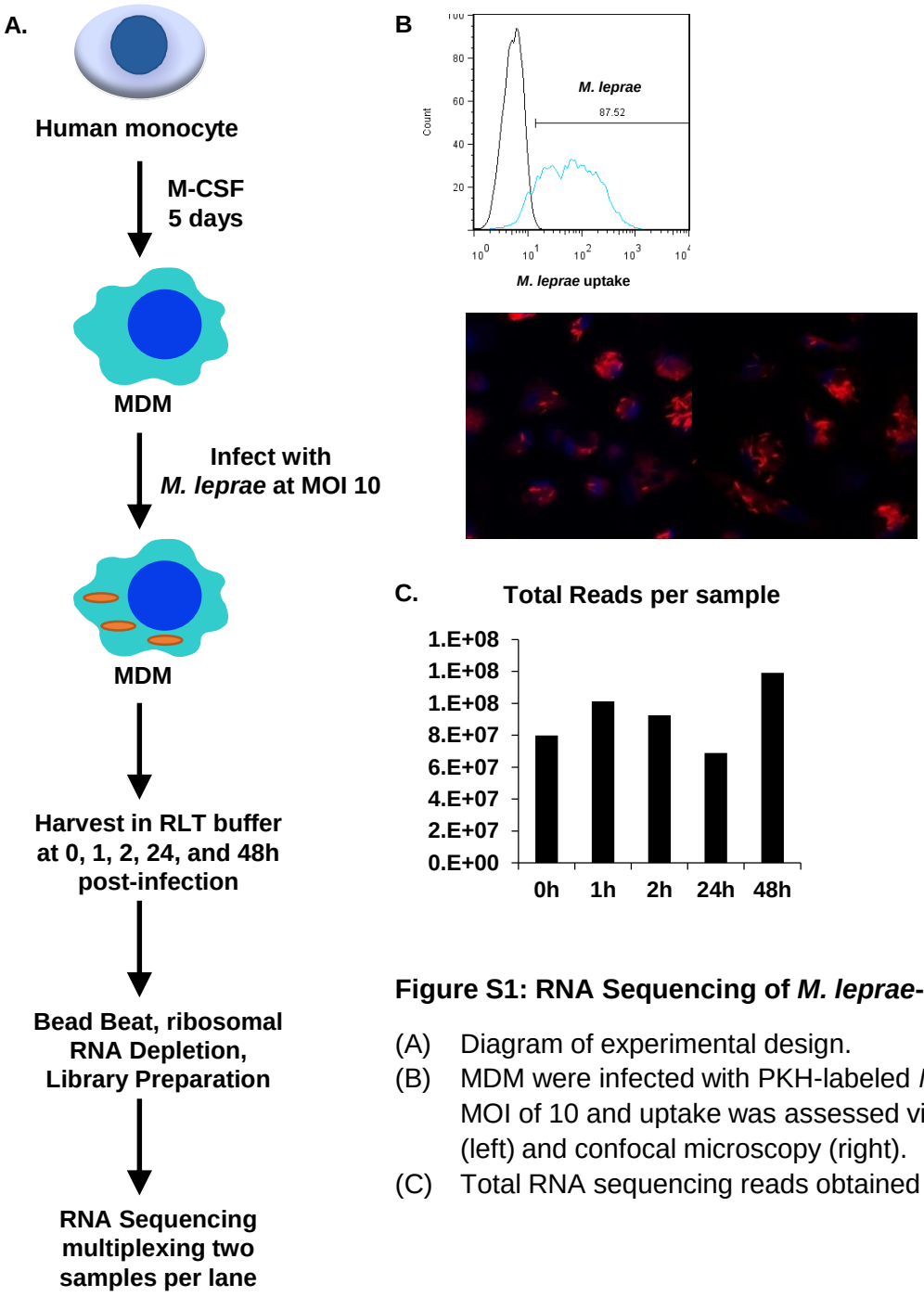

Figure S1: RNA Sequencing of *M. leprae*-infected MDM

(A) Diagram of experimental design.
(B) MDM were infected with PKH-labeled *M. leprae* at an MOI of 10 and uptake was assessed via flow cytometry (left) and confocal microscopy (right).
(C) Total RNA sequencing reads obtained per sample.

SUPPLEMENTAL FIGURE 2: Validation of RNA sequencing results

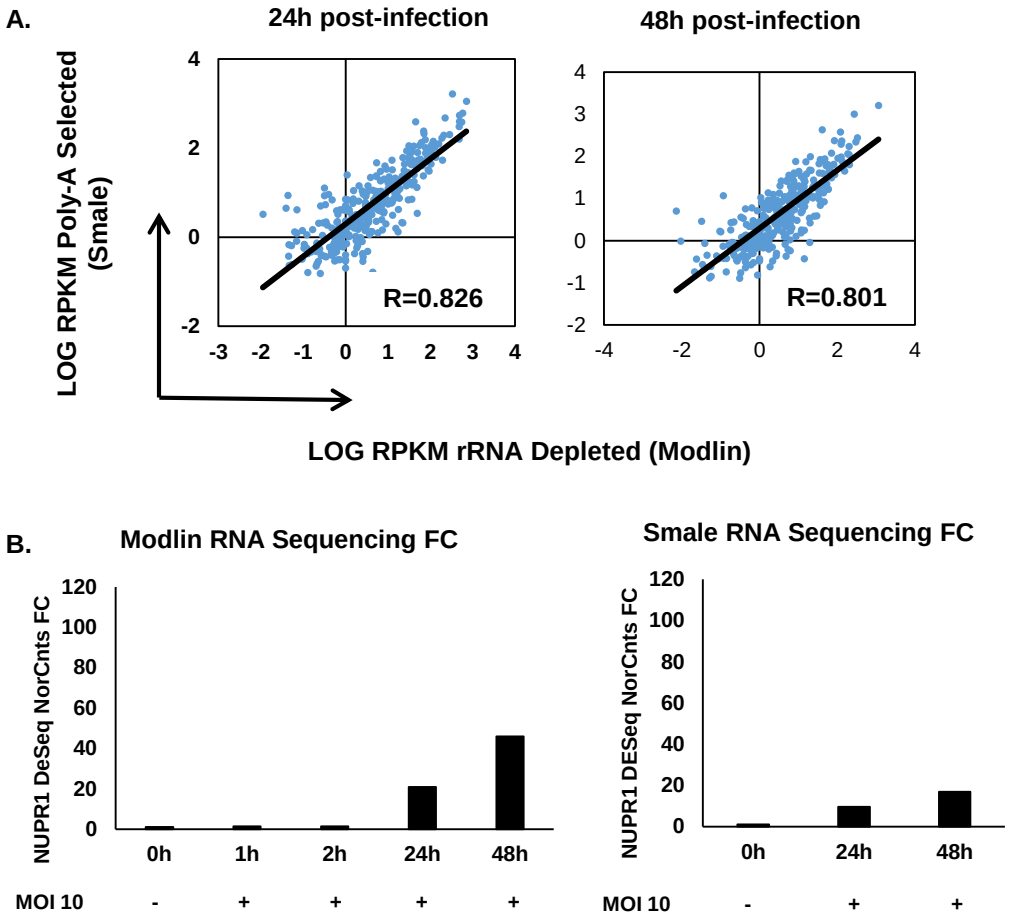

Figure S2: Validation of RNA sequencing results

(A) Assessment of the effect of rRNA-depletion (x-axis) versus poly-A selection (y-axis) on RNA sequencing data obtained on technical replicates of *M. leprae*-infected MDM taken at 24h (left) and 48h (right) post-infection. Trend line and R correlation score are as indicated. Data are representative of n=1.

(B) Comparison of NUPR1 FC obtained from Modlin RNA sequencing (left; n=1) versus Smale RNA Sequencing (right; n=4).

SUPPLEMENTAL FIGURE 3: Top 500 *M. leprae*-induced genes are enriched for L-lep and T-lep signatures

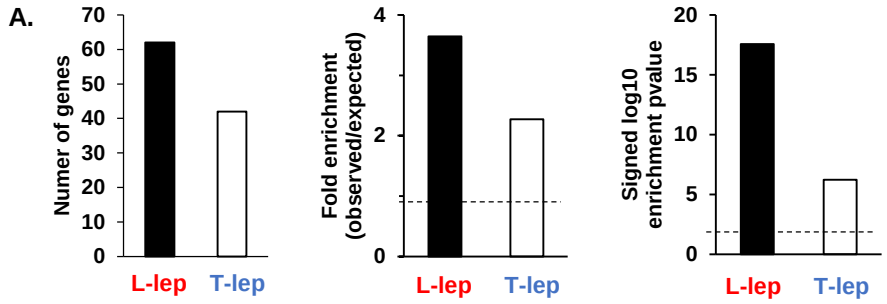

Figure S3: Top 500 *M. leprae*-induced genes are enriched for L-lep and T-lep signatures

(A) Hypergeometric enrichment analysis of overlap of *M. leprae*-induced gene signature with genes more highly expressed in L-lep and T-lep lesions (induced >1.5, p-value<.05, >3 fold change versus other stimulation). Hypergeometric enrichment analysis shown as FC enrichment (observed/expected) with dotted line indicating greater than expected. Significant of enrichment depicted as signed log10 enrichment p-value with dotted line indicating significance (signed log10 pvalue = 1.3).

FIGURE 2: *M. leprae*-induced genes cluster into a significant WGCNA module enriched for autophagy genes

A.

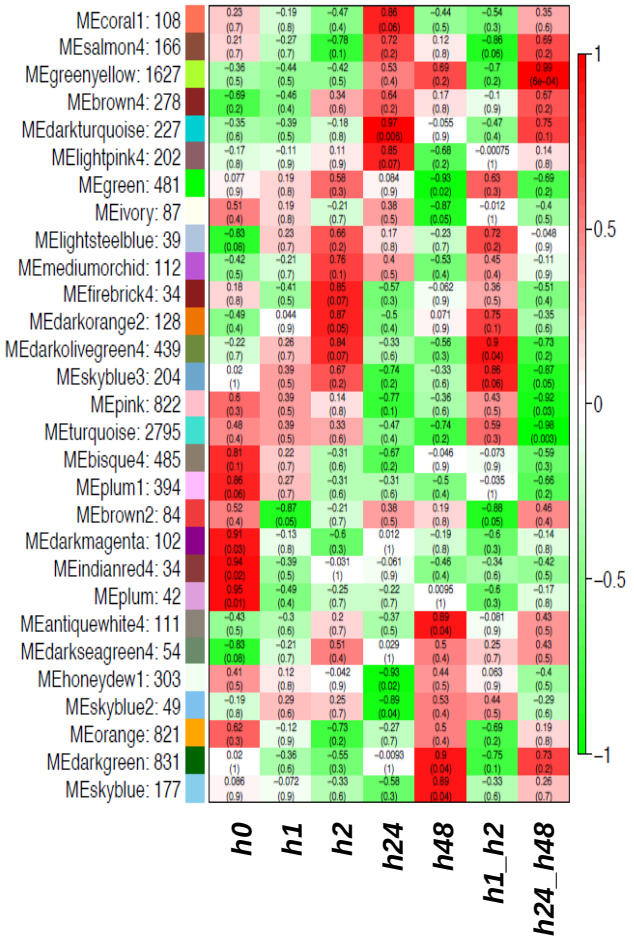

B.

Ingenuity Canonical Pathways	-log(p-value)	Ratio
Interferon Signaling	7.83E+00	4.17E-01
phagosome maturation	6.74E+00	2.25E-01
Antigen Presentation Pathway	6.72E+00	3.78E-01
Activation of IRF by Cytosolic Pattern Recognition Receptors	5.72E+00	2.74E-01
Death Receptor Signaling	5.49E+00	2.28E-01
Role of RIG1-like Receptors in Antiviral Innate Immunity	5.02E+00	3.02E-01
UVA-Induced MAPK Signaling	4.66E+00	2.16E-01
NRF2-mediated Oxidative Stress Response	4.15E+00	1.61E-01
Prolactin Signaling	4.11E+00	2.19E-01
Retinoic acid Mediated Apoptosis Signaling	3.89E+00	2.30E-01
Reelin Signaling in Neurons	3.68E+00	2.03E-01
FLT3 Signaling in Hematopoietic Progenitor Cells	3.49E+00	2.03E-01
Oncostatin M Signaling	3.17E+00	2.65E-01
Polyamine Regulation in Colon Cancer	3.09E+00	3.18E-01
autophagy	2.98E+00	2.50E-01
Type I Diabetes Mellitus Signaling	2.89E+00	1.64E-01
CNTF Signaling	2.86E+00	2.12E-01
Protein Ubiquitination Pathway	2.84E+00	1.29E-01
Cdc42 Signaling	2.82E+00	1.44E-01
PDGF Signaling	2.81E+00	1.82E-01

C.

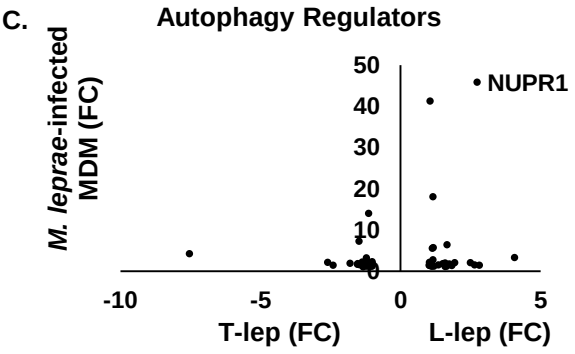

D.

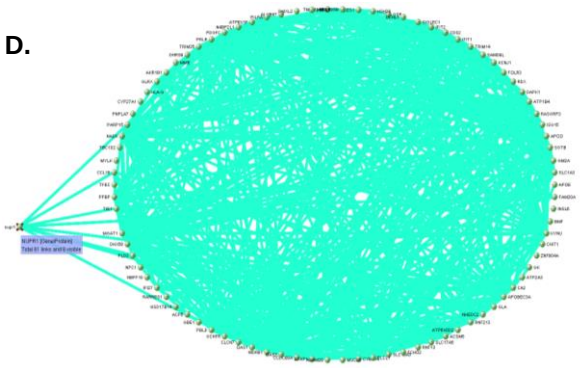

FIGURE 2: *M. leprae*-induced genes cluster into a significant WGCNA module enriched for autophagy genes

A) Heat map depicting correlation of infection conditions (x-axis) with WGCNA modules (y-axis), with red representing an enrichment and green a deenrichment of module genes. Correlation score (top) and corresponding p-value (bottom) denoted on each square.
B) Top canonical pathways enriched in MEgreenyellow module as determined by Ingenuity IPA analysis. Rows highlighted in yellow represent pathways also enriched in L-lep versus T-lep lesions.
C) Autophagy regulator genes in MEgreenyellow module denoting differential expression in leprosy lesions (x-axis) versus induction in *M. leprae*-infected MDM (y-axis).
D) Graphical representation of gene connections of autophagy regulators as determined by VisANT analysis of Megreenyellow module

SUPPLEMENTAL FIGURE 4: Correlation scores of WGCNA module MEgreenyellow

A.

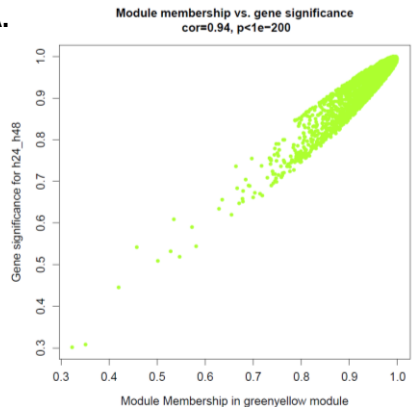

FIGURE S4: Correlation scores of WGCNA module MEgreenyellow

A) p-value of each gene's correlation to other genes within the module (module membership) versus significance of each gene within the h24_h48 cluster.

FIGURE 3: *M. leprae* induction of NUPR1 is dependent on Type I IFN signaling

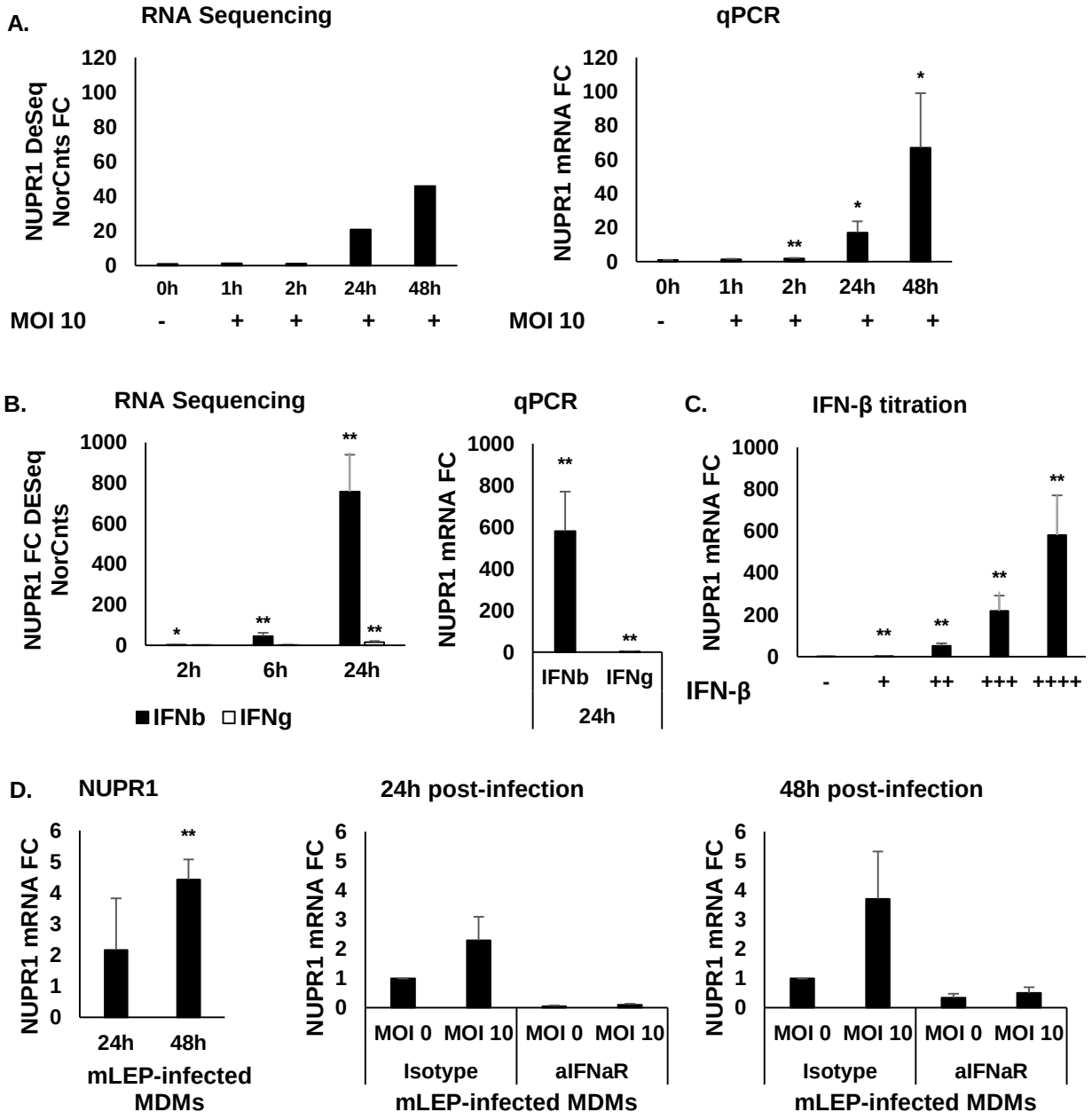

Figure 3: *M. leprae*-mediated induction of NUPR1 is dependent on Type I IFN signaling

(A) Fold change of NUPR1 normalized DESeq counts as compared to time 0 obtained from RNASeq of *M. leprae*-infected MDMs (n=1). Experimental replicates assessed via qPCR for NUPR1 mRNA normalized to housekeeping gene h36b4 are representative of n=9.

(B) Fold change of NUPR1 normalized DESeq counts obtained from RNASeq of IFN-b (conc.) or IFN-g (conc.)-stimulated MDM as compared to media controls at each time point (n=5). qPCR replicates assessed for NUPR1 24h post-treatment normalized to housekeeping gene h36b4 are representative of n=3.

(C) NUPR1 FC after 24h treatment with increasing concentrations of IFN-b: +: 2.7u/ml, ++: 27.7u/ml, +++: 92.3u/ml, ++++: 277u/ml

(D) MDM infected with *M. leprae* after pre-incubation with aIFNAR blocking antibody or IgG2a Isotype control and assessed for NUPR1 FC at 24h or 48h (n=4).

$p<.05$ (*), $p<.001$ (**), qPCR experiments are representative of at least three experiments

SUPPLEMENTAL FIGURE 5: Validation of αIFNAR antibody

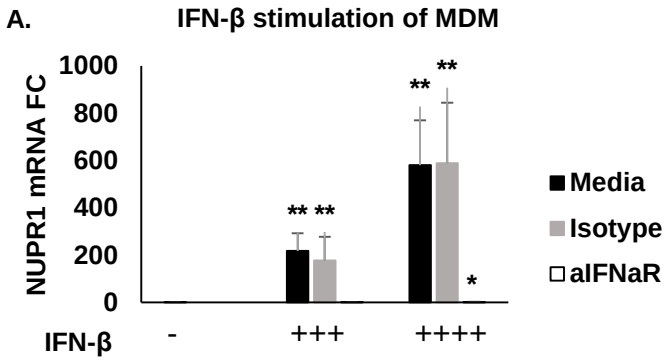

Figure S5: Validation of αIFNAR antibody

(A) MDM stimulated with increasing concentrations of IFN-β (+++: 92.3u/ml, ++++: 277u/ml) after pre-incubation with αIFNAR blocking antibody or IgG2a Isotype control and assessed for NUPR1 FC at 24h (n=3).

p<.05 (*), p<.001 (**)

FIGURE 4: NUPR1 protein is more highly expressed in lepromatous leprosy lesions

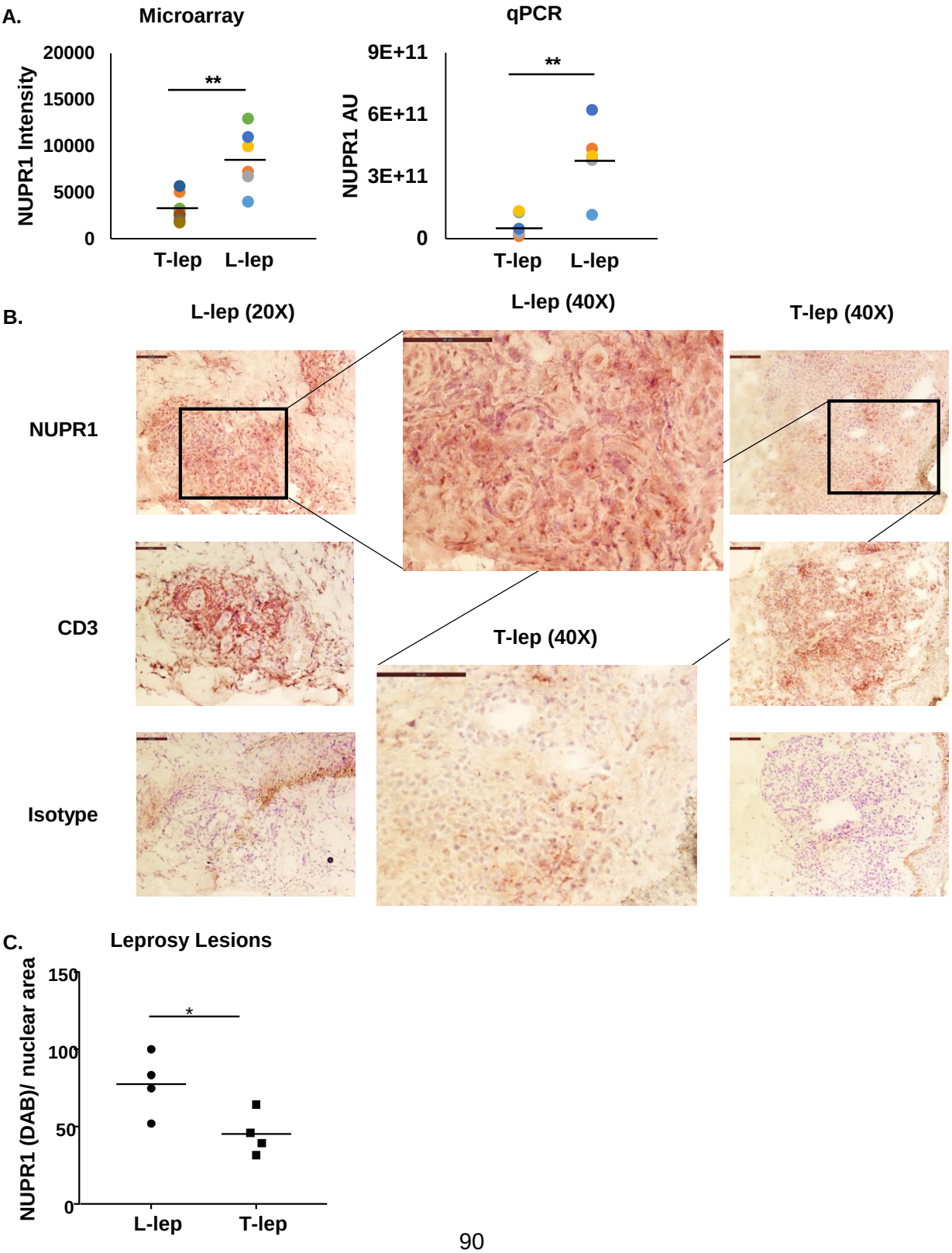

Figure 4: NUPR1 is more highly expressed in lepromatous leprosy lesions

(A) NUPR1 intensity values from microarray analysis of L-lep (n=6) and T-lep (n=5) leprosy lesions and relative NUPR1 arbitrary units on corresponding cDNA.
(B) Immunoperoxidase staining of L-lep and T-lep lesions tissue for NUPR1, CD3, or IgG2b Isotype control (20X with 40X insert). Pictures shown are representative of n=4.
(C) Immunoratio analysis quantifying NUPR1 immunoperoxidase staining (DAB) versus hematoxylin nuclear area of leprosy lesion tissue.

SUPPLEMENTAL FIGURE 6: Model Hypothesis

A.

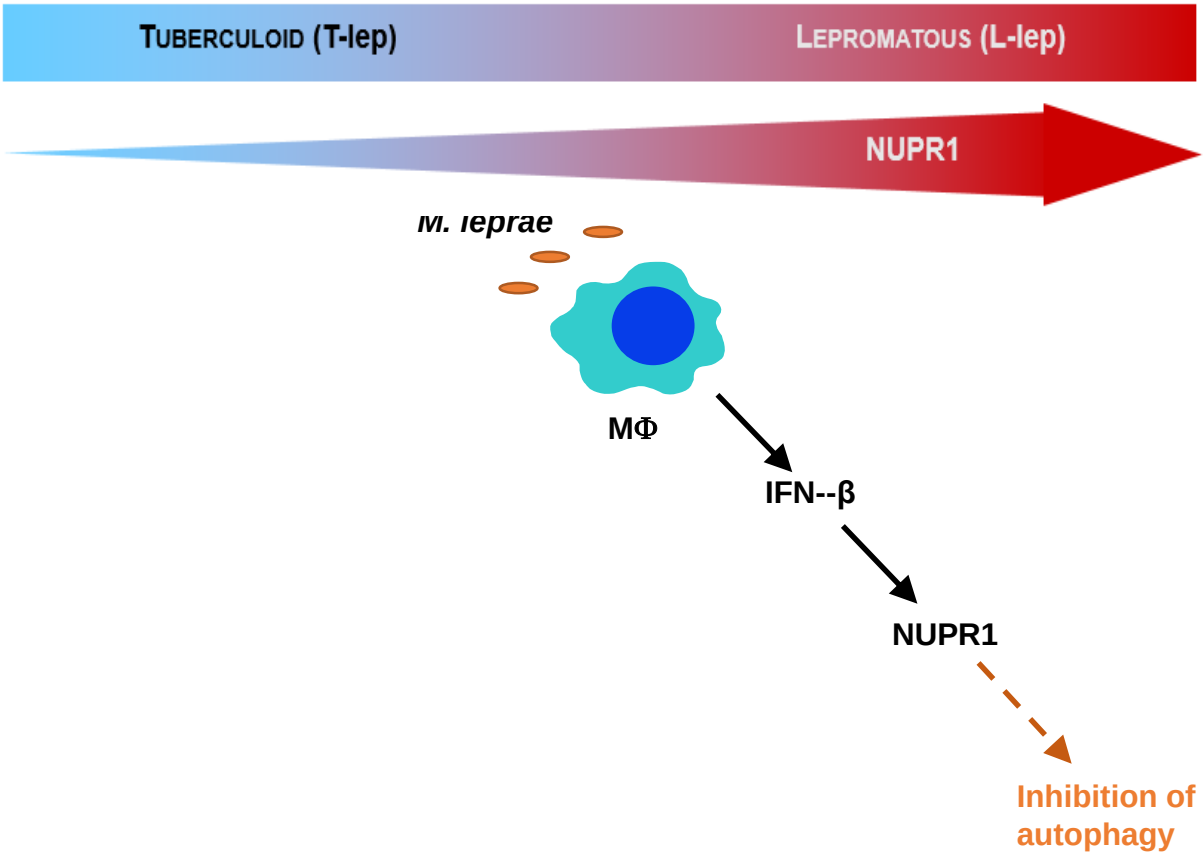

Figure S6: Model Hypothesis

(A) Graphical representation of data. NUPR1 is more highly expressed in L-lep versus T-lep lesions and is induced in MDM after *M. leprae* infection in a type I IFN-dependent manner.

CHAPTER 5:

Conclusions and Final Remarks

This dissertation address the ability of mycobacteria or mycobacterial products to modulate host immune responses in order to gain a clearer understanding of disease pathogenesis. Activated macrophages employ multiple mechanisms of antimicrobial activity to eliminate invading intracellular pathogens including the induction of antimicrobial peptide production, autophagolysosomal fusion, and delivery of antimicrobial peptides to the autophagosome. Mycobacterial infection, however, can stimulate the production of type I IFN and subsequent IL-10 expression to subvert type II IFN-mediated host immune responses, reeducation of M1 MΦ, and enabling of bacterial persistence. Through transcriptome analysis of gene expression profiles at the site of disease in leprosy, IL-10 and IL-15-derived M2 and M1 MΦ, and *in vitro M. leprae*-infected or IFN-stimulated MDM, we were able to identify multiple methods by which Mycobacteria can alter MΦ phenotype, gene expression, and function that can play a role in outcome of infection.

It was previously shown that disseminated L-lep lesions display differential expression of cytokines and macrophage activation states in comparison to self-limiting T-lep lesions, mirroring the immune response to infection. Gene expression profiling of microRNAs expressed in L-lep versus T-lep lesions cross-referenced with mRNA targeting algorithms identified microRNA-21 (miR-21) as being highly expressed in L-lep lesions and a potential regulator of the vitamin D antimicrobial pathway. *M. leprae*-mediated induction of miR-21 suppressed expression of antimicrobial gene CYP27b1 and production of downstream antimicrobial peptides cathelicidin and defensin-beta 2, contributing to the inhibition of mycobacterial killing. Intriguingly, investigation into the mechanism of miR-21 induction led to the discovery that miR-21 is induced by the mycobacterial cell wall component phenolic glycolipid-1 (PGL-1), which is expressed in *M. leprae* but not other mycobacteria, providing an explanation for how *M. leprae*, but not *M. tuberculosis*, is able to escape vitamin D-dependent antimicrobial activity. Here we provide evidence illustrating the ability of a specific microRNA, miR-21, induced during infection to modify the host immune response and influence the outcome of infection.

Several other microRNAs were more expressed in L-lep versus T-lep lesions and could potentially target components of the vitamin D pathway or Th1-related genes during infection. Among these are microRNAs differentially expressed in other mycobacterial infections and with known functions modifying the host immune response, including miR-146a and miR-29c. miR-

146a, induced following *M. leprae* infection of monocytes (unpublished data), is predicted to target CYP27b1, the enzyme responsible for conversion of vitamin D to its active form. miR-146a is also induced following *M. bovis* BCG infection of mice but is significantly lower in the peripheral blood mononuclear cells (PBMCs) of tuberculosis patients compared to healthy controls[129], suggesting a role in control of chronic inflammation. Through targeting the TLR signaling cascade, miR-146a[130] may dampen the uncontrolled inflammation that leads to tissue damage, a major cause of pulmonary morbidity and mortality in tuberculosis[131], significantly impacting the outcome of infection and disease pathogenesis. In addition, microRNA single nucleotide polymorphism (SNP) analysis has revealed a correlation between a miR-146a SNP (rs2910164) and increased pulmonary tuberculosis susceptibility in certain populations[132], further highlighting the protective role of miR-146a in containment of uncontrolled host immune responses during mycobacterial infection. Contrary to miR-146a, infection of mice with *M. bovis* BCG results in decreased expression of miR-29 in T-cells, which targets and down regulates the critical Th1 cytokine IFN-γ[133]. Ablation of miR-29 in mice renders them more resistant to both *M. bovis* BCG and *M. tuberculosis* infections, suggesting that induction of miR-29 in T-cells during infection is a facilitator of bacterial virulence. Further studies are needed to decipher the role of these and other microRNAs in the context of leprosy disease.

In addition to differential expression of microRNAs, L-lep and T-lep lesions are composed of MΦ with differing activation states. Our lab previously demonstrated that L-lep MΦ are $CD209^{+}CD163^{hi}$, similar to that seen in IL-10-derived MΦ, which exhibit enhanced phagocytic function and a decrease in antimicrobial gene expression. In contrast, T-lep MΦ are $CD209^{+}CD163^{lo}$, similar to IL-15-derived MΦ which are activated to express antimicrobial genes but exhibit a decrease in phagocytic capabilities. In the present study, we investigated whether MΦ polarization was reversible and identified mechanisms of reeducation of MΦ by stimulation with cytokines and mycobacterial ligands. Treatment with IL-10 induced and maintained M2 MΦ polarization as well as reeducated M1 MΦ to M2-like MΦ with an increase in phagocytic function. In contrast, IL-15 treatment of M2 MΦ was not sufficient to fully reprogram M2 MΦ; instead M2 MΦ required co-stimulation with TLR2/1L + IFN-γ to convert to M1 MΦ with an upregulation of antimicrobial gene expression. How this plays a role in leprosy during infection and whether this is occurring during reversal reactions still remains to be determined.

Gene expression profiles at the site of disease in leprosy integrated with transcriptome analysis of *in vitro* infected cells provides a means to identify genes important for bacterial survival during mycobacterial infection. Hierarchical clustering of gene expression profiles of *M. leprae*-infected MDM identified a cluster of genes upregulated after infection that were enriched for a leprosy gene signature and type I IFN-specific gene signature. WGCNA analysis led to the identification of a highly significant module, 'MEgreenyellow', enriched for the autophagy pathway. Expression of autophagy regulators in leprosy skin lesions and *M. leprae*-infected MDM identified a strong upregulation of the novel gene NUPR1, which to date has not been shown to play a role in bacterial infections. *M. leprae* induces NUPR1 in a type I IFN-dependent manner, suggesting *M. leprae* can stimulate type I IFN production and regulate autophagy through NUPR1. Further studies are still needed to tease out the role of NUPR1 during mycobacterial infection, including its effect on autophagy, antigen presentation, and bacterial viability. Of note, multiple significant WGCNA modules deenriched in *M. leprae*-infected macrophages showed an enrichment for genes within the antigen presentation pathway.

The work presented in this dissertation provides evidence that *Mycobacterium leprae* infection can alter host immune responses to influence the outcome of infection. Although the chapters are distinct, it is interesting to note commonalities between them. IFN-β is now known to upregulate miR-21 expression in a STAT3- and NFkB-dependent manner in various cancer cell lines[134], providing a potential mechanism by which *M. leprae* can induce miR-21 and IFN-β can induce IL-10. Thus, the effect of IFN-β and miR-21 on the vitamin D pathway may occur through a linear pathway (*M. leprae* → IFN-β → miR-21 → IL-10), culminating in a decrease of CYP27b1, an inability to convert vitamin D to its active form, and inhibition of antimicrobial peptide production.

The role of NUPR1 in mycobacterial infection may mirror miR-21. Similar to miR-21, NUPR1 is induced by IFN-β and contains NFkB binding motifs within its promoter. NUPR1 is not, however, induced by IL-10 (data not shown), indicating either NUPR1 is upstream of IL-10 or induced in parallel. Interestingly, NUPR1 is stabilized the same protein that is required for IFN-β-mediated induction of IL-10, glycogen synthase kinase 3 beta (GSK3b), and has been reported to influence the methylation status of VDR. Further investigation into where NUPR1 falls in this pathway and whether NUPR1 plays a role in the expression of IL-10 and

components within the vitamin D pathway would be of great interest to study in the context of mycobacterial disease. In addition, whether NUPR1 exhibits positive feedback on IFN-β signaling could be of interest due to biochemical similarities of NUPR1 to HMG-I:Y proteins which comprise part of the IFN-β enhanceosome complex.

The response to *M. leprae* and IFN-β may also be dependent on the activation state of the host MΦ. IL-10 MΦ display higher basal miR-21 expression than IL-15 MΦ (unpublished data). In addition, IL-10 MΦ induce much greater amounts of NUPR1 in response to *M. leprae* and IFN-β in comparison to IL-15 MΦ. These distinct responses to *M. leprae* can be explained by the disparities in phagocytic function and bacterial loads. How IL-10 and IL-15 MΦ can differentially respond to IFN-β is still unclear.

In summary, the work presented in this dissertation provides evidence that *Mycobacterium leprae* infection can upregulate specific genes capable of modifying host immune responses. More studies investigating whether other microRNAs and mRNAs differentially expressed during infection favor or target the immune response when the host cell and *M. leprae* are engaged could give further insight in determining the outcome of the infection. As more data are gathered on (i) the functional consequences of microRNA regulation during mycobacterial infections, (ii) methods of MΦ reeducation to facilitate effective immune responses and iii) mechanisms of immune evasion through upregulation of inappropriate host genes, they may provide an opportunity for directed therapeutic intervention.

References:

[1]Bennett BH, Parker DL, Robson M. Leprosy: Steps Along the Journey of Eradication. *Public Health Rep*. **123**, 198-205 (2008).

[2]Fine PE. Leprosy: the epidemiology of a slow bacterium. *Epidemiol Rev.* **4**, 161-188 (1982).

[3]Lockwood D, Shetty V, Penna GO. Hazards of setting targets to eliminate disease: lessons from the leprosy elimination campaign. *BMJ*. **348**, g1136 (2014).

[4]Staples J. Interrogating leprosy stigma: why qualitative insights are vital. *Lepr Rev.* **82**, 91-97 (2011).

[5]Lockwood D, Sanderson PR. Nerve damage in leprosy: a continuing challenge to scientists, clinicians, and service providers. *Int Health*. **4**, 240-252 (2012).

[6]Scollard DM, Adams LB, Gillis TP et al. The continuing challenges of leprosy. *Clin Microbiol Rev*. **19**, 338-381 (2006).

[7]Richardus JH, Habbema JD. The impact of leprosy control on the transmission of *M. leprae*: is elimination being attained? *Lepr Rev.* **78**, 330-337 (2007).

[8]Meima A, Gupte MD, van Oortmarssen GJ et al. Trends in leprosy case detection rates. *Int J Lepr Other Mycobact Dis.* **65**, 305-319 (1997).

[9]Fine PE, Warndorff DK. Leprosy by the year – what is being eliminated? *Lepr Rev*. **68**, 201-202 (2000).

[10]Smith WC. We need to know what is happening to the incidence of leprosy. *Lepr Rev.* **68**, 195-200 (1997).

[11]World Health Organization. Global leprosy update, 2013; reducing disease burden. *Wkly Epidemiol Rec*. **89**(36), 389-400 (2014).

[12]Ridley DS, Jopling WH. Classification of leprosy according to immunity. A five-group system. *Int J Lepr Other Mycobact Dis.* **34**, 255-273 (1966).

[13]Teles RM, Graeber TG, Krutzik SR et al. Type I interferon suppresses type II interferontriggered human anti-mycobacterial responses. *Science.* **339**(6126), 1448-53 (2013).

[14]Montoya D, Cruz D, Teles RM, et al. Divergence of macrophage phagocytic and antimicrobial programs in leprosy. *Cell Host Microbe*. **6**, 343–53 (2009).

[15]Klug-Micu GM, Stenger S, Sommer A, et al. CD40 ligand and interferon-gamma induce an antimicrobial response against *Mycobacterium tuberculosis* in human monocytes. *Immunology*. **139**(1), 121–128 (2013).

[16]Dupuis S, et al. Human interferon-gamma-mediated immunity is a genetically controlled continuous trait that determines the outcome of mycobacterial invasion. *Immunol Rev.* **178,** 129–137 (2000).

[17]Dorman SE, Holland SM. Mutation in the signal-transducing chain of the interferon-gamma receptor and susceptibility to mycobacterial infection. *J Clin Invest.* **101,** 2364–2369 (1998).

[19]Filipe-Santos O, et al. Inborn errors of IL-12/23- and IFN-gamma-mediated immunity: molecular, cellular, and clinical features. *Semin Immunol.* **18**, 347–361 (2006).

[20]Bustamante J, Zhang SY, von Bernuth H, Abel L, Casanova JL. From infectious diseases to primary immunodeficiencies. *Immunol Allergy Clin North Am.* **28,** 235–258 (2008).

[21]Newport MJ, et al. A mutation in the interferon-gamma-receptor gene and susceptibility to mycobacterial infection. *N Engl J Med.* **335**, 1941–1949 (1996).

[22]Jouanguy E, et al. Interferon-gamma-receptor deficiency in an infant with fatal bacilli CalmetteGuerin infection. *N Engl J Med*. **335**, 1956–1961 (1996).

[23]Jouanguy E, et al. Partial interferon-gamma receptor 1 deficiency in a child with tuberculoid bacillus Calmette-Guerin infection and a sibling with clinical tuberculosis. *J Clin Invest*. **100**, 2658–2664 (1997).

[24]Jouanguy E, et al. A human IFNGR1 small deletion hotspot associated with dominant susceptibility to mycobacterial infection. *Nat Genet*. **21,** 370–378 (1999).

[25]Jouanguy E, et al. In a novel form of IFNgamma receptor 1 deficiency, cell surface receptors fail to bind IFN-gamma. *J Clin Invest*. **105,** 1429–1436 (2000).

[26]Allende LM, et al. A point mutation in a domain of gamma interferon receptor 1 provokes severe immunodeficiency. *Clin Diagn Lab Immunol*. **8,** 133–137 (2001).

[27]Pierre-Audigier C, et al. Fatal disseminated *Mycobacterium smegmatis* infection in a child with inherited interferon gamma receptor deficiency. *Clin Infect Dis*. **24**, 982–984 (1997).

[28]Altare F, et al. A causative relationship between mutant IFNgR1 alleles and impaired cellular response to IFN gamma in a compound heterozygous child. *Am J Hum Genet*. **62**, 723–726 (1998).

[29]Koscielniak E, de Boer T, Dupuis S, Naumann L, Casanova JL, Ottenhoff TH. Disseminated *Mycobacterium peregrinum* infection in a child with complete interferon-gamma receptor-1 deficiency. *Pediatr Infect Dis J*. **22**, 378–380 (2003).

[30]Dorman SE, et al. Clinical features of dominant and recessive interferon gamma receptor 1 deficiencies. *Lancet*. **364**, 2113–2121 (2004).

[31]Doffinger R, et al. Partial interferon-gamma receptor signaling chain deficiency in a patient with bacille Calmette-Guerin and *Mycobacterium abscessus* infection. *J Infect Dis.* **181,** 379– 384 (2000).

[32]Farrar MA, Schreiber RD. The molecular cell biology of interferon-gamma and its receptor. *Annu Rev Immunol.* **11**, 571–611 (1993).

[33]Fabri M, Stenger S, Shin DM et al. Vitamin D is required for IFN-g-mediated antimicrobial activity of human macrophages. *Sci Transl Med.* **3**, 104ra2 (2011).

[34]Stanley SA, Johndrow JE, Manzanillo P, Cox JS. The Type I IFN response to infection with *Mycobacterium tuberculosis* requires ESX-1-mediated secretion and contributes to pathogenesis. *J Immunol*. **178**, 3143-52 (2007).

[35]Manca C, Tsenova L, Bergtold A, Freeman S, Tovey M, Musser JM, et al. Virulence of a *Mycobacterium tuberculosis* clinical isolate in mice is determined by failure to induce Th1 type immunity and is associated with induction of IFN-alpha/beta. *Proc Natl Acad Sci USA*. **98**, 57527 (2001).

[36]Fortune SM, Solache A, Jaeger A, Hill PJ, Belisle JT, Bloom BR, et al. *Mycobacterium tuberculosis* inhibits macrophage responses to IFN-gamma through myeloid differentiation factor 88-dependent and –independent mechanisms. *J Immunol*. **172**, 6272-80 (2004).

[37]Pai RK, Pennini ME, Tobian AA, Canaday DH, Boom WH, Harding CV. Prolonged toll-like receptor signaling by *Mycobacterium tuberculosis* and its 19-kilodalton lipoprotein inhibits

gamma interferon-induced regulation of selected genes in macrophages. *Infect Immun*. **72**, 6603-14 (2004).

[38]Pennini ME, Pai RK, Schultz DC, Boom WH, Harding CV. *Mycobacterium tuberculosis* 19 kDa lipoprotein inhibits IFN-gamma-induced chromatin remodeling of MHC2TA by TLR2 and MAPK signaling. *J Immunol*. **176**, 4323-30 (2006).

[39]Benson SA, Ernst JD. TLR2-dependent inhibition of macrophage responses to IFN-gamma is mediated by distinct, gene-specific mechanisms. *PLoS One.* **4**, 6329 (2009).

[40]Yamamura, M. *et al.* Defining protective responses to pathogens: cytokine profiles in leprosy lesions. *Science* **254**, 277–279 (1991).

[41]Jullien D, Sieling, PA, Uyemura K et al. IL-15, an immunomodulator of T cell responses in intracellular nfection. *J. Immunol*. **158**, 800–806 (1997).

[42]Cruz D, Watson AD, Miller CS et al. Host-derived oxidized phospholipids and HDL regulate innate immunity in human leprosy. *J. Clin. Invest*. **118**, 2917–2928 (2008).

[43]Krutzik SR, Ochoa MT, Sieling PA et al. Activation and regulation of Toll-like receptors 2 and 1 in human leprosy. *Nat. Med.* **9**, 525–532 (2003).

[44]Liu PT, Stenger S, Li H et al. Toll-like receptor triggering of a vitamin D-mediated human antimicrobial response. *Science.* **311**, 1770–1773 (2006).

[45]Krutzik SR, Hewison M, Liu PT et al. IL-15 links TLR2/1-induced macrophage differentiation to the vitamin D-dependent antimicrobial pathway. *J. Immunol.* **181**, 7115–7120 (2008).

[46]Liu PT, Schenk M, Walker VP et al. Convergence of IL-1beta and VDR activation pathways in human TLR2/1-induced antimicrobial responses. *PLoS ONE.* **4**, e5810 (2009).

[47]Rodriguez A, Griffiths-Jones S, Ashurst JL, Bradley A. Identification of mammalian microRNA host genes and transcription units. *Genome Res*. **14**, 1902–1910 (2004).

[48]Hsu PW, Huang HD, Hsu SD et al. miRNAMap: genomic maps of microRNA genes and their target genes in mammalian genomes. *Nucleic Acids Res*. **34**, D135–139 (2006).

[49]Lee Y, Kim M, Han J, Yeom KH, Lee S, Baek SH, Kim VN. MicroRNA genes are transcribed by RNA polymerase II. *EMBO J*. **23**, 4051–4060 (2004).

[50]Bortolin-Cavaille ML, Dance M, Weber M, Cavaille J. C19MC microRNAs are processed from introns of large Pol-II, non-protein-coding transcripts. *Nucleic Acids Res*. **37**, 3464–3473 (2009).

[51]Cai X, Hagedorn CH, Cullen BR. Human microRNAs are processed from capped, polyadenylated transcripts that can also function as mRNAs. *RNA.* **10**, 1957–1966 (2004).

[52]Lee Y, Ahn C, Han J, Choi H, Kim J, Yim J, Lee J, Provost P, Radmark O, Kim S, Kim VN. The nuclear RNase III Drosha initiates microRNA processing. *Nature.* **425**, 415–419 (2003).

[53]Lee Y, Jeon K, Lee JT, Kim S, Kim VN. MicroRNA maturation: stepwise processing and subcellular localization. *EMBO J*. **21**, 4663–4670 (2002).

[54]Ballarino M, Pagano F, Girardi E, Morlando M, Cacchiarelli D, Marchioni M, Proudfoot NJ, Bozzoni I. Coupled RNA processing and transcription of intergenic primary microRNAs. *Mol. Cell. Biol*. **29**, 5632–5638 (2009).

[55]Morlando M, Ballarino M, Gromak N, Pagano F, Bozzoni I, Proudfoot NJ. Primary microRNA transcripts are processed co-transcriptionally. *Nat. Struct. Mol. Biol*. **15**, 902–909 (2008).

[56]Yi R, Qin Y, Macara IG, Cullen BR. Exportin-5 mediates the nuclear export of premicroRNAs and short hairpin RNAs. *Genes Dev.* **17**, 3011–3016 (2003).

[57]Lund E, Guttinger S, Calado A, Dahlberg JE, Kutay U. Nuclear export of microRNA precursors. *Science.* **303**, 95–98 (2004).

[58]Bohnsack MT, Czaplinski K, Gorlich D. Exportin 5 is a RanGTP-dependent dsRNA binding protein that mediates nuclear export of pre-miRNAs. *RNA.* **10**, 185–191 (2004).

[59]Hutvagner G, McLachlan J, Pasquinelli AE, Balint E, Tuschl T, Zamore PD. A cellular function for the RNA-interference enzyme Dicer in the maturation of the let-7 small temporal RNA. *Science.* **293**, 834–838 (2001).

[60]Ketting RF, Fischer SE, Bernstein E, Sijen T, Hannon GJ, Plasterk RH. Dicer functions in RNA interference and in synthesis of small RNA involved in developmental timing in *C. elegans*, *Genes Dev*. **15**, 2654–2659 (2001).

[61]Lewis BP, Shih IH, Jones-Rhoades MW, Bartel DP, Burge CB. Prediction of mammalian microRNA targets. *Cell.* **115**, 787–798 (2003).

[62]Horvitz HR and Sulston JE. Isolation and genetic characterization of cell-lineage mutants of the nematode *Caenorhabditis elegans. Genetics.* **96**, 435–454 (1980).

[63]Ardekani AM, and Naeini MM. The role of microRNAs in human diseases. *Avicenna*. *J. Med. Biotechnol.* **2**, 161–179 (2010).

[64]Mehta MD and Liu PT. microRNAs in mycobacterial disease: friend or foe? *Front. Genet*. **5**, 231 (2014).

[65]Sheedy, F.J. *et al.* Negative regulation of TLR4 via targeting of the proinflammatory tumor suppressor PDCD4 by the microRNA miR-21. *Nat. Immunol.* **11**, 141–147 (2010).

[66]Yao Q, Cao S, Li C, Mengesha A, Kong B, Wei M. Micro-RNA-21 regulates TGF-beta-induced myofibroblast differentiation by targeting PDCD4 in tumor-stroma interaction. *Int J Cancer*. **128**, 1783–1792 (2011).

[67]Lu TX, Munitz A., Rothenberg ME. MicroRNA-21 is up-regulated in allergic airway inflammation and regulates IL-12p35 expression. *J. Immunol.* **182**, 4994–5002 (2009).

[68]Lum JJ, DeBerardinis RJ, Thompson CB. Autophagy in metazoans: cell survival in the land of plenty. *Nat Rev Mol Cell Biol*, **6**(6), 439-48 (2005).

[69]Shibutani ST, et al. Autophagy and autophagy-related proteins in the immune system. *Nat Immunol*, **16**(10), 1014-24 (2015).

[70]Fujita N, et al. An Atg4B mutant hampers the lipidation of LC3 paralogues and causes defects in autophagosome closure. *Mol Biol Cell*. **19**(11), 4651-9 (2003).

[71]Li WW, Li J, Bao JK. Microautophagy: lesser-known self-eating. *Cell Mol Life Sci*, **69**(7), 112536 (2012).

[72]Chiang HL, et al. A role for a 70-kilodalton heat shock protein in lysosomal degradation of intracellular proteins. *Science*. **246**(4928), 382-5 (1989).

[73]Agarraberes FA and Dice JF. A molecular chaperone complex at the lysosomal membrane is required for protein translocation. *J Cell Sci*, **114**(13), 2491-9 (2001).

[74]Deretic V, Saitoh T, Akira S. Autophagy in infection, inflammation and immunity. *Nat Rev Immunol*, **13**(10), 722-37 (2013).

[75]Huang J and Brumell JH. Bacteria-autophagy interplay: a battle for survival. *Nat Rev Microbiol*, **12**(2), 101-14 (2014).

[76]Barnett TC, et al. The globally disseminated M1T1 clone of group A Streptococcus evades autophagy for intracellular replication. *Cell Host Microbe*. **14**(6), 675-82 (2013).

[77]Zang F, et al. Autophagy is involved in regulating the immune response of dendritic cells to influenza A (H1N1) pdm09 infection. *Immunology*. **148**(1), 56-69 (2016).

[78]Gutierrez MG, Master SS, Singh SB, Taylor GA, Colombo MI, Deretic V. Autophagy is a defense mechanism inhibiting BCG and Mycobacterium tuberculosis survival in infected macrophages. *Cell*. **119**, 753–766 (2004).

[79]Singh SB, Davis AS, Taylor GA, Deretic V. Human IRGM induces autophagy to eliminate intracellular mycobacteria. *Science.* **313**, 1438–1441 (2006).

[80]Vergne I, Singh S, Roberts E, et al. Autophagy in immune defense against *Mycobacterium tuberculosis*. *Autophagy*. **2**(3), 175–178 (2006).

[81]Fratti RA, et al. *Mycobacterium tuberculosis* glycosylated phosphatidylinositol causes phagosome maturation arrest. *Proc Natl Acad Sci USA*. **100**(9), 5437-42 (2003).

[82]Vergne I, et al. *Mycobacterium tuberculosis* phagosome maturation arrest: mycobacterial phosphatidylinositol analog phosphatidylinositol mannoside stimulates early endosomal fusion. *Mol Biol Cell*. **15**(2), 751-60 (2004).

[83]Deretic V, Singh S, Master S, Harris J, Roberts E, Kyei G, et al. *Mycobacterium tuberculosis* inhibition of phagolysosome biogenesis and autophagy as a host defence mechanism. *Cell Microbiol*. **8**(5), 719–27 (2006).

[84]Rovetta AI, et al. IFNG-mediated immune responses enhance autophagy against *Mycobacterium tuberculosis* antigens in patients with active tuberculosis. *Autophagy*. **10**(12), 2109-21 (2014).

[85]Matsuzawa T, et al. IFN-gamma elicits macrophage autophagy via the p38 MAPK signaling pathway. *J Immunol*, **189**(2), 813-8 (2012).

[86]Juárez E, Carranza C, Hernández-Sánchez F, León-Contreras JC, Hernández-Pando R, Escobedo D, et al. NOD2 enhances the innate response of alveolar macrophages to *Mycobacterium tuberculosis* in humans. *Eur J Immunol.* **42**, 880–889 (2012).

[87]Mallo GV, Fiedler F, Calvo EL, Ortiz EM, Vasseur S, Keim V, Morisset J, Iovanna JL. Cloning and expression of the rat p8 cDNA, a new gene activated in pancreas during the acute phase of pancreatitis, pancreatic development, and regeneration, and which promotes cellular growth. *J Biol Chem*. **272**, 32360–32369 (1997).

[88]Zinke I, Schutz CS, Katzenberger JD, Bauer M, Pankratz MJ. Nutrient control of gene expression in Drosophila: Microarray analysis of starvation and sugar-dependent response. *EMBO J*. **21**, 6162–6173 (2002).

[89]Plant SR, Wang Y, Vasseur S, Thrash JC, McMahon EJ, Bergstralh DT, Arnett HA, Miller SD, Carson MJ, Iovanna JL, Ting JP. Upregulation of the stress-associated gene p8 in mouse models of demyelination and in multiple sclerosis tissues. *Glia.* **53**, 529–537 (2006).

[90]Valacco MP, Varone C, Malicet C, Canepa E, Iovanna JL, Moreno S. Cell growth dependent subcellular localization of p8. *J Cell Biochem.* **97**, 1066–1079 (2006).

[91]Garcia-Montero AC, Vasseur S, Giono LE, Canepa E, Moreno S, Dagorn JC, Iovanna JL. Transforming growth factor beta-1 enhances Smad transcriptional activity through activation of p8 gene expression. *Biochem J*. **357**, 249–253 (2001).

[92]Kallwellis K, Grempler R, Gunther S, Path G, Walther R. Tumor necrosis factor alpha induces the expression of the nuclear protein p8 via a novel NFkappaB binding site within the promoter. *Horm Metab Res.* **38**, 570–574 (2006).

[93]Goruppi S, Patten RD, Force T, Kyriakis JM. Helix-loop-helix protein p8, a transcriptional regulator required for cardiomyocyte hypertrophy and cardiac fibroblast matrix metalloprotease induction. *Mol Cell Biol.* **27**, 993–1006 (2007).

[94]Path G, Opel A, Knoll A, Seufert J. Nuclear protein p8 is associated with glucose induced pancreatic beta-cell growth. *Diabetes.* **53**, S82–S85 (2004).

[95]Bratland A, Risberg K, Maelandsmo GM et al. Expression of a novel factor, com1, is regulated by 1,25-dihydroxyvitamin D3 in breast cancer cells. *Cancer Res.* **60**, 5578–5583 (2000).

[96]Igarashi T, Kuroda H, Takahashi S, Asashima M. Cloning and characterization of the Xenopus laevis p8 gene. *Dev Growth Differ.* **43**, 693–698 (2001).

[97]Encinar JA, Mallo GV, Mizyrycki C, Giono L, Gonzalez-Ros JM, Rico M, Canepa E, Moreno S, Neira JL, Iovanna JL. Human p8 is a HMG-I/Y-like protein with DNA binding activity enhanced by phosphorylation. *J Biol Chem.* **276**, 2742–2751 (2001).

[98]Gironella M, Malicet C, CanoC, Sandi MJ,Hamidi T, Tauil RM, BastonM, Valaco P, Moreno S, Lopez F, Neira JL, Dagorn JC, Iovanna JL. p8/nupr1 regulates DNA-repair activity after doublestrand gamma irradiation-induced DNA damage. *J Cell Physiol.* **221**, 594–602 (2009).

[99]Kong DK, Georgescu SP, Cano C, Aronovitz MJ, Iovanna JL, Patten RD et al. Deficiency of the transcriptional regulator p8 results in increased autophagy and apoptosis, and causes impaired heart function. *Mol Biol Cell*, **21**, 1335–1349 (2010).

[100]Hamidi T, Algul H, Cano CE, Sandi MJ, Molejon MI, Riemann M et al. Nuclear protein 1 promotes pancreatic cancer development and protects cells from stress by inhibiting apoptosis. *J Clin Invest*. **122**, 2092–2103 (2012).

[101]Lorente M, Carracedo A, Torres S et al. Amphiregulin is a factor for resistance of glioma cells to cannabinoid-induced apoptosis. *Glia* **57**, 1374–1385 (2009).

[102]Huang S. *et al* A new microRNA signal pathway regulated by long noncoding RNA TGFB2OT1 in autophagy and inflammation of vascular endothelial cells. *Autophagy.* **11**, 2172–2183 (2015).

[103]Carracedo A, Lorente M, Egia A et al. The stress-regulated protein p8 mediates cannabinoidinduced apoptosis of tumor cells. *Cancer Cell.* **9**, 301–312 (2006).

[104]Malicet C, Giroux V, Vasseur S, Dagorn JC, Neira JL, Iovanna JL. Regulation of apoptosis by the p8/prothymosin alpha complex. *Proc Natl Acad Sci USA.* **103**, 2671–2676 (2006).

[105]Hoffmeister A, Ropolo A, Vasseur S et al. The HMG-I/Y-related protein p8 binds to p300 and Pax2 trans-activation domain-interacting protein to regulate the transactivation activity of the

Pax2A and Pax2B transcription factors on the glucagon gene promoter. *J Biol Chem.* **277**, 22314–22319 (2002).

[106]Sambasivan R, Cheedipudi S, Pasupuleti N, Saleh A, Pavlath GK, Dhawan J. The small chromatin-binding protein p8 coordinates the association of anti-proliferative and promyogenic proteins at the myogenin promoter. *J Cell Sci.* **122**, 3481–3491 (2009).

[107]Clark DW, Mitra A, Fillmore RA, Jiang WG, Samant RS, Fodstad O, Shevde LA. NUPR1 interacts with p53, transcriptionally regulates p21 and rescues breast epithelial cells from doxorubicin-induced genotoxic stress. *Curr Cancer Drug Targets.* 8, 421–430 (2008).

[108]Murray PJ, Wynn TA. Protective and pathogenic functions of macrophage subsets. *Nat Rev Immunol*. **11**, 723–37 (2011).

[109]Mantovani A. Macrophage diversity and polarization: in vivo veritas. *Blood*. **108**, 408–9 (2006).

[110]Mosser DM, Edwards JP. Exploring the full spectrum of macrophage activation. *Nat Rev Immunol*. **8**, 958–69 (2008).

[111]Huang H, Fletcher A, Niu Y, Wang TY, Yu L. Characterization of lipopolysaccharidestimulated cytokine expression in macrophages and monocytes. *Inflamm Res*. **61**, 1329–38 (2012).

[112]Gordon S, Martinez FO. Alternative activation of macrophages: mechanism and functions. *Immunity*. **32**, 593–604 (2010).

[113]Martinez FO, Helming L, Gordon S. Alternative activation of macrophages: an immunologic functional perspective. *Annu Rev Immunol*. **27**, 451–83 (2009).

[114]Biswas SK, Mantovani A. Macrophage plasticity and interaction with lymphocyte subsets: cancer as a paradigm. *Nat Immunol.* **11**, 889-96 (2010).

[115]Weaver LK, Pioli PA, Wardwell K, Vogel SN, Guyre PM. Up-regulation of human monocyte CD163 upon activation of cell-surface Toll-like receptors. *J Leukoc Biol*. **81**, 663–71 (2007).

[116]Peiser L, Mukhopadhyay S, Gordon S. Scavenger receptors in innate immunity. *Curr. Opin. Immunol*. **14**, 123–128 (2002).

[117]Jiang J, Jia T, Gong W, Ning B, Wooley PH, Yang SY. Macrophage Polarization in IL10 Treatment of Particle-Induced Inflammation and Osteolysis. *Am J Pathol.* **186**(1), 57-66 (2016).

[118]Aharoni S, Lati Y, Aviram M, Fuhrman B. Pomegranate juice polyphenols induce a phenotypic switch in macrophage polarization favoring a M2 anti-inflammatory state. *BioFactors*. **41**(1), 44–51 (2015).

[119]Ponce NE, Sanmarco LM, Eberhardt N, García NC, Rivarola HW, Cano RC, Aoki MP. CD73 Inhibition Shifts Cardiac Macrophage Polarization toward a Microbicidal Phenotype and Ameliorates the Outcome of Experimental Chagas Cardiomyopathy. *J Immunol*. **197**, 814-823 (2016).

[120]Perise-Barrios AJ, Gomez R, Corbi AL, de la Mata J, Domiguez-Soto A, Munoz-Fernandez MA. Use of carbosilane dendrimer to switch macrophage polarization for the acquisition of antitumor functions. *Nanoscale*. **7**(9), 3857-66 (2015).

[121]Domínguez-Soto A, de las Casas-Engel M, Bragado R, Medina-Echeverz J, AragonesesFenoll L, et al. Intravenous immunoglobulin promotes antitumor responses by modulating macrophage polarization. *J Immunol*. **193**, 5181–5189 (2014).

[122]Hamilton JA. Therapeutic potential of targeting inflammation. *Inflamm Res*. **62**, 653–65 (2013).

[123]Berry MP, Graham CM, McNab FW, Xu Z, Bloch SA, Oni T, et al. An interferon-inducible neutrophil-driven blood transcriptional signature in human tuberculosis. *Nature*. **466**(7309), 973–7 (2010).

[124]Lorenzi PL, Claerhout S, Mills GB, Weinstein JN. A curated census of autophagy-modulating proteins and small molecules: candidate targets for cancer therapy. *Autophagy*. **10**(7), 1316-26 (2014).

[125]Tuominen VJ, Ruotoistenmaki S, Viitanen A, Jumppanen M, Isola J. ImmunoRatio: a publicly available web application for quantitative image analysis of estrogen receptor (ER), progesterone receptor (PR), and Ki-67. *Breast Cancer Res*. **12**, R56 (2010).

[126]Su SB, Motoo Y, Iovanna JL, Xie MJ, MouriH, Ohtsubo K, Yamaguchi Y, WatanabeH, Okai T, Matsubara F, Sawabu N. Expression of p8 in human pancreatic cancer. *Clin Cancer Res.* **7**, 309–313 (2001).

[127]Ito Y, Yoshida H, Motoo Y, Miyoshi E, Iovanna JL, Tomoda C, Uruno T, Takamura Y, Miya A, Kobayashi K, Matsuzuka F, Matsuura N, Kuma K, Miyauchi A. Expression and cellular localization of p8 protein in thyroid neoplasms. Elsevier. **25**, 3419–3423 (2003).

[128]Realegeno S, Kelly-Scumpia KM, Dang AT et al. S100A12 is part of the antimicrobial network against Mycobacterial leprae in human macrophages. *PLoS Pathog*. **12**(6), e1005705 (2016).

[129]Ghorpade DS, Holla S, Kaveri SV et al. Sonic hedgehog-dependent induction of microRNA 31 and microRNA 150 regulates *Mycobacterium* bovis BCG-driven toll-like receptor 2 signaling. *Mol. Cell Biol.* **33**, 543–556 (2013).

[130]Taganov KD, Boldin MP, Chang KJ, Baltimore D. NF-kappaB-dependent induction of microRNA miR-146, an inhibitor targeted to signaling proteins of innate immune responses. *Proc. Natl. Acad. Sci. USA.* **103**, 12481–12486 (2006).

[131]Lazar-Molnar E, Chen B, Sweeney KA et al. Programmed death-1 (PD-1)-deficient mice are extraordinarily sensitive to tuberculosis. *Proc. Natl. Acad. Sci. USA.* **107**, 13402–13407 (2010).

[132]Li D, Wang T, Song X et al. Genetic study of two single nucleotide polymorphisms within corresponding microRNAs and susceptibility to tuberculosis in a Chinese Tibetan and Han population. *Hum. Immunol.* **72**, 598–602 (2011).

[133]Ma F, Xu S, Liu X et al. The microRNA miR-29 controls innate and adaptive immune responses to intracellular bacterial infection by targeting interferon-gamma. *Nat. Immunol.* **12**, 861–869 (2011).

[134]Yang CH, Yue J, Fan M, Pfeffer LM. IFN induces miR-21 through a signal transducer and activator of transcription 3-dependent pathway as a suppressive negative feedback on IFN-induced apoptosis. *Cancer Res*. **70**, 8108–8116 (2010).